CR-130132

STAR

Final Report

April 1969 to August 1972

DETERMINATION OF CONTAMINATION CHARACTER OF MATERIALS IN SPACE TECHNOLOGY TESTING

By: DANIEL L. HAYNES and DALE M. COULSON

Prepared for:

GODDARD SPACE FLIGHT CENTER
NATIONAL AERONAUTICS AND SPACE ADMINISTRATION
GLENN ROAD
GREENBELT, MARYLAND 20771

Attention: MR. HAROLD SHAPIRO, CODE 332
TECHNICAL OFFICER

N73-14878

Unclas
G3/31 50896

(NASA-CR-130132) DETERMINATION OF CONTAMINATION CHARACTER OF MATERIALS IN SPACE TECHNOLOGY TESTING Final Report, D.L. Haynes, et al (Stanford Research Inst.) Aug. 1972 130 p CSCL 22B

STANFORD RESEARCH INSTITUTE
Menlo Park, California 94025 · U.S.A.

STANFORD RESEARCH INSTITUTE
Menlo Park, California 94025 · U.S.A.

Final Report
April 1969 to August 1972

DETERMINATION OF CONTAMINATION CHARACTER OF MATERIALS IN SPACE TECHNOLOGY TESTING

By: DANIEL L. HAYNES and DALE M. COULSON

Prepared for:

GODDARD SPACE FLIGHT CENTER
NATIONAL AERONAUTICS AND SPACE ADMINISTRATION
GLENN ROAD
GREENBELT, MARYLAND 20771
Attention: MR. HAROLD SHAPIRO, CODE 332
TECHNICAL OFFICER

CONTRACT NAS5-11697

SRI Project PSU-7907

Approved by:

MARION E. HILL, *Director*
Chemistry Laboratory

CHARLES J. COOK, *Executive Director*
Physical Sciences Division

SUMMARY

This work was undertaken to measure the contamination effects on mirror surfaces of vacuum condensable material (VCM) from various materials used in space technology testing. The measurement of these effects was made in a simulated space environment. The objective was to obtain a direct measure of the contamination characteristics of these materials when used in spacecraft or spacecraft simulators.

Samples of the materials studied were heated at 125°C, and the outgases were emitted into a vacuum environment. Outgases were condensed on cold mirror surfaces that were dark or irradiated with ultraviolet light. The degree of contamination of the mirrors was measured in terms of deposit thickness and degradation of reflectivity. Materials tested included items such as shrinkable tubing, insulated wire, foams, elastomers, tapes, lubricants, and adhesives.

It was found that outgases from these materials degraded the mirror's reflectivity primarily at ultraviolet and visible wavelengths. The reflectivity at infrared wavelengths was much less degraded. The primary cause of the loss of reflected light is attributed to scattering.

Areas of the mirrors exposed to ultraviolet irradiation showed polymerization in the deposited VCM from some of the materials tested. Heating the mirrors after VCM had deposited on them improved their reflectivity, particularly when the deposit had not polymerized.

Materials whose VCM deposits noticeably degraded the reflectivity more on the nonirradiated area of the mirror were Thermofit RNF-100, insulated wire TRT-24-19-V-93, and Eccofoam FS and FPH. Deposits that

PRECEDING PAGE BLANK NOT FILMED

degraded the reflectivity more on the irradiated area of the mirror were experienced with Moxness MS60 S08, RTV-41 liquid silicone rubber, Epon 934 epoxy adhesive, Stycast 1090 epoxy foam, Epon 828 epoxy adhesive, Silastic 55U silicone elastomer, Adiprene L-100 polyurethane elastomer, and Scotch tape Y-9050. Materials that gave light deposits and degraded the reflectivity about the same amount on both areas of the test mirror were polyimide tape X1156, Insulgrease G-640, Dow Corning high vacuum silicone grease, RTV-577 liquid silicone rubber, RTV-602 liquid silicone rubber, Mystic 7100 double-faced tape, and Rexolite 2200 copper-clad polystyrene.

CONTENTS

SUMMARY iii

LIST OF ILLUSTRATIONS vii

LIST OF TABLES xi

INTRODUCTION 1

EXPERIMENTAL APPARATUS AND PROCEDURES 3

RESULTS AND DISCUSSION 11

Thermofit RNF-100 11
Insulated Wire TRT-24-19-V-93 25
Eccofoam FS 27
Moxness MS60 S08 30
Raychem Wire 44/0411 30
Polyimide Tape X1156 32
Insulgrease G-640 37
Dow Corning High Vacuum Silicone Grease 38
Scotch Pressure-Sensitive Tape No. Y-9050 39
Eccofoam FPH 41
RTV-41 Liquid Silicone Rubber 46
RTV-577 Liquid Silicone Rubber 46
RTV-602 Liquid Silicone Rubber 50
Epon 934 Epoxy Adhesive 51
Stycast 1090 Epoxy Foam 52
Epon 828 Epoxy Adhesive 52
Mystic 7100 Double-faced Tape, The Borden Co. 58
Rexolite 2200 Copper-clad Polystyrene, American Enka Corp. . . 64
Silastic 55U Silicone Elastomer, Dow Corning Co. 68
Adiprene L-100 Polyurethane Elastomer, E. I. du Pont de Nemours & Co., Inc. 75

CONCLUSIONS 81

APPENDIX REFLECTION AND SCATTERING FROM COATED AND UNCOATED ALUMINUM MIRRORS A-1

ILLUSTRATIONS

1	Thermal-Vacuum Chamber	4
2	Location of Test Mirror and Crystals of the Microbalance	5
3	Optical Path from the Test Mirror to the Cary Model 14M Spectrophotometer	6
4	Distribution of Outgases in the Thermal-Vacuum Apparatus	8
5	Photographs of Test Mirrors Contaminated with Outgases from Materials Subjected to Thermal-Vacuum Treatment	13
6	Reflectivity of a Mirror Contaminated with Outgases from Thermofit RNF-100 (After 5 Hours)	19
7	Reflectivity of a Mirror Contaminated with Outgases from Thermofit RNF-100 (After 24 Hours)	20
8	Reflectivity of a Mirror Contaminated with Outgases from Thermofit RNF-100 (After 96 Hours)	21
9	Reflectivity of a Mirror Contaminated with Outgases from Thermofit RNF-100 (After Heating Chill-Plate)	22
10	Quadrupole Mass Spectrum for Outgases from Polyolefin Shrinkable Tubing, Thermofit RNF-100	24
11	Reflectivity of a Mirror Contaminated with Outgases from Insulated Wire TRT-24-19-V-93 (After Heating Chill-Plate)	25
12	Quadrupole Mass Spectrum for Outgases from Insulated Wire TRT-24-19-V-93 (Sample Heater On)	26
13	Reflectivity of a Mirror Contaminated with Outgases from Eccofoam FS (After Heating Chill-Plate)	28
14	Quadrupole Mass Spectrum for Outgases from Eccofoam FS (Sample Heater On)	29
15	Reflectivity of a Mirror Contaminated with Outgases from Moxness Material MS60 S08 (After Heating Chill-Plate)	31
16	Reflectivity of a Mirror Contaminated with Outgases from Raychem Wire 44/0411 (After Heating Chill-Plate)	32
17	Reflectivity of a Mirror Contaminated with Outgases from 3M Polyimide Tape X1156 (After 5 Hours)	33

PRECEDING PAGE BLANK NOT FILMED

18 Reflectivity of a Mirror Contaminated with Outgases from 3M Polyimide Tape X1156 (After 24 Hours) 34

19 Reflectivity of a Mirror Contaminated with Outgases from 3M Polyimide Tape X1156 (After 96 Hours) 35

20 Reflectivity of a Mirror Contaminated with Outgases from 3M Polyimide Tape X1156 (After Heating Chill-Plate) 36

21 Reflectivity of a Mirror Contaminated with Outgases from Insulgrease G-640 (After Heating Chill-Plate) 37

22 Reflectivity of a Mirror Contaminated with Outgases from Dow Corning High Vacuum Silicone Grease (After Heating Chill-Plate) 38

23 Reflectivity of a Mirror Contaminated with Outgases from 3M Scotch Tape Y-9050 (After 96 Hours) 40

24 Reflectivity of a Mirror Contaminated with Outgases from 3M Scotch Tape Y-9050 (After Heating Chill-Plate) 40

25 Reflectivity of a Mirror Contaminated with Outgases from Eccofoam FPH (After 5 Hours) 42

26 Reflectivity of a Mirror Contaminated with Outgases from Eccofoam FPH (After 24 Hours) 43

27 Reflectivity of a Mirror Contaminated with Outgases from Eccofoam FPH (After 96 Hours) 44

28 Reflectivity of a Mirror Contaminated with Outgases from Eccofoam FPH (After Heating Chill-Plate) 45

29 Mass Spectrum of Eccofoam FPH 47

30 Reflectivity of a Mirror Contaminated with Outgases from G.E. RTV-41 (After 138 Hours) 48

31 Reflectivity of a Mirror Contaminated with Outgases from G.E. RTV-41, After Chill-Plate Was Heated at 80°C for One-half Hour 48

32 Reflectivity of a Mirror Contaminated with Outgases from G.E. RTV-577 (After Heating Chill-Plate) 49

33 Reflectivity of a Mirror Contaminated with Outgases from G.E. RTV-602 (After Heating Chill-Plate) 50

34 Reflectivity of a Mirror Contaminated with Outgases from Shell Epon 934 (After Heating Chill-Plate) 51

35 Reflectivity of a Mirror Contaminated with Outgases from Stycast 1090 (After 5 Hours) 53

36 Reflectivity of a Mirror Contaminated with Outgases from Stycast 1090 (After 24 Hours) 54

37 Reflectivity of a Mirror Contaminated with Outgases from Stycast 1090 (After 96 Hours) 55

38 Reflectivity of a Mirror Contaminated with Outgases from Stycast 1090 (After Heating Chill-Plate) 56

39 Mass Spectrum for Outgases from Stycast 1090 57

40 Reflectivity of a Mirror Contaminated with Outgases from Shell Epon 828 (After Heating Chill-Plate) 58

41 Reflectivity of a Mirror Contaminated with Outgases from Mystic Tape No. 7100 (After 5 Hours) 59

42 Reflectivity of a Mirror Contaminated with Outgases from Mystic Tape No. 7100 (After 24 Hours) 60

43 Reflectivity of a Mirror Contaminated with Outgases from Mystic Tape No. 7100 (After 96 Hours) 61

44 Reflectivity of a Mirror Contaminated with Outgases from Mystic Tape No. 7100 (After Heating Chill-Plate) 62

45 Mass Spectrum of Outgases from Mystic Tape No. 7100 63

46 Reflectivity of a Mirror Contaminated with Outgases from Rexolite 2200 (After 5 Hours) 64

47 Reflectivity of a Mirror Contaminated with Outgases from Rexolite 2200 (After 24 Hours) 65

48 Reflectivity of a Mirror Contaminated with Outgases from Rexolite 2200 (After 96 Hours) 66

49 Reflectivity of a Mirror Contaminated with Outgases from Rexolite 2200 (After Heating Chill-Plate) 67

50 Mass Spectrum of Outgases from Rexolite 2200 69

51 Reflectivity of a Mirror Contaminated with Outgases from Silastic 55U (After 5 Hours) 70

52 Reflectivity of a Mirror Contaminated with Outgases from Silastic 55U (After 24 Hours) 71

53 Reflectivity of a Mirror Contaminated with Outgases from Silastic 55U (After 96 Hours) 72

54 Reflectivity of a Mirror Contaminated with Outgases from Silastic 55U (After Heating Chill-Plate) 73

55 Mass Spectrum of Outgases from Silastic 55U 74

56 Reflectivity of a Mirror Contaminated with Outgases from Adiprene L-100 (After 5 Hours) 76

57 Reflectivity of a Mirror Contaminated with Outgases from Adiprene L-100 (After 24 Hours) 77

58 Reflectivity of a Mirror Contaminated with Outgases from Adiprene L-100 (After 96 Hours) 78

59 Reflectivity of a Mirror Contaminated with Outgases from Adiprene L-100 (After Heating Chill-Plate) 79

60 Mass Spectrum of Outgases from Adiprene L-100 80

TABLES

I	Reflectivity Degradation of the Mirror Surface and Deposit Thicknesses on Mirrors	2
II	Materials Subjected to Thermal-Vacuum Treatment	12
III	Microbalance and Pressure Results	18

INTRODUCTION

This final report under Contract NAS5-11697 summarizes the work done in the study of the contamination character of selected materials used in space technology testing. Many of these materials contain components that become volatile in a space environment. Most previous data were limited to weight loss or vapor pressure. However, these parameters are not necessarily a direct measure of the contamination character of these materials.

In this project selected materials were exposed to a thermal-vacuum environment, and the degree of contamination was measured by collecting the outgases from these materials on a cold test mirror surface. The degradation of reflectivity of the mirror was measured over a spectral range from 1100 Å to 2.5 μ. Half the mirror's surface was also exposed to uv irradiation to determine its effects on the contaminative character of the depositing outgases. The amount of deposit per unit area was measured by microbalances mounted near the mirror; the sensor of one microbalance was uv irradiated. A quadrupole mass spectrometer was used to determine the composition of the outgases.

Table I summarizes the effects of outgases from the materials on a mirror surface. It must be kept in mind that all materials tested were of the same sample weight (1 g) and were subjected to the same testing procedure. The amount of the material actually used in a spacecraft and the conditions under which it is used must be considered when extrapolating these results to obtain the effects expected in spacecraft and spacecraft simulators.

Table 1

REFLECTIVITY DEGRADATION OF THE MIRROR
SURFACE AND DEPOSIT THICKNESSES ON MIRRORS

Material	Extent of Reflectivity Degradation below 1 μ		Deposit Thickness (micron)
	Irradiated Area	Nonirradiated Area	
Thermofit RNF-100	Moderate	Severe	0.3 - 0.5
TRT-24-19-V-93	Slight	Severe	0.03 - 0.05
Eccofoam FS	Slight	Moderate	0.1 - 0.3
Moxness MS60 S08	Moderate	Slight	0.03 - 0.05
Raychem wire 44/0411	Slight	Very slight	0.01 - 0.03
Polyimide tape X1156 (electrical tape No. 92)	Very slight	Very slight	<0.01
Insulgrease G-640	Slight	Slight	0.01 - 0.03
High vacuum silicone grease	Very slight	Very slight	<0.01
Scotch tape No. Y-9050	Moderate	Slight	<0.05
Eccofoam FPH	Very slight	Very slight	<0.01
RTV-41	Slight	Very slight	0.01 - 0.03
RTV-577	Slight	Slight	0.10 - 0.15
RTV-602	Very slight	Very slight	<0.01
Epon 934	Moderate	Slight	0.01 - 0.03
Stycast 1090	Moderate	Slight	0.05 - 0.08
Epon 828	Slight	Very slight	0.01 - 0.03
Mystic 7100	Slight	Slight	0.07 - 0.10
Rexolite 2200	Very slight	Very slight	<0.01
Silastic 55U	Moderate	Slight	0.07 - 0.10
Adiprene L-100	Moderate	Slight	0.01 - 0.03

EXPERIMENTAL APPARATUS AND PROCEDURES

The first year of the project was devoted largely to developing a thermal-vacuum apparatus for testing the contamination character of the materials used in space technology. The apparatus finally developed for these studies is described below and is shown in Figures 1, 2, and 3. In this apparatus a test mirror is mounted on a copper block that can be cooled to -20°C and heated to 80°C. The chill-plate is cooled by a refrigerator charged with monochlorodifluoromethane and heated by a 250-W cartridge heater. Test mirrors consist of a quartz plate (2 x 2 x 1/8 inch) onto which a mirror surface of aluminum was deposited. The aluminum surface is approximately 2000 Å thick with an overcoating of MgF_2 that is approximately 150 Å thick. A port in the thermal-vacuum wall admits uv irradiation to half of the mirror; the other half is not irradiated. Quartz crystal microbalances are mounted near the mirror (in both the irradiated and nonirradiated areas) to measure deposited outgases. The sample is placed in a heater that is in direct line with the mirror and the ionizer of the quadrupole mass spectrometer. The heater can heat the sample to 125°C using a Calrod heating element.

Several changes were made to the sample heater during the course of this project. The original sample heater was made from a 1-inch i.d. copper cylinder with 1/8-inch-thick walls. The heater was 2-1/2 inches long and narrowed to a 5/16-inch-diameter mouth. It will be referred to as sample heater No. 1 in this report. When this heater was used, the flux of the outgases from the sample was much higher on the mirror than it was on the microbalances. This led to deposition of a much thicker film of contaminants on the mirror than on the microbalance crystals,

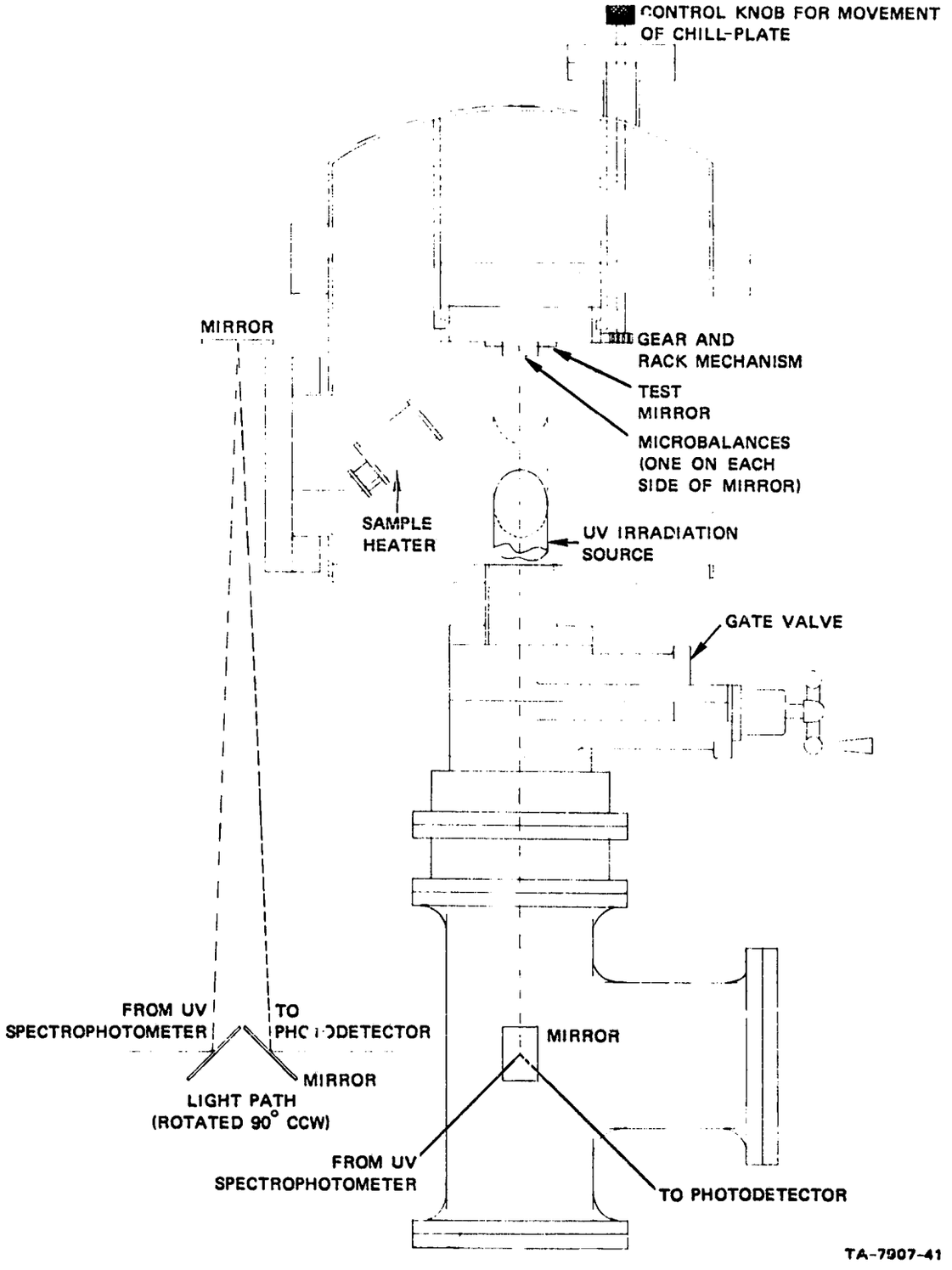

FIGURE 1 THERMAL-VACUUM CHAMBER

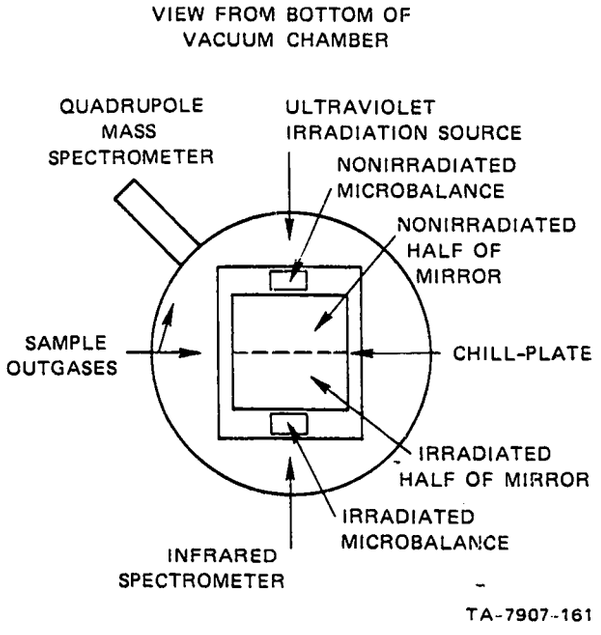

FIGURE 2 LOCATION OF TEST MIRROR AND CRYSTALS OF THE MICROBALANCE

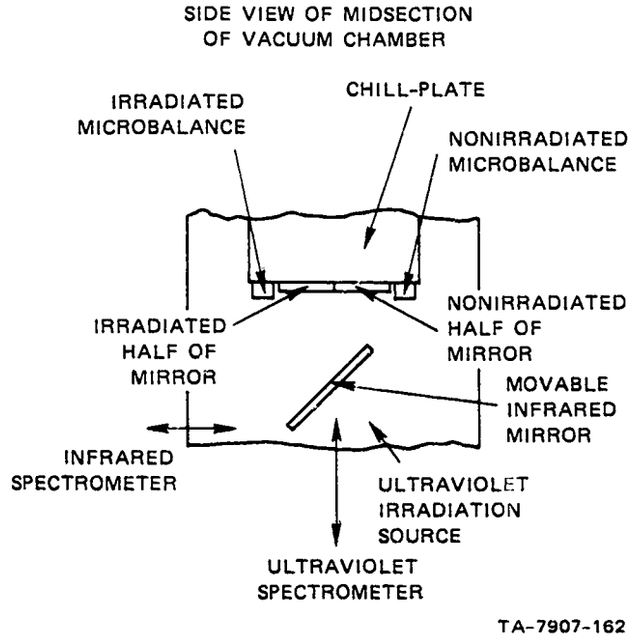

FIGURE 3 OPTICAL PATH FROM THE TEST MIRROR TO THE CARY MODEL 14M SPECTROPHOTOMETER

making it difficult to correlate the microbalance results with the weight of the deposit on the mirror.

Sample heater No. 2 was constructed with a 1-inch-diameter mouth and having the approximate flux distribution shown in Figure 4. If all the outgases reached the mirror, the flux would be approximately 1.0. This represents the outgases from the sample passing through a 4-sq-in. area. It can be seen from this curve that the flux at the mirror is at least five times that at the microbalances.

Another refinement was made later by adding a 3/8-inch-diameter side-arm that brought the outgasing sample into direct line of sight with the ionizer of the quadrupole mass spectrometer (Electronics Associates, Inc., Model 300). This was done to increase the intensity of the mass spectral patterns so that more information could be read from them. This heater will be referred to as sample heater No. 3 in this report.

Two spectrophotometers are connected to the thermal-vacuum chamber to measure the reflectivity of the mirror over a spectral range from 1100 Å to 2.5 μ. The thermal-vacuum chamber is mounted on a McPherson Model 225 vacuum spectrophotometer. This instrument is used to measure the reflectivity of the mirror between 1100 and 6000 Å. The reflectivity of the mirror between 5000 Å and 2.5 μ is measured with a Cary Model 14M spectrophotometer. Originally these infrared reflectivity measurements were made after the run was finished and the mirror removed from the chamber. Later, we constructed optics, including the movable infrared mirror in Figure 3, to connect the Cary spectrophotometer to the test chamber. This made it possible to make in situ infrared reflectivity measurements on the Cary spectrophotometer. The chill-plate on which the mirror is mounted is movable so that the reflectivity of both the irradiated and nonirradiated areas of the mirror can be measured.

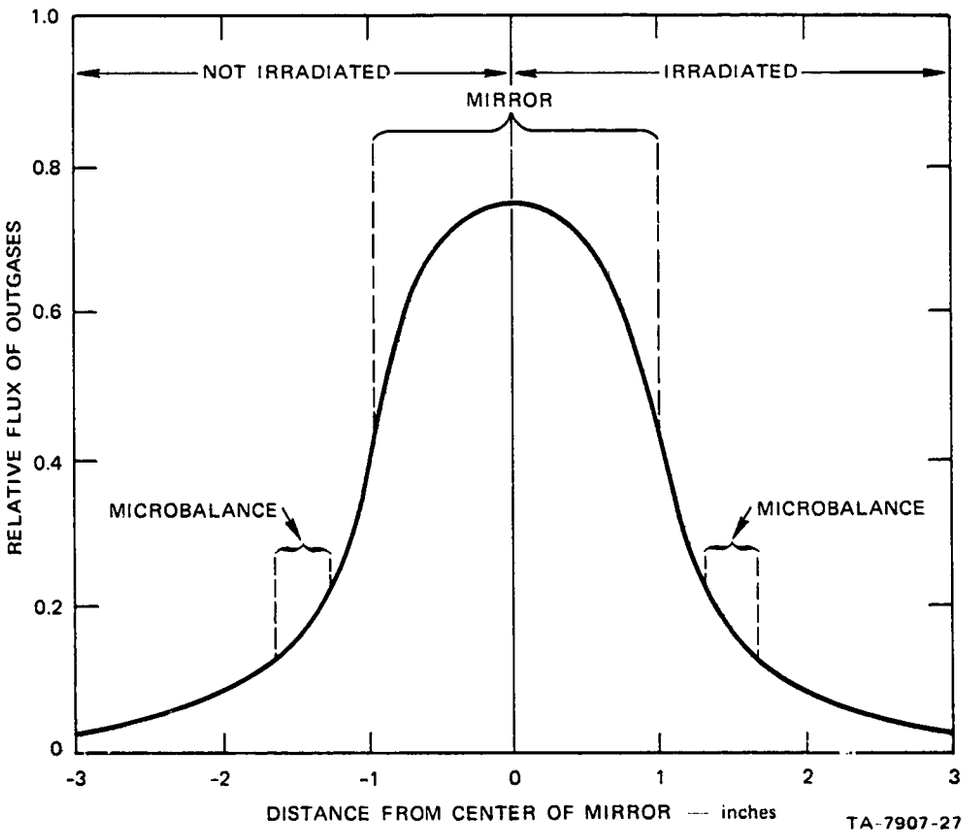

FIGURE 4 DISTRIBUTION OF OUTGASES IN THERMAL-VACUUM APPARATUS

After these changes were made, including the addition of a side-arm on sample heater No. 3, a series of experiments was carried out to check the results of these changes and, in the case of the Cary spectrophotometer, to see whether previous data taken outside the test chamber were consistent with those taken during a test. When the data were found to be consistent and mass spectral patterns improved, the tests of materials continued. Mystic 7100 was the first material to be tested after these changes were complete.

The uv irradiation source is a high pressure mercury short-arc lamp (Illumination Industry Model 202). This lamp provides approximately 5 solar constants in the wavelength range from 2000 to 4000 Å.

Other parts of the thermal-vacuum chamber not shown in Figures 1 through 3 are the pumping system, consisting of a 4-inch diffusion pump charged with Dow Corning diffusion pump fluid 705, and a CVC Type GLC-110 ionization vacuum gauge. Pressures in the 10^{-7} torr range are attained.

The experimental procedure was as follows: a 1-g sample of finely divided material was placed in the sample heater. The thermal-vacuum chamber was pumped down overnight. For tests lasting 96 hours, the chamber was pumped over the weekend. The pressure at the beginning of a test was in the 10^{-7} torr range.

The gate valve connecting the thermal-vacuum chamber to the McPherson spectrophotometer (see Figure 1) was opened, and the reflectivity of the clean test mirror was measured in the uv and visible regions. The gate valve was then closed, and the reflectivity of the mirror was measured in the infrared region with the Cary spectrophotometer.

The chill-plate refrigerator was turned on, cooling the test mirror to -20°C in 20 minutes. The uv irradiation source was turned on at the same time, and the test chamber was left to equilibrate for approximately 1 hour.

The sample heater was turned on to heat the sample from ambient temperature to 125°C in 20 minutes. The power to the heater was then reduced to maintain the sample temperature at 125°C for the rest of the experiment. Mass spectra of the sample outgases were taken during the first two hours after the sample heater was turned on.

In later tests, the reflectivity of the test mirror was measured 3 times during the test at 5, 24, and 96 hours so that the degradation of the optical surface could be monitored throughout the run. In the first few tests the intermediate reflectivity measurements were not made. The duration of the tests originally ranged from 5 to 137 hours. However, for tests of the last four materials (Mystic 7100, Rexolite 2200, Silastic 55U, and Adiprene L-100), it was decided to limit the test to 96 hours. This time is adequate to define the outgasing characteristics of the materials and is a more convenient working time frame.

After the reflectivity measurements were made at 96 hours, the chill-plate refrigerator and the sample heater were turned off. The chill-plate was heated to 80°C in about 20 minutes and held at that temperature for 30 minutes. Mass spectra were taken while the chill-plate was being heated.

The reflectivities of the two areas of the test mirror were measured again after heating the chill-plate. The chamber was held under vacuum for several hours to allow the chill-plate to come to ambient temperature. The chamber was then opened and the test mirror removed for examination and photographs.

Microbalance and pressure readings were taken during the entire course of the test.

RESULTS AND DISCUSSION

The materials studied in this project are listed in Table II. Photographs of the test mirrors after exposure to the outgases from these materials and to uv irradiation are given in Figure 5. The top half of each photograph corresponds to the irradiated area of the mirror, the bottom half to the nonirradiated area.

Microbalance results for each material, taken at 5, 24, 48, and 96 hours, are tabulated in Table III. These data must be corrected in accordance with Figure 4 to arrive at a value for the amount of deposit on the test mirror. The rate of deposition of the outgases from the various samples tested can be determined over the course of any particular experiment. Pressure results taken immediately before and during the heating of the material are also presented in Table III.

Thermofit RNF-100

Thermofit RNF-100 was tested several times during the project, under several different sets of experimental conditions. The following is a summary of the results of those tests.

A 1-g sample was prepared by cutting the 1/2-inch-diameter tubing into 1/8- to 1/4-inch long segments and preshrinking them at a temperature of 200-300°C.

Reflectivity data reported in Figures 6 through 9 were measured *in situ*. They show that the reflectivity of the mirror was severely degraded in the short wavelength region. The relative curves in Figures 6 and 7 indicate that the reflectivity of both the irradiated and nonirradiated areas of the mirror was about the same after 5 and 24 hours.

Table II

MATERIALS SUBJECTED TO THERMAL-VACUUM TREATMENT

Material	Manufacturer	Description
Thermofit RNF-100	Raychem Corporation	Polyolefin shrinkable tubing
TRT-24-19-V-93	Raychem Corporation	Insulated wire
Eccofoam FS	Emerson & Cuming, Inc.	Polyurethane foam
Moxness MS60 S08	Moxness Products, Inc.	Silicone elastomer
Raychem wire 44/0411	Raychem Corporation	Insulated wire
Polyimide tape X1156 (electrical tape No. 92)	3M Company	Polyimide film with thermosetting silicone pressure-sensitive tape
Insulgrease G-640	General Electric	Dielectric silicone grease
High vacuum silicone grease	Dow Corning	Silicone lubricant
Scotch tape No. Y-9050	3M Company	Pressure-sensitive tape
Eccofoam FPH	Emerson & Cuming, Inc.	Polyurethane foam
RTV-41	General Electric	Liquid silicone rubber
RTV-577	General Electric	Liquid silicone rubber
RTV-602	General Electric	Liquid silicone rubber
Epon 934	Shell Chemical Company	Epoxy adhesive
Stycast 1090	Emerson & Cuming, Inc.	Epoxy foam
Epon 828	Shell Chemical Company	Epoxy adhesive
Mystic 7100	The Borden Company	Double-faced tape
Rexolite 2200	American Enka Corporation	Copper clad polystyrene
Silastic 55U	Dow Corning Company	Silicone elastomer
Adiprene L-100	E.I. du Pont de Nemours & Co., Inc.	Polyurethane elastomer

THERMOFIT RNF-100

TRT-24-13-V-93

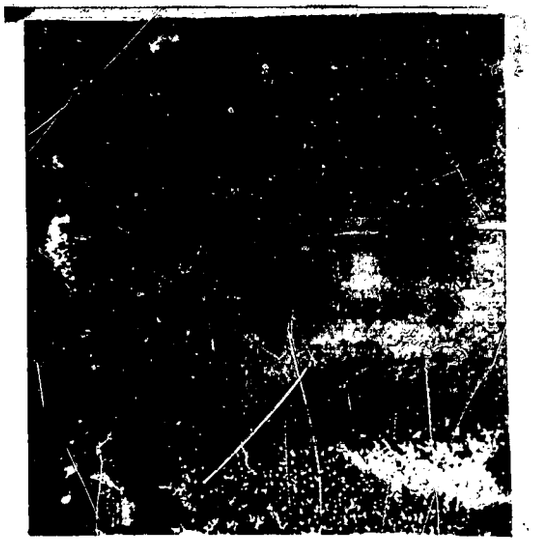

ECCOFOAM FS

MOXNESS MS60 S08

FIGURE 5 PHOTOGRAPHS OF TEST MIR[illegible] CONTAMINATED WITH OUTGASES FROM MATERIALS SUBJECTED TO [illegible] TREATMENT

RAYCHEM WIRE 44/0411

POLYIMIDE TAPE X1156

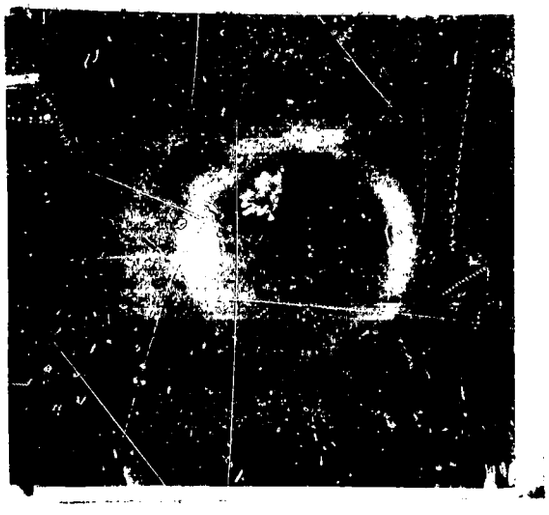

INSULGREASE G-640

HIGH VACUUM SILICONE GREASE

FIGURE 5 PHOTOGRAPHS OF TEST MIRRORS CONTAMINATED WITH OUTGASES FROM MATERIALS SUBJECTED TO THERMAL-VACUUM TREATMENT (Continued)

SCOTCH TAPE NO. Y-9050

ECCOFOAM FPH

RTV-41

RTV-577

FIGURE 5 PHOTOGRAPHS OF TEST MIRRORS CONTAMINATED WITH OUTGASES FROM MATERIALS SUBJECTED TO THERMAL-VACUUM TREATMENT (Continued)

RTV-602

EPON 934

STYCAST 1090

EPON 828

FIGURE 5 PHOTOGRAPHS OF TEST MIRRORS CONTAMINATED WITH OUTGASES FROM MATERIALS SUBJECTED TO THERMAL-VACUUM TREATMENT (Continued)

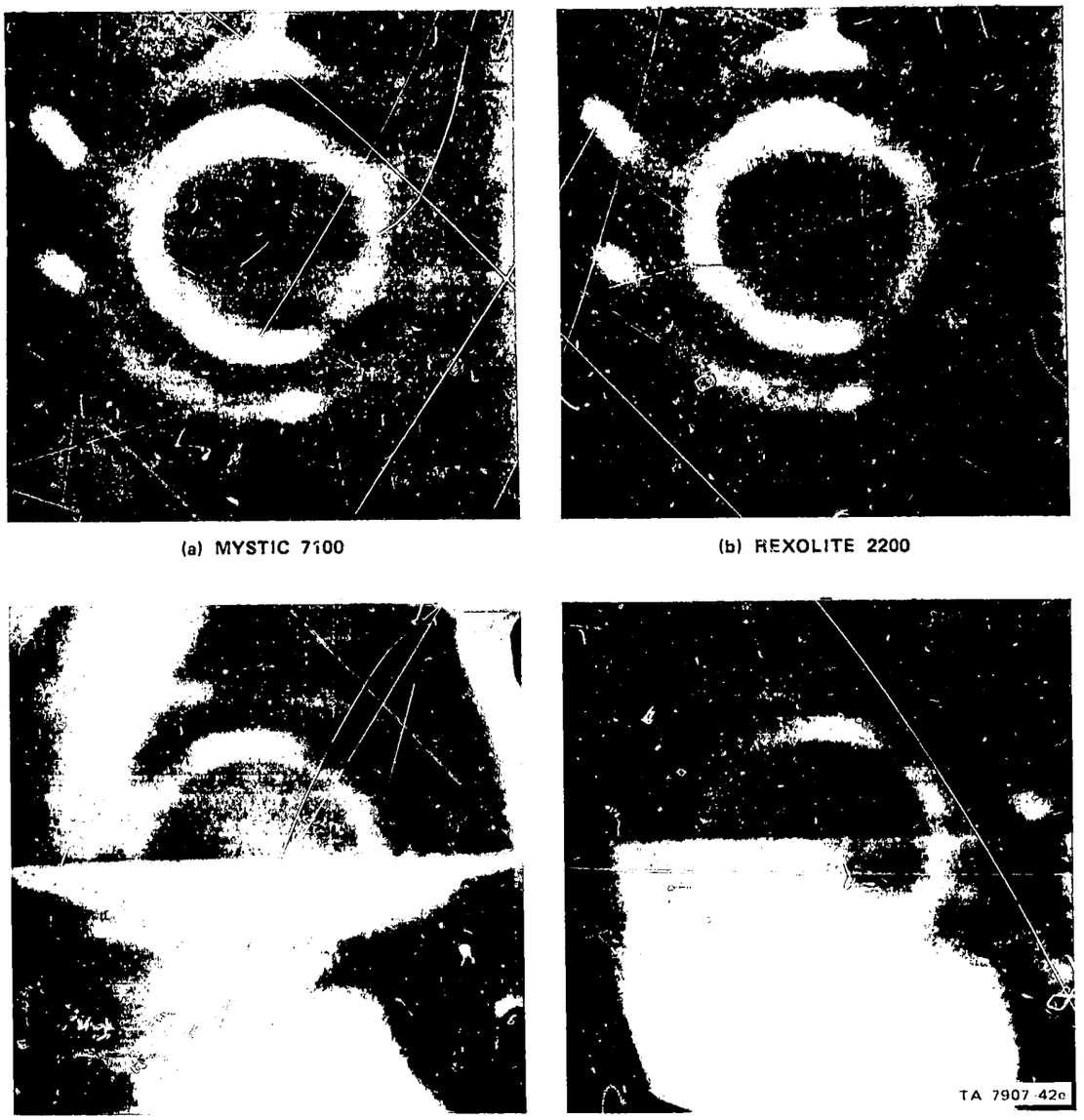

(a) MYSTIC 7100

(b) REXOLITE 2200

(c) SILASTIC 55U

(d) ADIPRENE L-100

FIGURE 5 PHOTOGRAPHS OF TEST MIRRORS CONTAMINATED WITH OUTGASES FROM MATERIALS SUBJECTED TO THERMAL-VACUUM TREATMENT (Concluded)

Table III

MICROBALANCE AND PRESSURE RESULTS

Material	Microbalance Results ($\mu g/cm^2$)								Initial Pressure (torr)	Highest Pressure Attained While Heating Material (torr)
	After 5 hr		After 24 hr		After 48 hr		After 96 hr			
	Irradiated	Nonirradiated	Irradiated	Nonirradiated	Irradiated	Nonirradiated	Irradiated	Nonirradiated		
Thermofit RNF-100	0.5 (2.5)	0.4 (2.0)	1.7 (8.5)	1.4 (7.0)	2.7 (13.5)	2.3 (11.5)	4.2 (21.0)	4.5 (22.5)	6×10^{-7}	2.6×10^{-6}
TRT 24-19-V-93	0.66								2×10^{-7}	4.1×10^{-6}
Eccofoam FS	0.26		0.73*						7×10^{-7}	3.5×10^{-6}
Moxness MS60 S08	0.77 (3.85)								8×10^{-7}	3.3×10^{-6}
Raychem Wire 44/0411	0.05 (0.25)		0.13* (0.65)						1.2×10^{-6}	7.6×10^{-6}
Polyimide tape X1156	0.18 (0.90)	0.20 (1.00)	0.35 (1.75)	0.41 (2.05)	0.50 (2.50)	0.58 (2.90)	0.73 (3.65)	0.85 (4.25)	7×10^{-7}	5.3×10^{-6}
Insulgrease G-640	0.61 (3.05)		0.85* (4.25)						3×10^{-7}	5.8×10^{-6}
Dow Corning high vacuum grease	0.22 (1.10)		0.39* (1.95)						2.0×10^{-6}	9.8×10^{-6}
Scotch tape No. Y-9050	0.33 (1.65)	0.33 (1.65)	0.61 (3.05)	0.36 (1.80)	0.80 (1.00)	0.38 (1.90)	1.04 (5.20)	0.44 (2.20)	6×10^{-7}	6.4×10^{-6}
Eccofoam FPH	0	0	0	0	0	0	0	0	6×10^{-7}	5.0×10^{-6}
RTV-41	0.78 (3.90)		0.81 (4.05)		0.75 (3.75)		0.64 (3.20)		5×10^{-7}	2.2×10^{-6}
RTV-577	2.3 (11.5)	2.3 (1.15)	2.8 (14.0)	2.7 (13.5)	2.9 (14.5)	2.7 (13.5)	3.0 (15.0)	2.9 (14.5)	2.0×10^{-6}	5.2×10^{-6}
RTV-602	2.2 (11.0)	2.5 (12.5)	2.4 (12.0)	2.8 (14.0)	2.3 (11.5)	2.8 (14.0)	1.7† (8.5)	2.2† (11.0)	5×10^{-7}	4.4×10^{-6}
Epon 934	0.40 (2.00)	0.27 (1.35)	0.56 (2.80)	0.35 (1.75)	0.61 (3.05)	0.38 (1.90)	0.58 (2.90)	0.37 (1.85)	1.4×10^{-6}	1.5×10^{-5}
Stycast 1090	0.20 (1.00)	0.25 (1.25)	0.18 (0.90)	0.25 (1.25)	0.12 (0.60)	0.22 (1.10)	0.07 (0.35)	0.18 (0.90)	6×10^{-7}	8.0×10^{-6}
Epon 828	0.16 (0.80)	0.18 (0.90)	0.29 (1.45)	0.24 (1.20)	0.29 (1.15)	0.30 (1.50)	0.24 (1.20)	0.22 (1.10)	7×10^{-7}	2.7×10^{-6}
Mystic tape 7100	0.15 (0.75)	0.24 (1.20)	0.38 (1.90)	0.63 (3.15)	0.54 (2.70)	0.87 (4.35)	0.78 (3.90)	1.2 (6.0)	9×10^{-7}	8.0×10^{-6}
Rexolite 2200	0.02 (0.10)	0.04 (0.20)	0	0	0	0.01 (0.05)	0	0.01 (0.05)	6×10^{-7}	2.0×10^{-6}
Silastic 550	0.15 (0.75)	0.21 (1.05)	0.34 (1.70)	0.46 2.30	0.43 (2.15)	0.56 (2.80)	0.54 (2.70)	0.68 (3.40)	8×10^{-7}	3.0×10^{-6}
Adiprene L-100	0.01 (0.05)	0.05 (0.25)	0.07 (0.35)	0.08 (0.40)	0.05 (0.25)	0.08 (0.40)	0.10 (0.50)	0.15 (0.75)	7×10^{-7}	3.0×10^{-6}

* Extrapolated to 24 hours.

† Extrapolated to 96 hours.

Note: Values in parentheses are corrected in accordance with flux distribution in Figure 4.

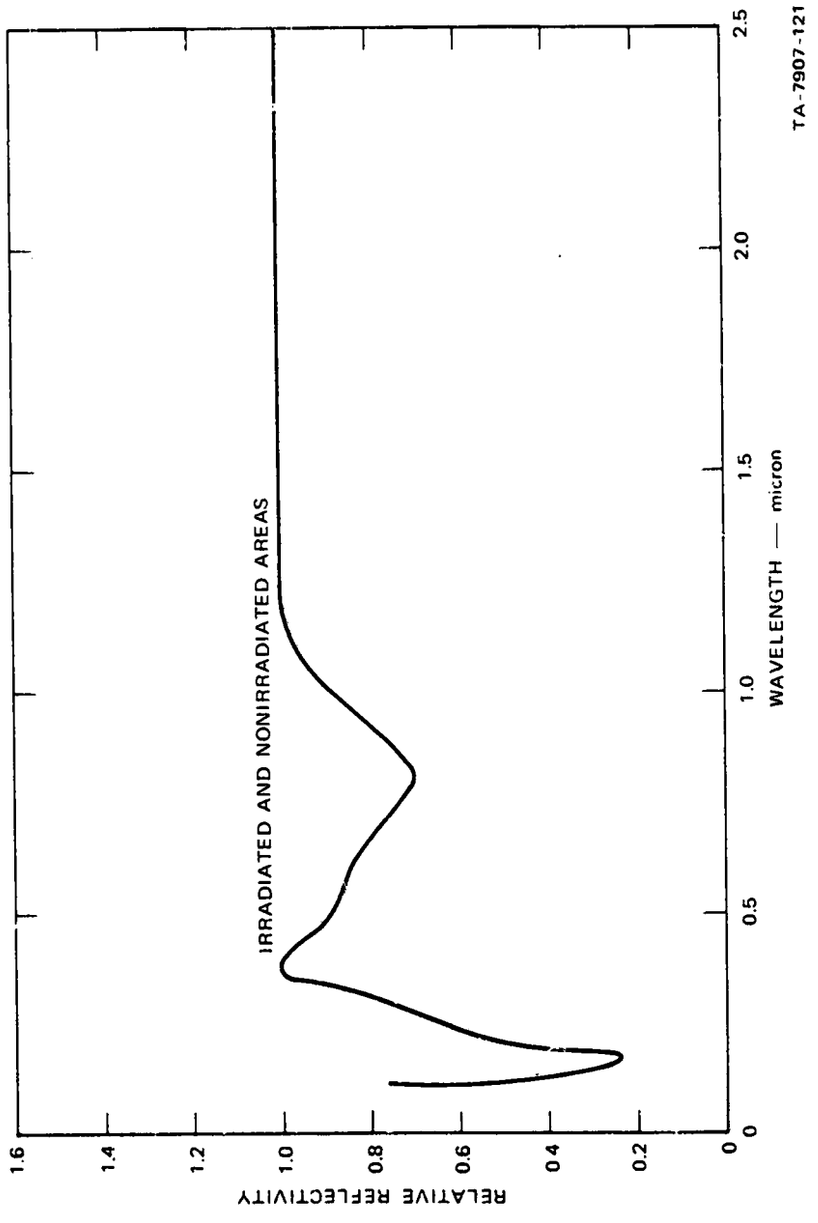

FIGURE 6 REFLECTIVITY OF A MIRROR CONTAMINATED WITH OUTGASES FROM THERMOFIT RNF-100 (AFTER 5 HOURS)

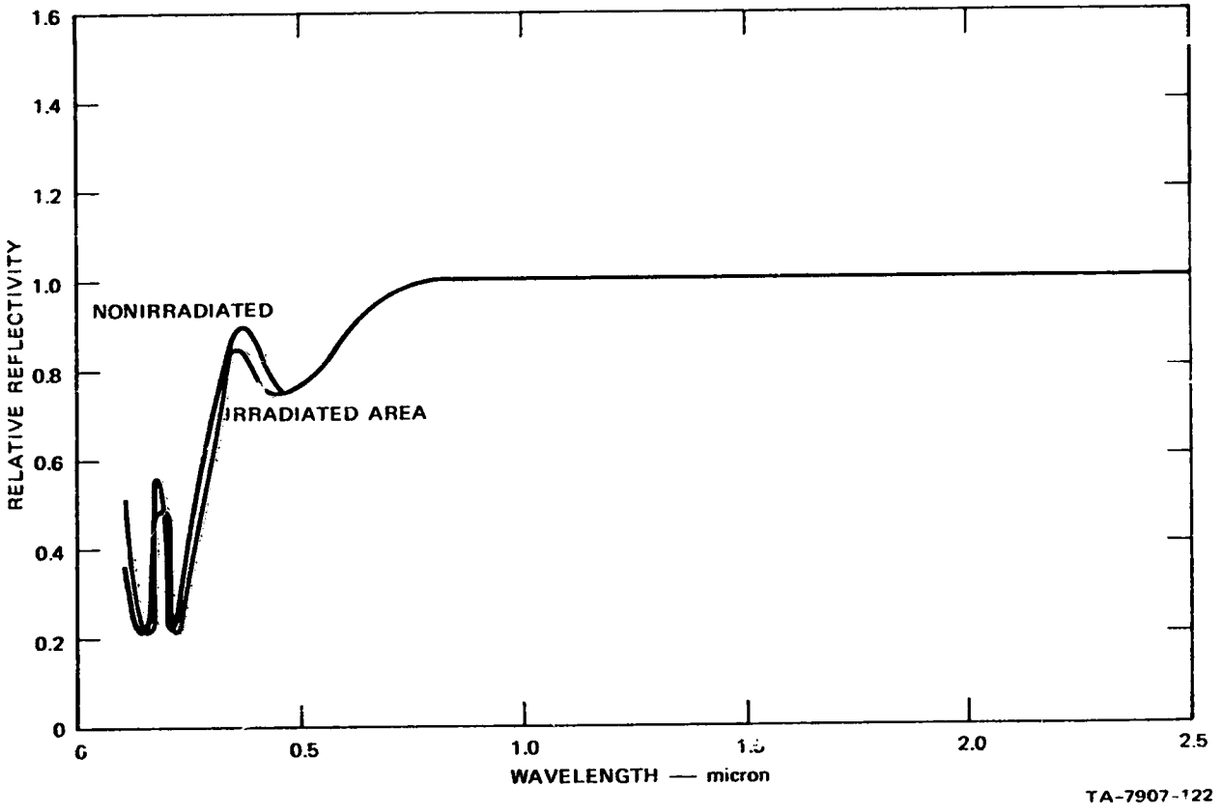

FIGURE 7 REFLECTIVITY OF A MIRROR CONTAMINATED WITH OUTGASES FROM THERMOFIT RNF-100 (AFTER 24 HOURS)

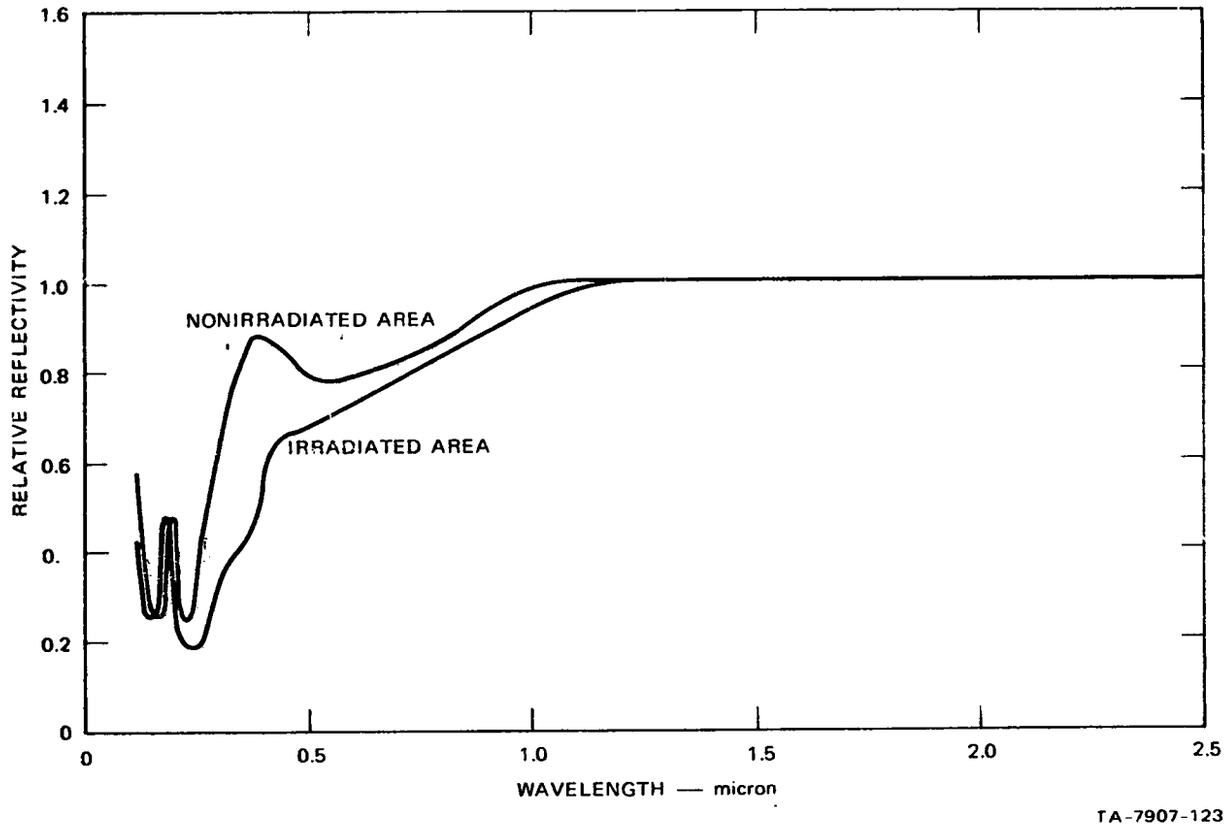

FIGURE 8 REFLECTIVITY OF A MIRROR CONTAMINATED WITH OUTGASES FROM THERMOFIT RNF-100 (AFTER 96 HOURS)

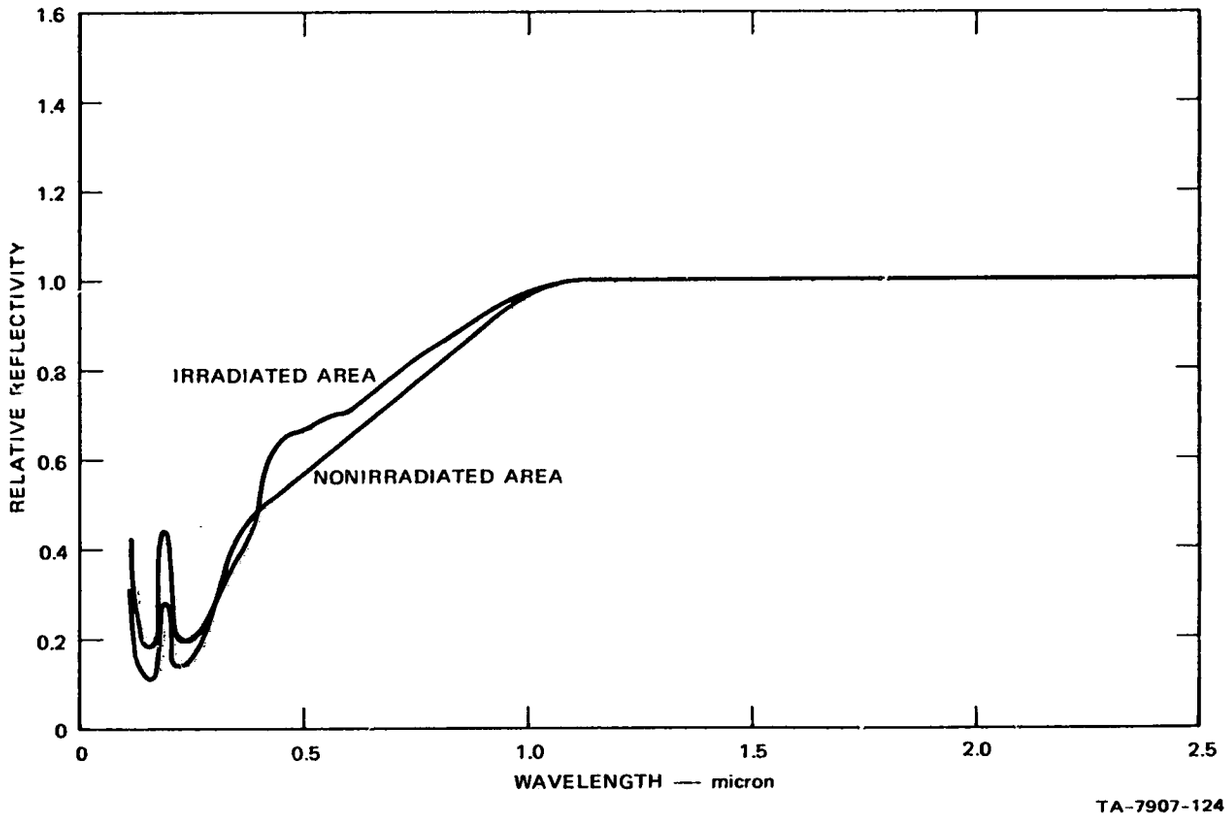

FIGURE 9 REFLECTIVITY OF A MIRROR CONTAMINATED WITH OUTGASES FROM THERMOFIT RNF-100 (AFTER HEATING CHILL-PLATE)

After 96 hours the irradiated area was noticeably less reflective than the nonirradiated area (Figure 8). The nonirradiated area of the mirror becomes the less reflective area after heating the mirror (Figure 9). It may be that the material on the irradiated area of the mirror is more volatile and lost at a greater rate than that on the nonirradiated area, or that heat causes a physical change in the deposit of one or both areas of the mirror, thereby altering its scattering properties, or a combination of these effects. Microbalance results in Table III show that deposits from this material were the heaviest of any of the materials tested. The thickness of the deposit was from 0.3 to 0.5 μ. The rate of deposition after 96 hours had slowed little from that at the beginning of the run, indicating that outgasing remained at about the same level throughout the run.

Visual examination of the mirror after the run confirms the heavy deposit and the reflectivity results (see Figure 5). Most of the material deposited on the nonirradiated area of the mirror was soluble in carbon tetrachloride, leaving a significant residual deposit only on the irradiated area. Most of the remaining deposit was soluble in acetone. In another test in which the mirror was not irradiated, the mirror was covered uniformly with a heavy deposit that was soluble in carbon tetrachloride. This evidence shows that the uv irradiation caused the deposit to polymerize.

The mass spectrum of the outgases from the sample in Figure 10 indicates the presence of C-6 hydrocarbons, most likely a dimer of propylene. However, this compound should be too volatile to deposit on the mirror.

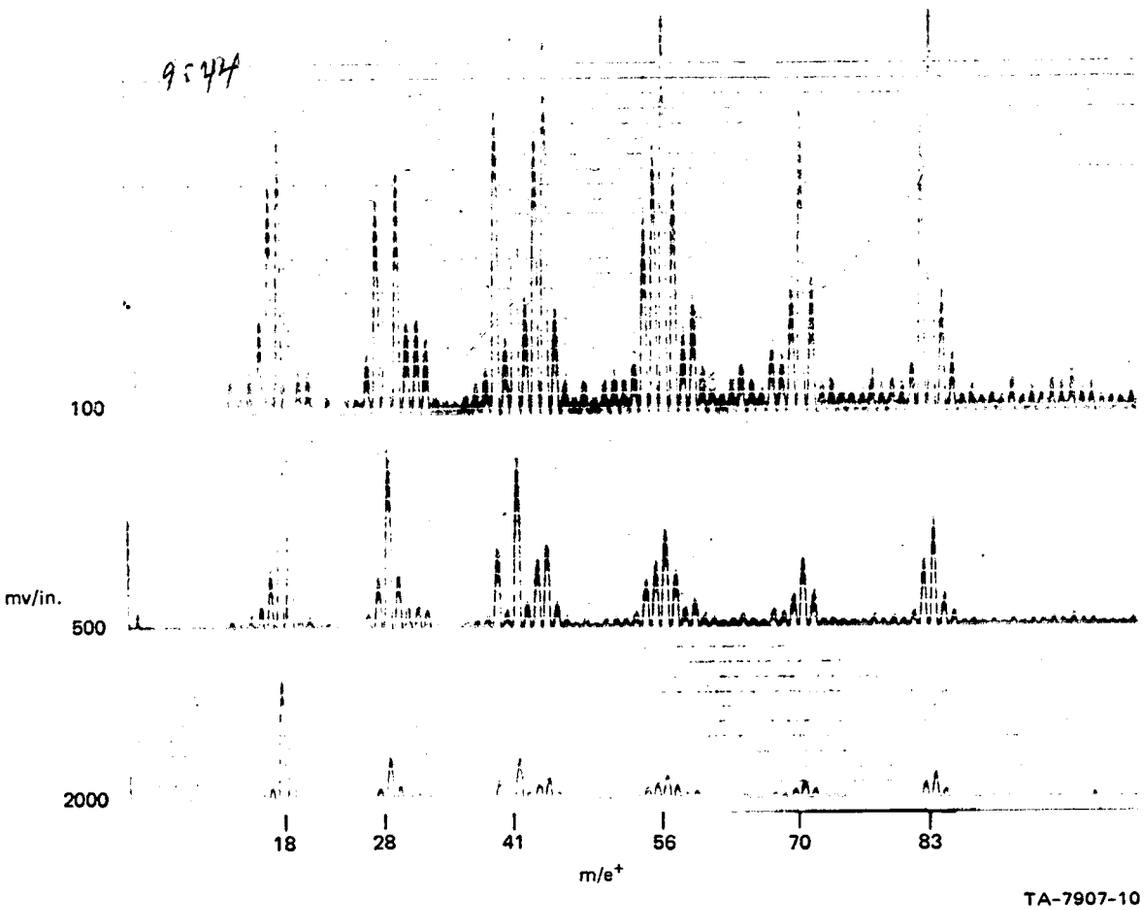

FIGURE 10 QUADRUPOLE MASS SPECTRUM FOR OUTGASES FROM POLYOLEFIN SHRINKABLE TUBING, THERMOFIT RNF-100

Insulated Wire TRT-24-19-V-93

The sample was prepared by cutting the wire into 3/4-inch lengths. Approximately 1 g of the material was placed in sample heater No. 1 and subjected to a 6-hour thermal-vacuum treatment.

The deposit was heaviest on the nonirradiated area of the mirror. Since sample heater No. 1 was used, the deposit is heavier than it would have been with the more opened-mouth sample heater No. 2 used in later runs. The rate of deposition slowed only slightly after 6 hours. The thickness of the deposit is estimated to be 0.03 to 0.05 μ.

The relative reflectivity of the test mirror after the chill-plate had been heated is shown in Figure 11. The portion of the curve from 0.5 to 2.5 μ was measured after the mirror was removed from the thermal-vacuum chamber. The lower relative reflectivity on the nonirradiated area of the mirror correlates with the visual examination (see Figure 5).

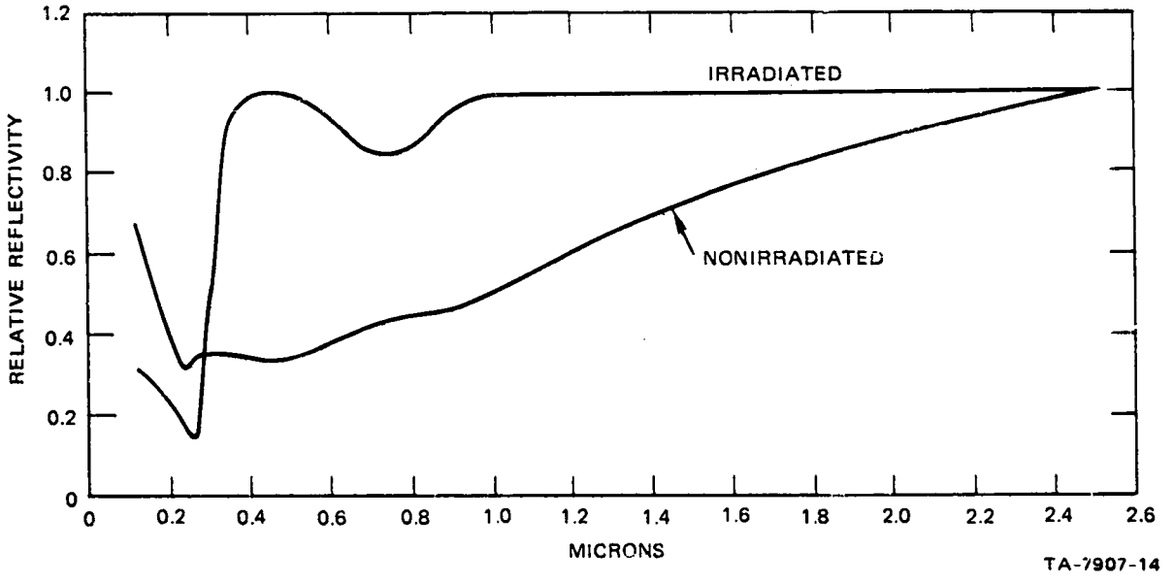

FIGURE 11 REFLECTIVITY OF A MIRROR CONTAMINATED WITH OUTGASES FROM INSULATED WIRE TRT-24-19-V-93 (AFTER HEATING CHILL-PLATE)

The mass spectrum of the outgases from this material is presented in Figure 12. The mass spectrum of the outgases from this material and that of Thermofit RNF-100 are very similar. It is suspected that the insulation of this wire is also a polyolefin and that it is the polyolefin degradation products that appear in the mass spectrum.

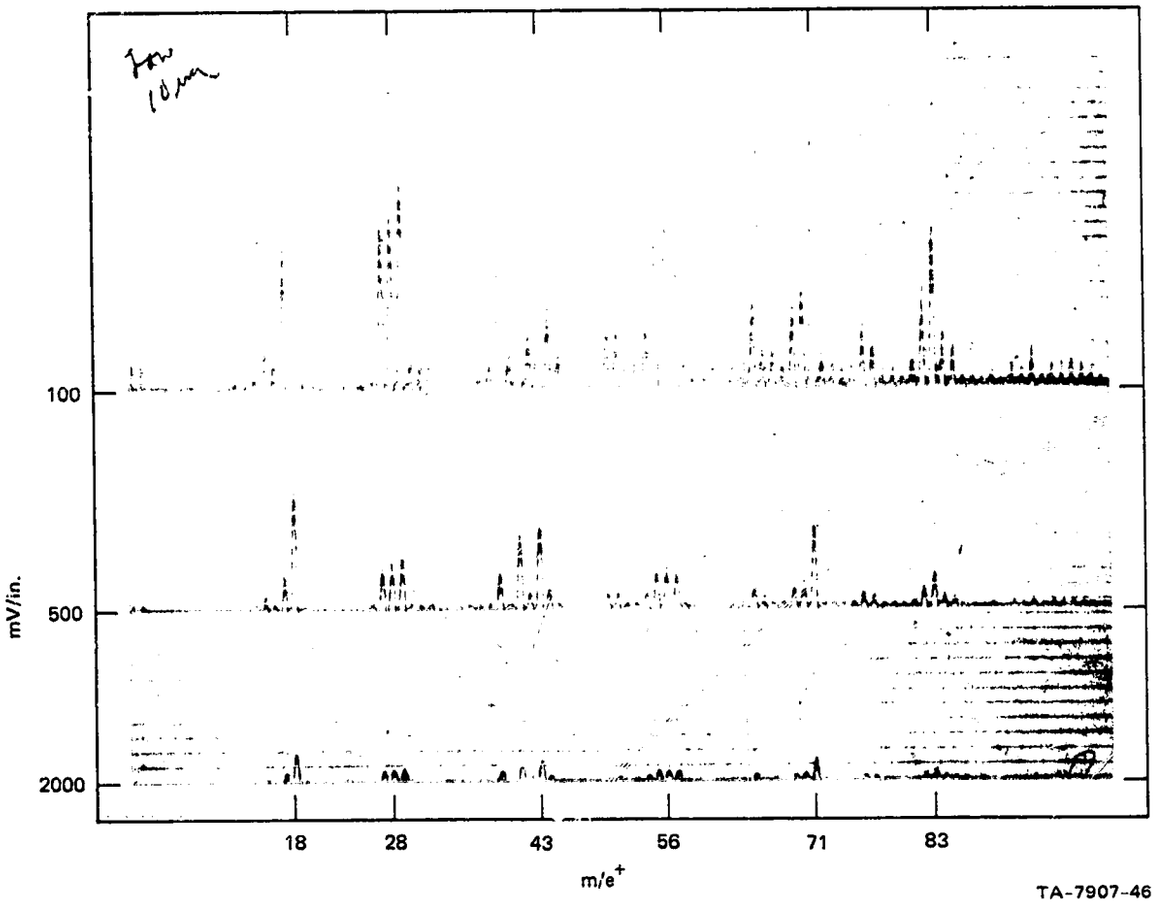

FIGURE 12 QUADRUPOLE MASS SPECTRUM FOR OUTGASES FROM INSULATED WIRE TRT-24-19-V-93 (SAMPLE HEATER ON)

Eccofoam FS

Approximately 1 g of sample was used for this 20-hour thermal-vacuum treatment of Eccofoam FS. The sample was prepared by cutting 1/4 x 1-1/2-inch pieces of Eccofoam FS from a preformed 1/8-inch sheet. Sample heater No. 1 was used for this test.

The rate of deposition on the test mirror was very high during the first two hours of the run. After that it slowed appreciably and was decreasing slightly at the end of the run. The deposit on the mirror was still accumulating at the end of 20 hours and was slightly heavier on the nonirradiated area of the test mirror. The nonirradiated deposit dissolved in acetone, leaving a residual deposit on the irradiated area. This remaining deposit was slightly soluble in benzene. The difference between these deposits indicates that polymerization took place in the irradiated deposit. Its thickness is estimated to be 0.1 to 0.3 μ. Because sample heater No. 1 was used in the run, the deposit was abnormally high in comparison with other materials tested with the more open mouthed sample heater No. 2.

The lower relative reflectivity of the nonirradiated area of the test mirror after heating the chill-plate (see Figure 13) corresponds to the visual observation. The relative reflectivity values from 0.5 to 2.5 μ were measured after taking the mirror from the thermal-vacuum chamber.

Figure 14 presents the mass spectrum of the outgases from Eccofoam FS. Although several significant peaks are present other than the usual water and low molecular peaks, not enough information is present to identify any specific material in the mass spectrum. Eccofoam FS is a preformed polyurethane foam.

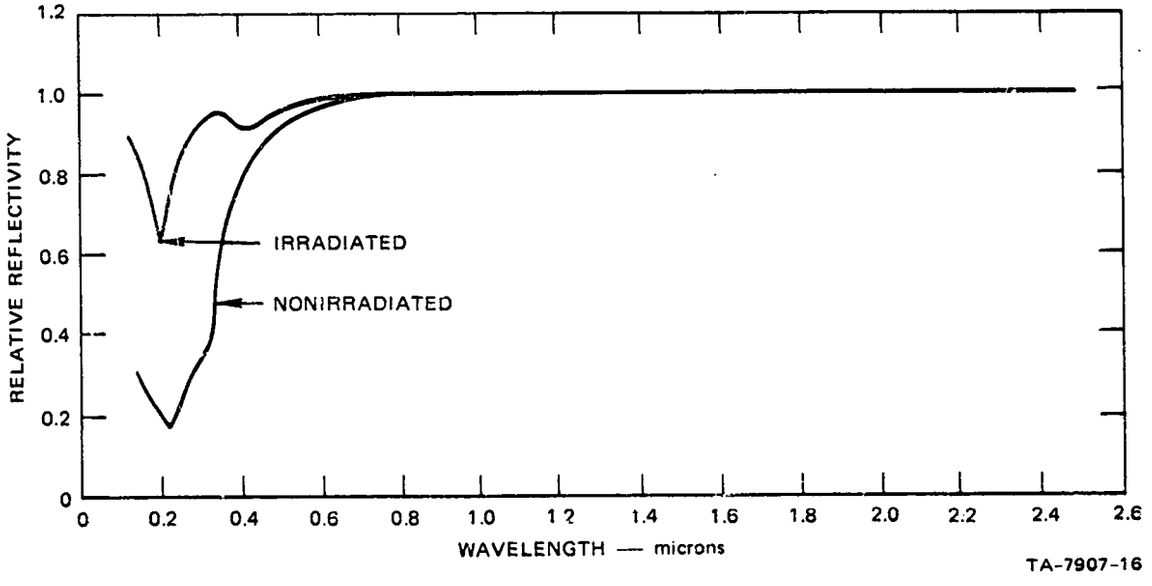

FIGURE 13 REFLECTIVITY OF A MIRROR CONTAMINATED WITH OUTGASES FROM ECCOFOAM FS (AFTER HEATING CHILL-PLATE)

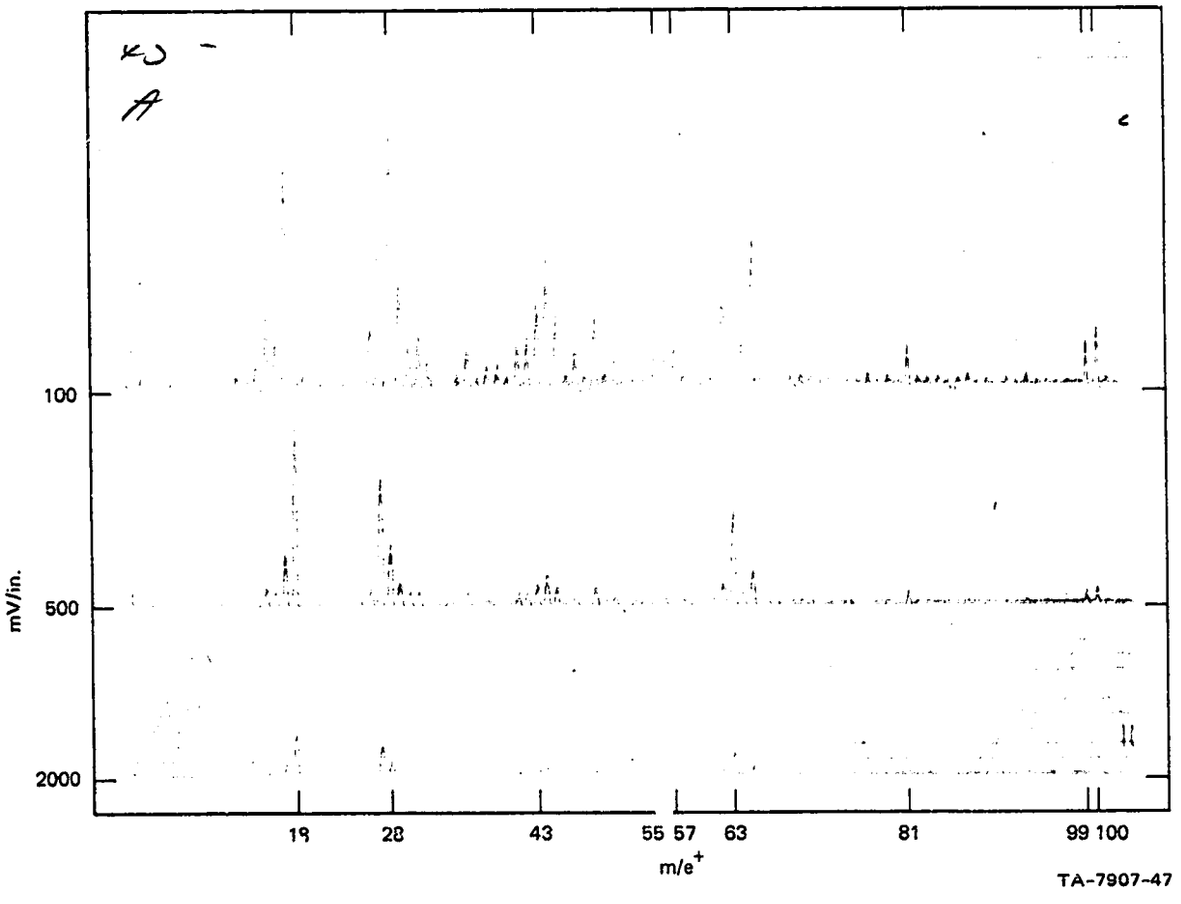

FIGURE 14 QUADRUPOLE MASS SPECTRUM FOR OUTGASES FROM ECCOFOAM FS (SAMPLE HEATER ON)

Moxness MS60 S08

For this and several subsequent tests, sample heater No. 2 was used. The mouth of the new sample heater was 1 inch in diameter. The more highly focused sample heater No. 1 had a mouth opening of only 5/16 inch.

The 1-g sample was prepared by cutting 1/32 x 3/4-inch strips from a 1/8-inch-thick sheet of the material. The sample was placed in the new sample heater and subjected to a 5-hour thermal-vacuum treatment.

The rate of increase of deposition continued at a fairly constant rate throughout the run, tapering off slightly after 2 hours. Visual inspection of the mirror indicated a heavier deposit on the irradiated area of the mirror. The thickness of the deposit was in the range of 0.03 to 0.05 μ.

The relative reflectivity of the irradiated area after heating the chill-plate was lower than that on the nonirradiated area (as shown in Figure 15). This correlates with visual observation of a heavier deposit on the irradiated area. The measurements between 0.5 and 2.5 μ were made after removal of the mirror from the thermal-vacuum chamber. Relative reflectivity values greater than 1 were obtained. It was observed that the mirror surface was so thin as to transmit light in the visible region. The addition of the thin film from depositing outgases apparently cut the loss of light and increased the reflectivity of the mirror. In subsequent runs, the thickness of the aluminum mirror surface was increased to 2000 Å from the original 1000 Å.

The quadrupole mass spectrum for the sample outgases consisted of only low-molecular-weight peaks, with water being the major constituent.

Raychem Wire 44/0411

The 1-g sample was prepared by cutting the wire into 3/4-inch lengths. This material was subjected to a 19-hour thermal-vacuum treatment.

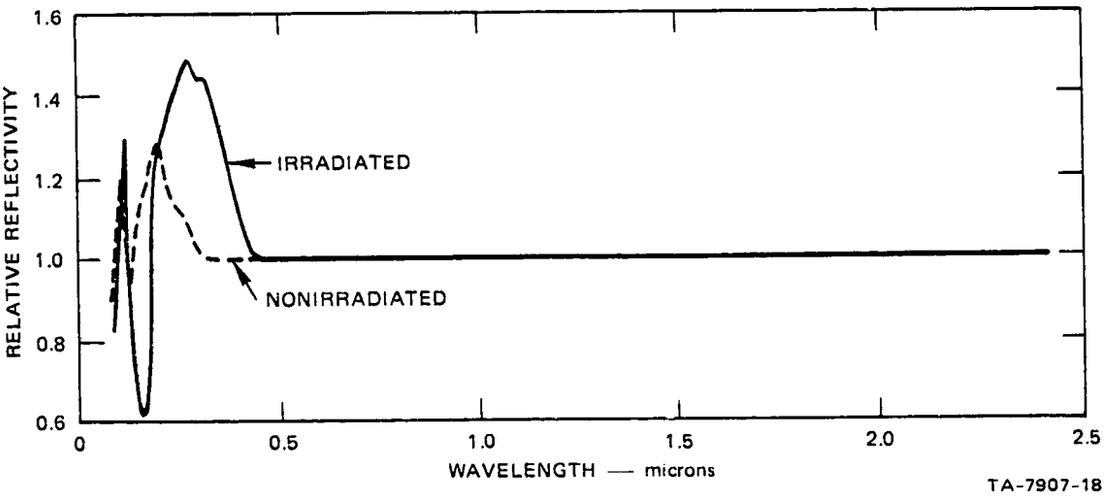

FIGURE 15 REFLECTIVITY OF A MIRROR CONTAMINATED WITH OUTGASES FROM MOXNESS MATERIAL MS 60 S08 (AFTER HEATING CHILL-PLATE)

The rate of deposition increased fairly rapidly over the first hour of the run. It then decreased and became constant after the first hour. The weight of the deposit increased only slightly from after the first hour. The thickness of the deposit is estimated to be 0.01 to 0.03 μ. The light deposit is spread fairly evenly on both areas of the mirror.

Figure 16 shows the relative reflectivity of the irradiated area of the test mirror to be lower than the nonirradiated area.

Except for water, no significant peaks were noted in the quadrupole mass spectrum of the outgases from this sample.

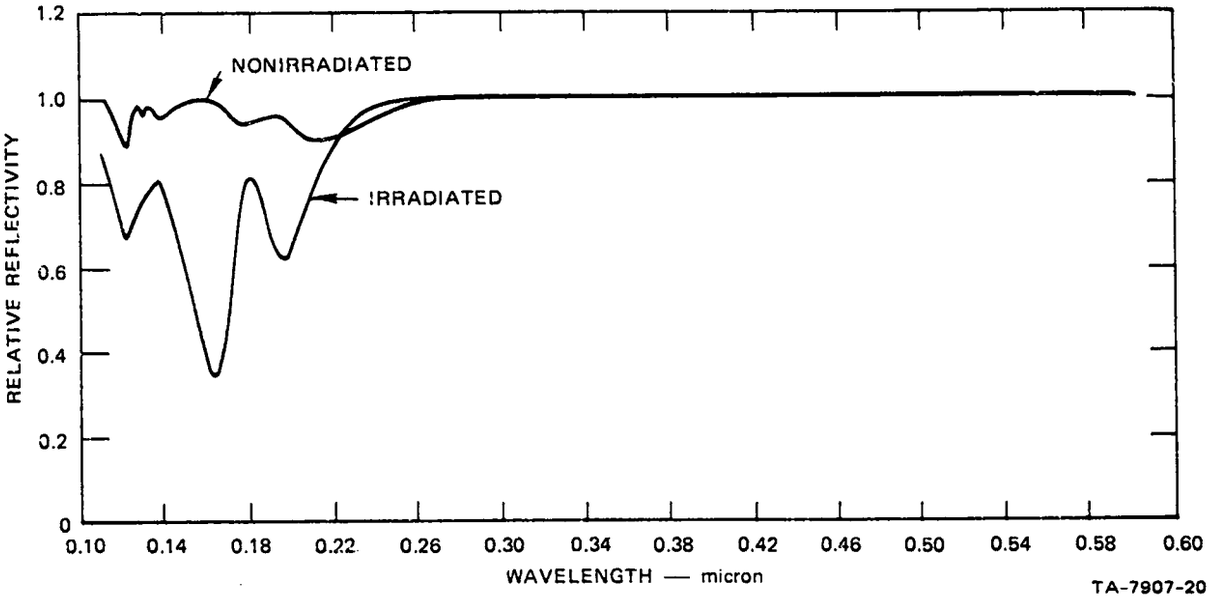

FIGURE 16 REFLECTIVITY OF A MIRROR CONTAMINATED WITH OUTGASES FROM RAYCHEM WIRE 44/0411 (AFTER HEATING CHILL-PLATE)

Polyimide Tape X1156

The following is a summary of the data collected in two tests of polyimide tape X1156. The sample was prepared by cutting the tape into 3-inch lengths and then doubling the tape and sticking it to itself. Both tests used 1-g samples.

Very little deposit was observed on the test mirror after removal from the thermal-vacuum chamber. The deposit was less than 0.01 μ thick. The outgases deposited quickly during the first 24 hours of the second test; after that the rate of deposition slowed. At the end of 96 hours, the sample continued to outgas, but deposit on the mirror accumulated very slowly (see Table III).

The relative reflectivity of the test mirror is shown in Figures 17 through 20. The reflectivity in Figure 20, although not complete because of equipment failure, indicates improved reflectivity after the chill-plate was heated. Data from a previous test after heating the chill-plate show the relative reflectivity to be 1.0 on the nonirradiated area and below 1.0 on the irradiated area only at wavelengths lower than 0.2 μ. The relative reflectivity measurements were made in situ.

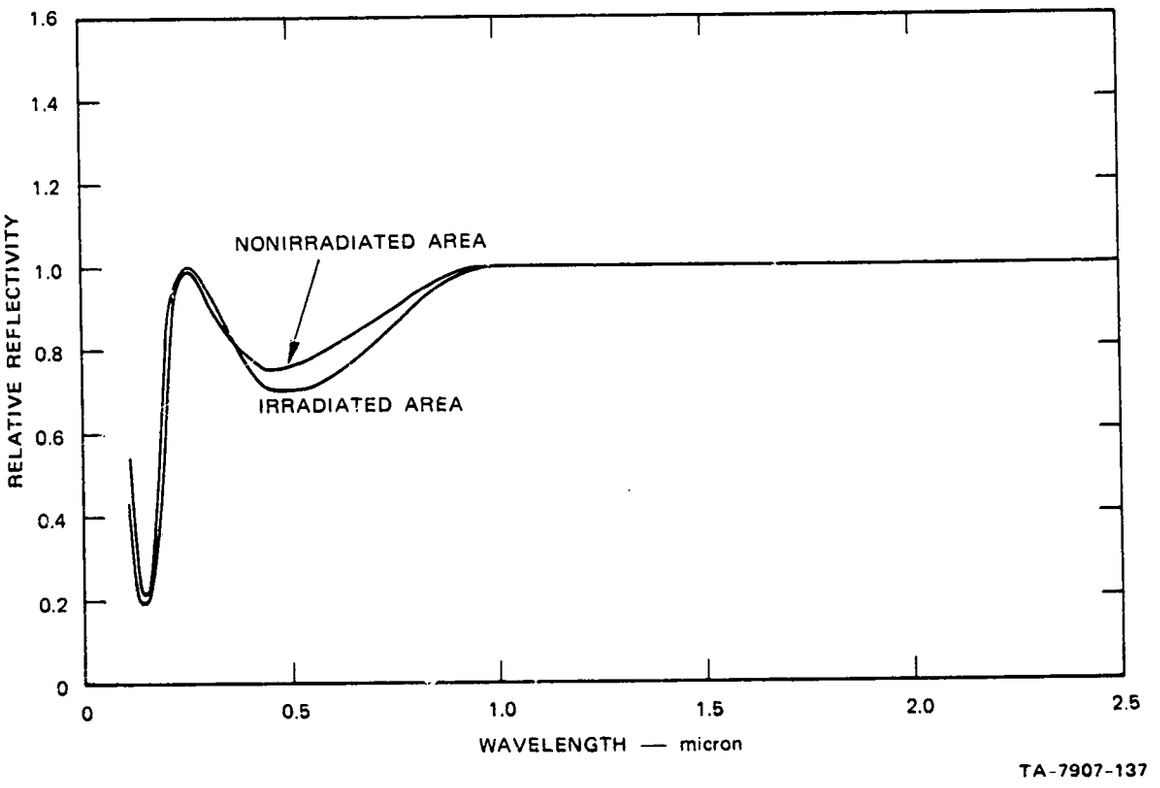

FIGURE 17 REFLECTIVITY OF A MIRROR CONTAMINATED WITH OUTGASES FROM 3M POLYIMIDE TAPE X1156 (AFTER 5 HOURS)

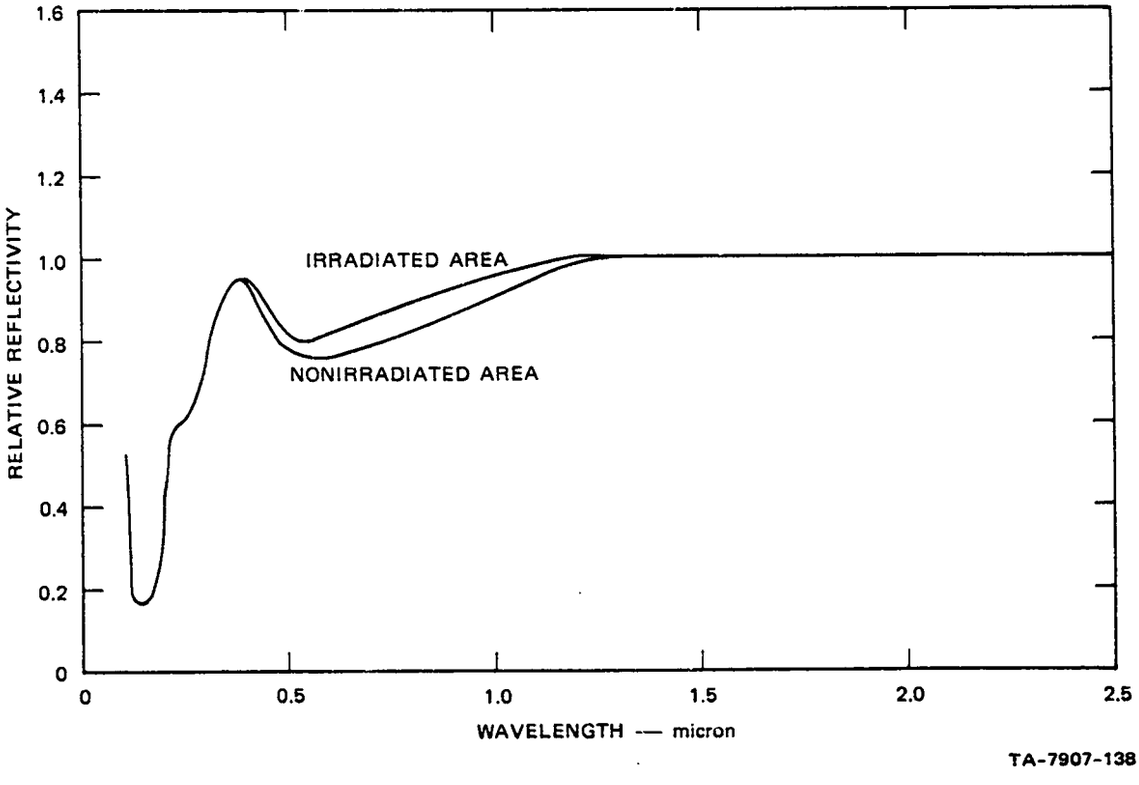

FIGURE 18 REFLECTIVITY OF A MIRROR CONTAMINATED WITH OUTGASES FROM 3M POLYIMIDE TAPE X1156 (AFTER 24 HOURS)

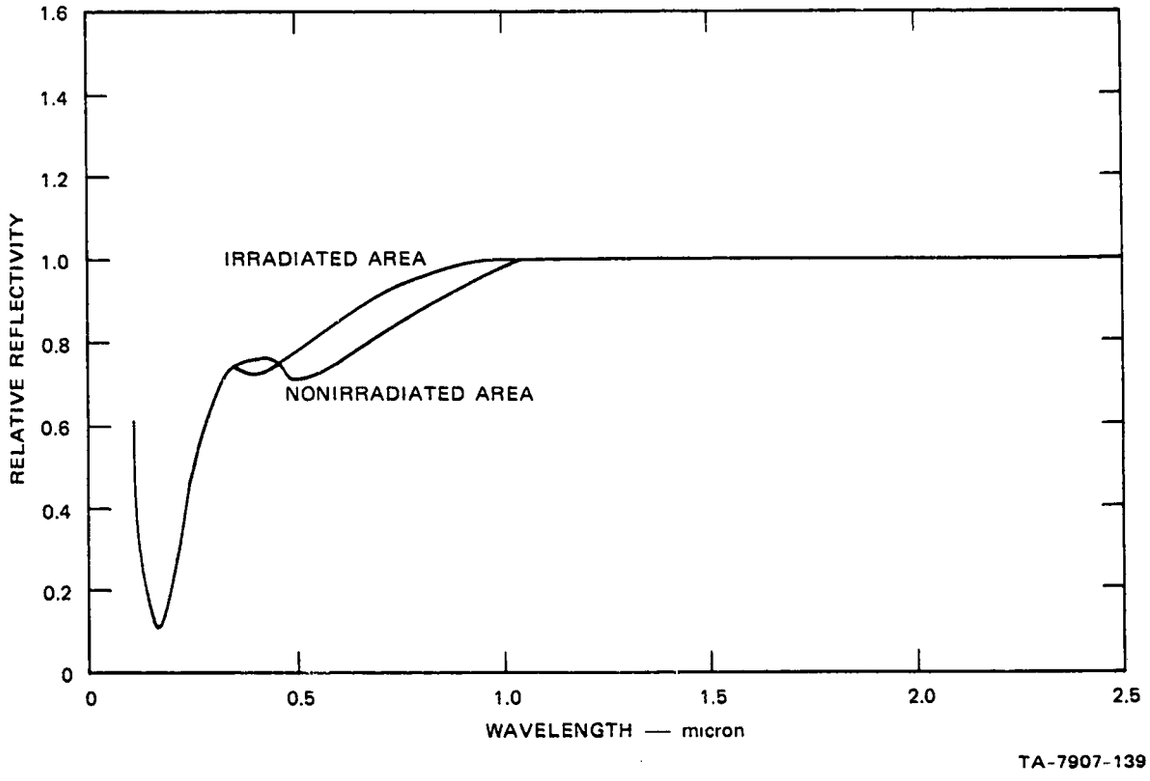

FIGURE 19 REFLECTIVITY OF A MIRROR CONTAMINATED WITH OUTGASES FROM 3M POLYIMIDE TAPE X1156 (AFTER 96 HOURS)

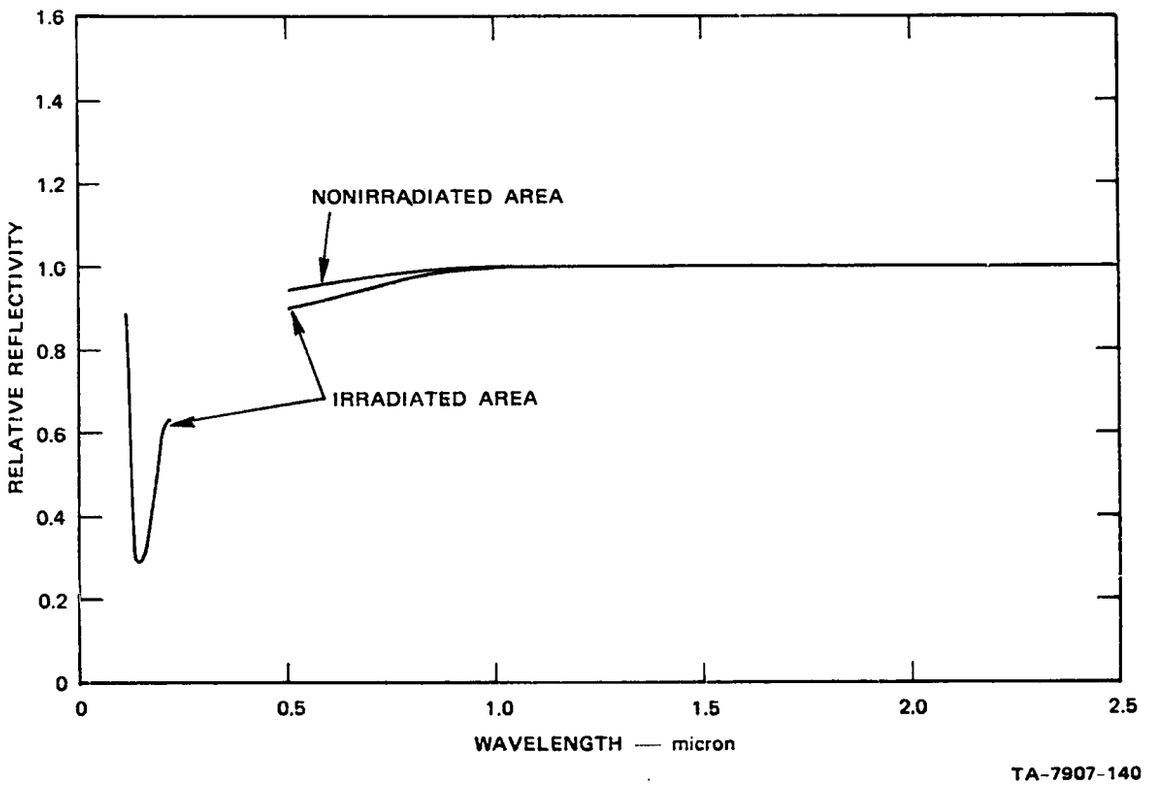

FIGURE 20 REFLECTIVITY OF A MIRROR CONTAMINATED WITH OUTGASES FROM 3M POLYIMIDE TAPE X1156 (AFTER HEATING CHILL-PLATE)

In both tests the mass spectra of the outgases from this material indicated that water was the only significant outgas. Polyimide tape X1156 is a thermosetting pressure-sensitive silicone adhesive on a polyimide film.

Insulgrease G-640

A 1-g portion of this material was smeared on the inside of an aluminum boat and placed in sample heater No. 2. It was then exposed to a 22-hour thermal-vacuum treatment.

The deposit on the test mirror was light, about 0.01 to 0.03 μ thick. It was only very slightly heavier on the irradiated area of the mirror. The deposit accumulated rapidly over the first 5 hours then slowed and was gaining very little weight by the end of the run.

The relative reflectivity measurements presented in Figure 21 show the irradiated area of the test mirror to be slightly less reflective than the nonirradiated. This would be expected from visual observation of the mirror.

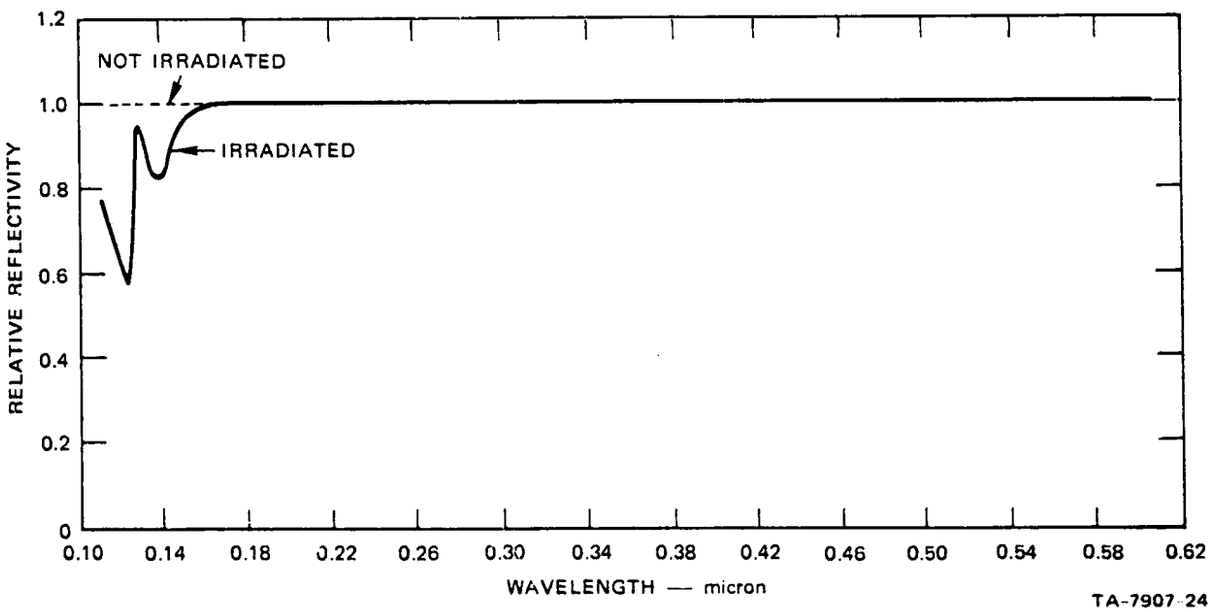

FIGURE 21 REFLECTIVITY OF A MIRROR CONTAMINATED WITH OUTGASES FROM INSULGREASE G-640 (AFTER HEATING CHILL-PLATE)

The quadrupole mass spectrum of the outgases of Insulgrease G-640 showed water to be the only significant component. Insulgrease G-640 is a high thermal conductivity grease-like silicone compound.

Dow Corning High Vacuum Silicone Grease

A 1-g sample of this material was smeared on the inside of an aluminum boat and placed in the sample heater. The sample was then exposed to a 16-hour thermal-vacuum treatment.

Almost immediately after the beginning of the run, the deposition rate began to slow, and the material deposited very slowly by the end of the run. The deposit was very light (< 0.01 μ thick) with the irradiated area being only very slightly heavier.

The relative reflectivity of the outgases from Dow Corning High Vacuum Grease after heating the chill-plate is presented in Figure 22. The reflectivity of the irradiated area is lower than that of the non-irradiated area.

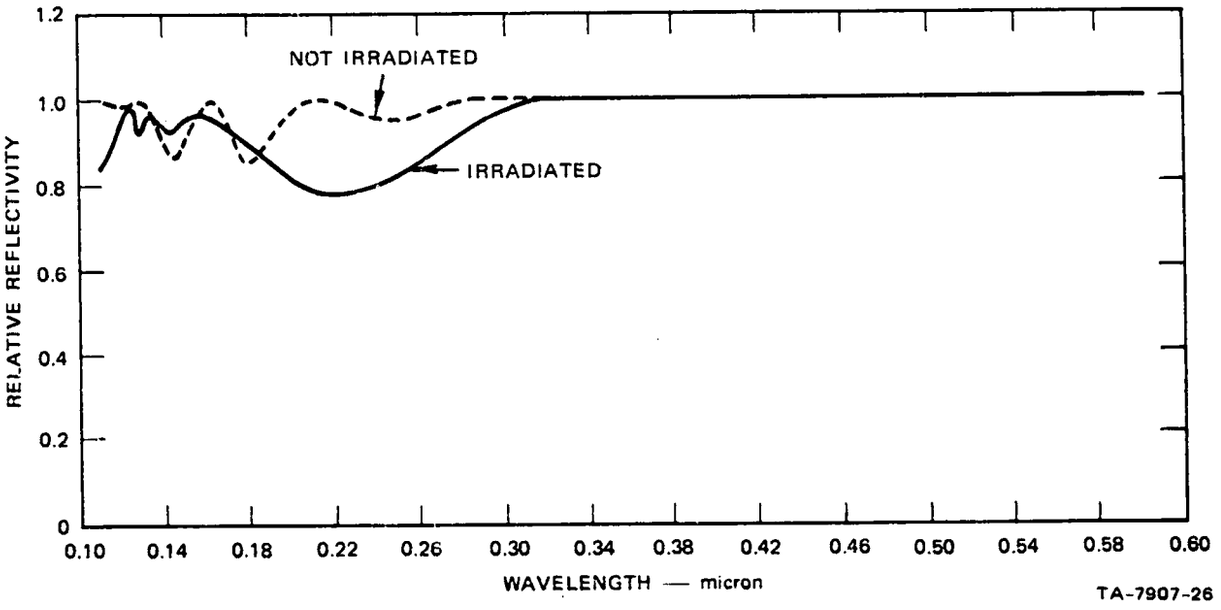

FIGURE 22 REFLECTIVITY OF A MIRROR CONTAMINATED WITH OUTGASES FROM DOW CORNING HIGH VACUUM SILICONE GREASE (AFTER HEATING CHILL-PLATE)

As determined by mass spectrometry, water was the major constituent of the outgases from this material. Dow Corning high vacuum grease is a silicone based lubricant.

Scotch Pressure-Sensitive Tape

Up to this point in the experiments materials were tested for only short periods of time (up to 20 hours), except for materials repeated later. Starting with this test, the time was extended to define more accurately the outgasing characteristics and resulting deposits for the materials.

The sample for this test was prepared by cutting the tape into 2-inch lengths, doubling it over, and sticking it together. The 1-g sample was placed in sample heater No. 2 and subjected to a 96-hour thermal-vacuum treatment.

The rate of deposition was rapid during the first few hours of the run. The deposit on the irradiated area of the mirror continued this rapid increase, but the deposit on the nonirradiated area slowed to an almost steady state. The deposit was very noticeably heavier on the irradiated area (see Table III). The thickness of the deposit was 0.05 μ or less.

The reflectivities of the test mirror at 96 hours and after heating the chill-plate are presented in Figure 23 and 24. The reflectivity of the irradiated area is lower after heating the chill-plate. Relative reflectivity values greater than 1 occur in Figure 24. These abnormally high reflectivities also occurred in subsequent runs. The problem of light leaking through the mirrors was corrected by increasing the thickness of the aluminum mirror surface from 1000 to 2000 Å. Small amounts of light may be lost in the MgF_2 overcoating of the mirror at short wavelengths by destructive interference. Light deposits from some sample

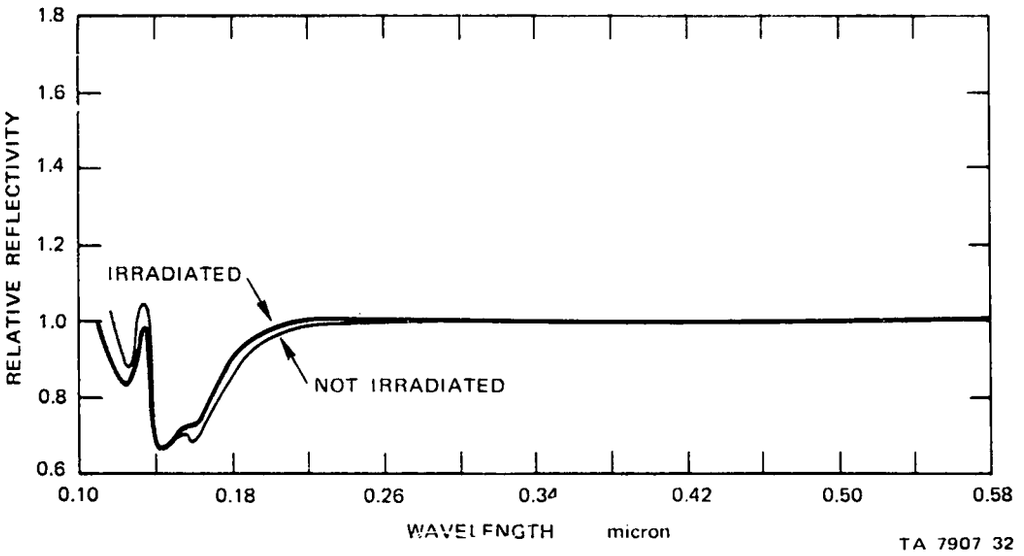

FIGURE 23 REFLECTIVITY OF A MIRROR CONTAMINATED WITH OUTGASES FROM 3M SCOTCH TAPE Y-9050 (AFTER 96 HOURS)

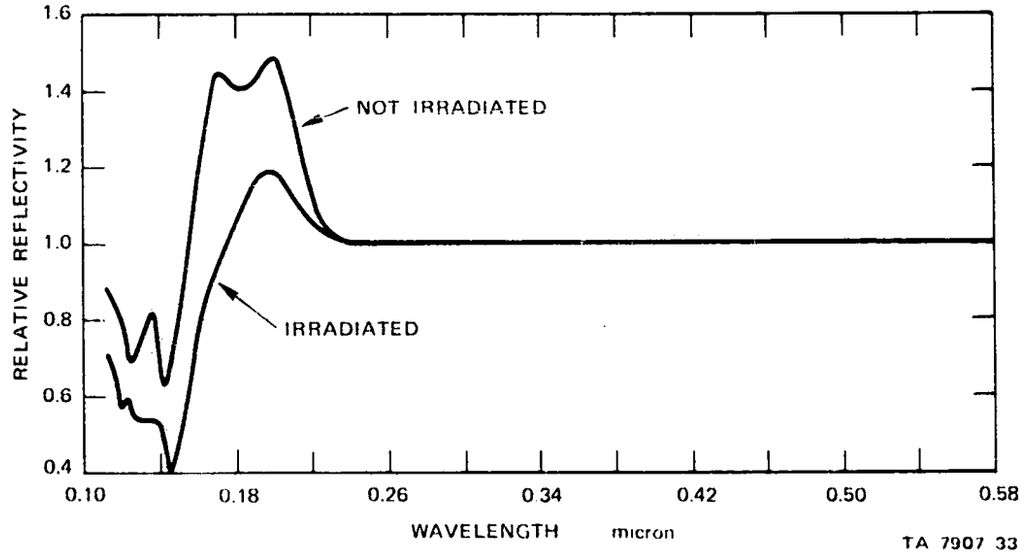

FIGURE 24 REFLECTIVITY OF A MIRROR CONTAMINATED WITH OUTGASES FROM 3M SCOTCH TAPE Y-9050 (AFTER HEATING CHILL-PLATE)

outgases produce a highly reflective surface and make the contaminated mirror more reflective than when it is clean.

These abnormally high reflectivity values are not seen for heavy deposits such as that from Thermofit RNF-100. In some of these cases, the values decrease with time as the deposit becomes heavier. In general, the relative reflectivity of the deposit remains near unity if the product of the extinction coefficient (in meters^{-1}) and the deposit thickness (in meters) is < 0.1 when the wavelength is > 1.0 μ.

The mass spectrum of the outgases from the sample showed water as the only significant component. Scotch tape No. Y-9050 is an aluminum-backed pressure-sensitive tape.

Eccofoam FPH

The following is a summary of data compiled from several tests of Eccofoam FPH. The sample was prepared according to instructions given in Technical Bulletin 6-2-2A from Emerson and Cuming, Inc., and cured at room temperatures. The material was then crushed into a coarse granular form. A 1-g sample was subjected to thermal-vacuum treatment for 96 hours.

In most of these tests no appreciable deposit was noted on the mirror or detected by the microbalances (see Table III). In the first run, however, some deposit was noticed. Since this material is made from a two-component system, it is not surprising that differences in the end product may result from batch to batch. The deposit, if any, was no thicker than 0.01 μ.

Relative reflectivity of a test mirror from a typical test is presented in Figures 25 through 28. No degradation of reflectivity is noted at wavelengths > 1.0 μ. Reflectivities > 1.0 were observed in the very short wavelengths.

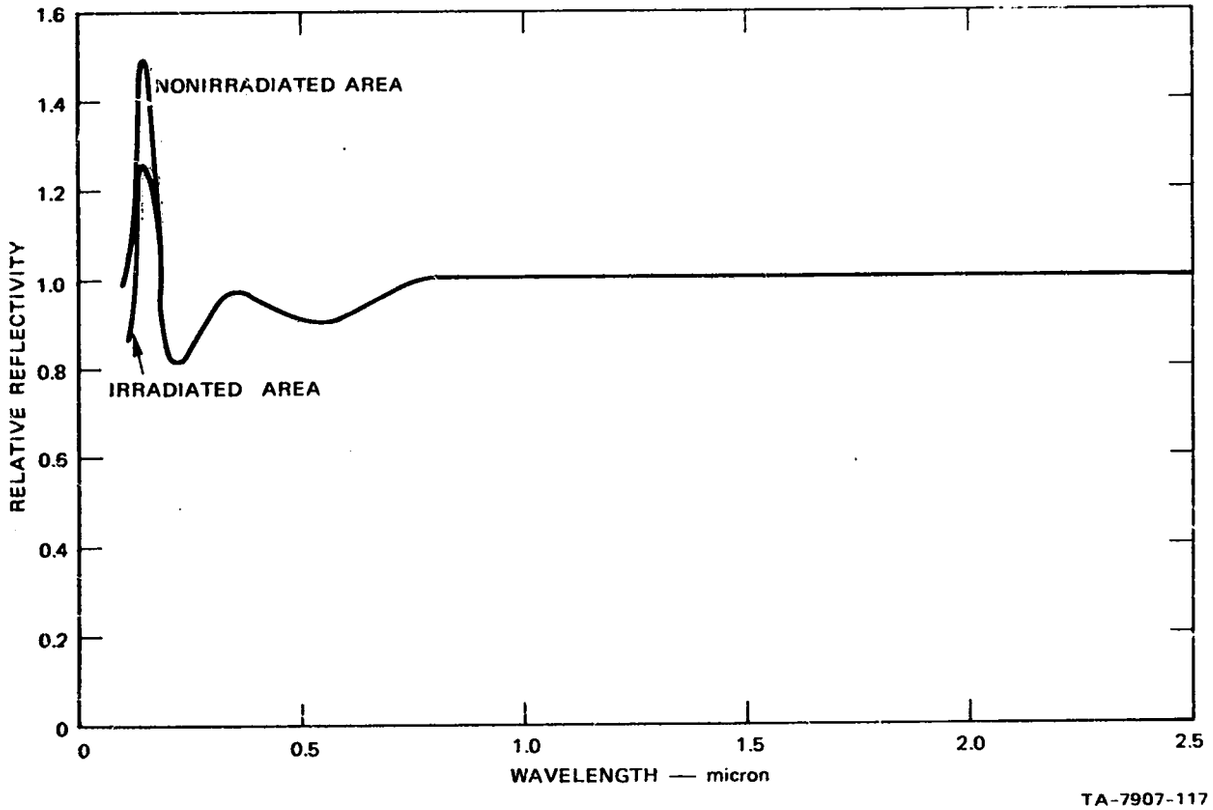

FIGURE 25 REFLECTIVITY OF A MIRROR CONTAMINATED WITH OUTGASES FROM ECCOFOAM FPH (AFTER 5 HOURS)

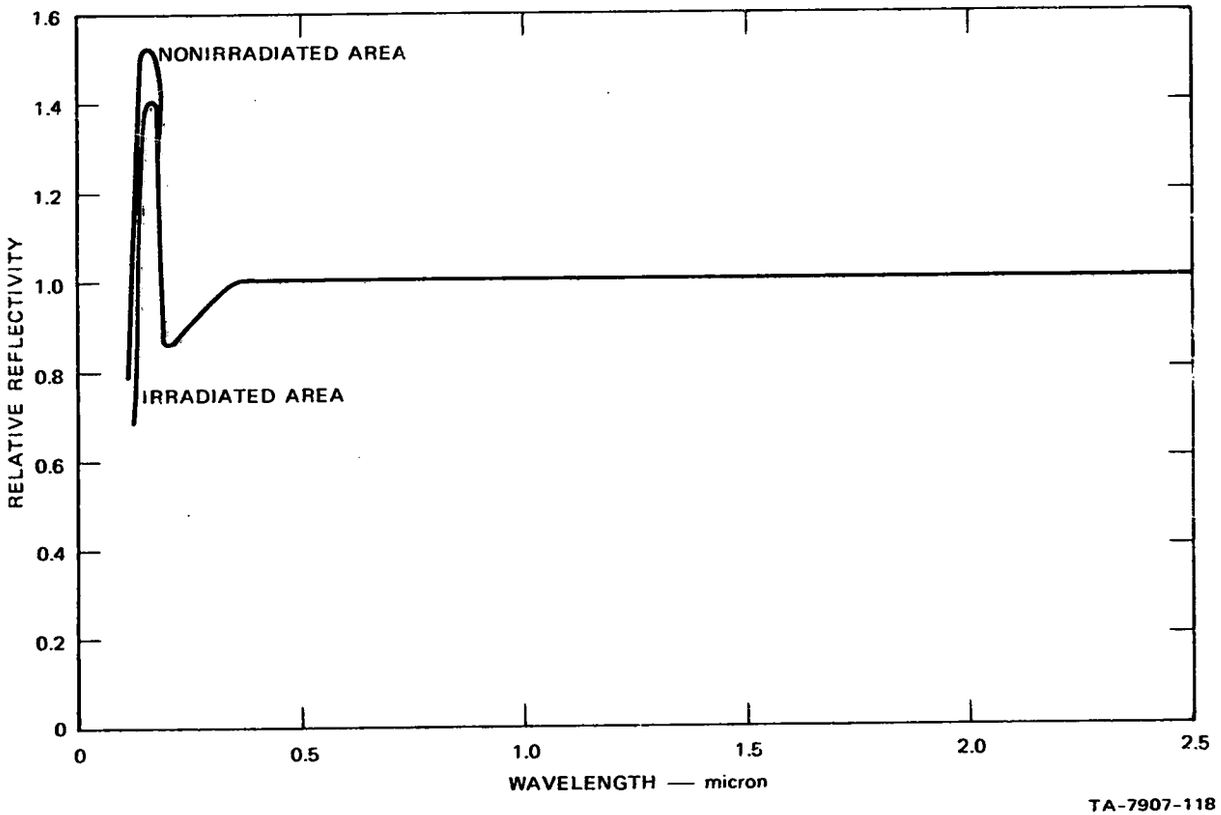

FIGURE 26 REFLECTIVITY OF A MIRROR CONTAMINATED WITH OUTGASES FROM ECCOFOAM FPH (AFTER 24 HOURS)

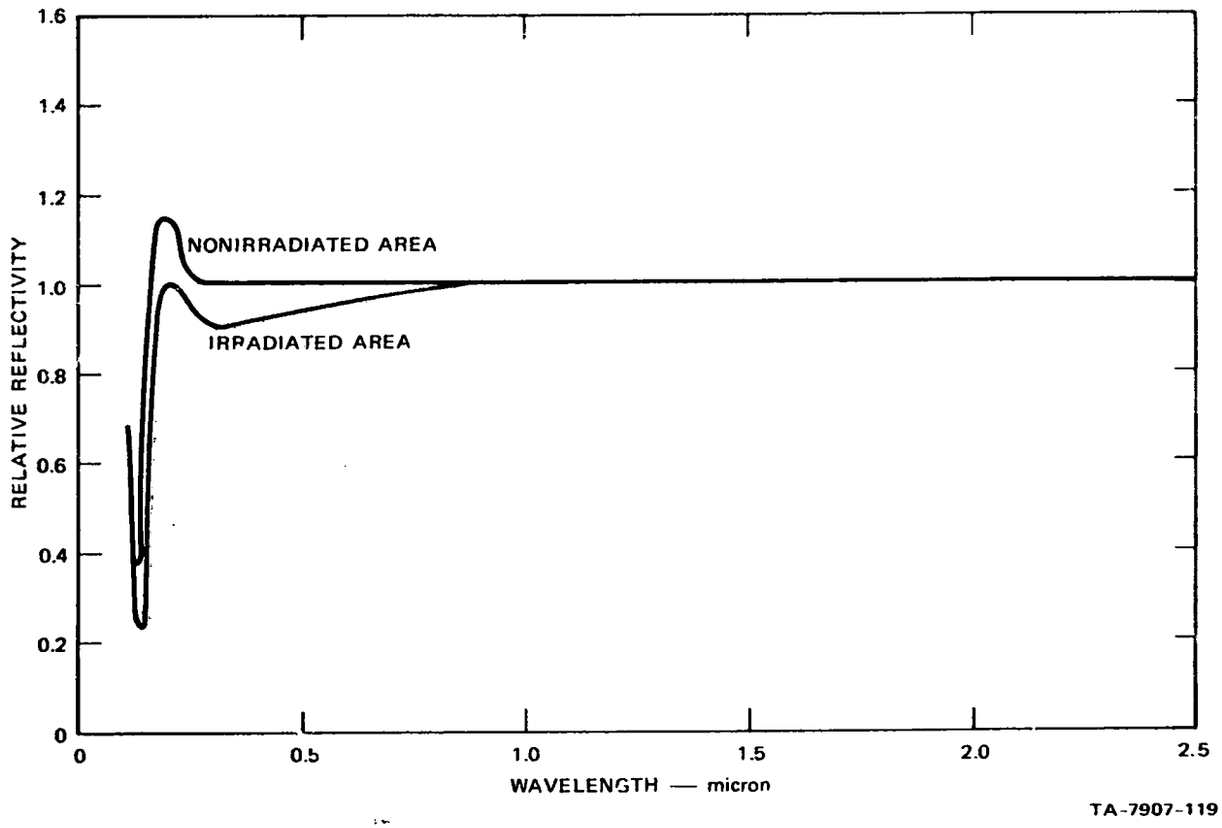

FIGURE 27 REFLECTIVITY OF A MIRROR CONTAMINATED WITH OUTGASES FROM ECCOFOAM FPH (AFTER 96 HOURS)

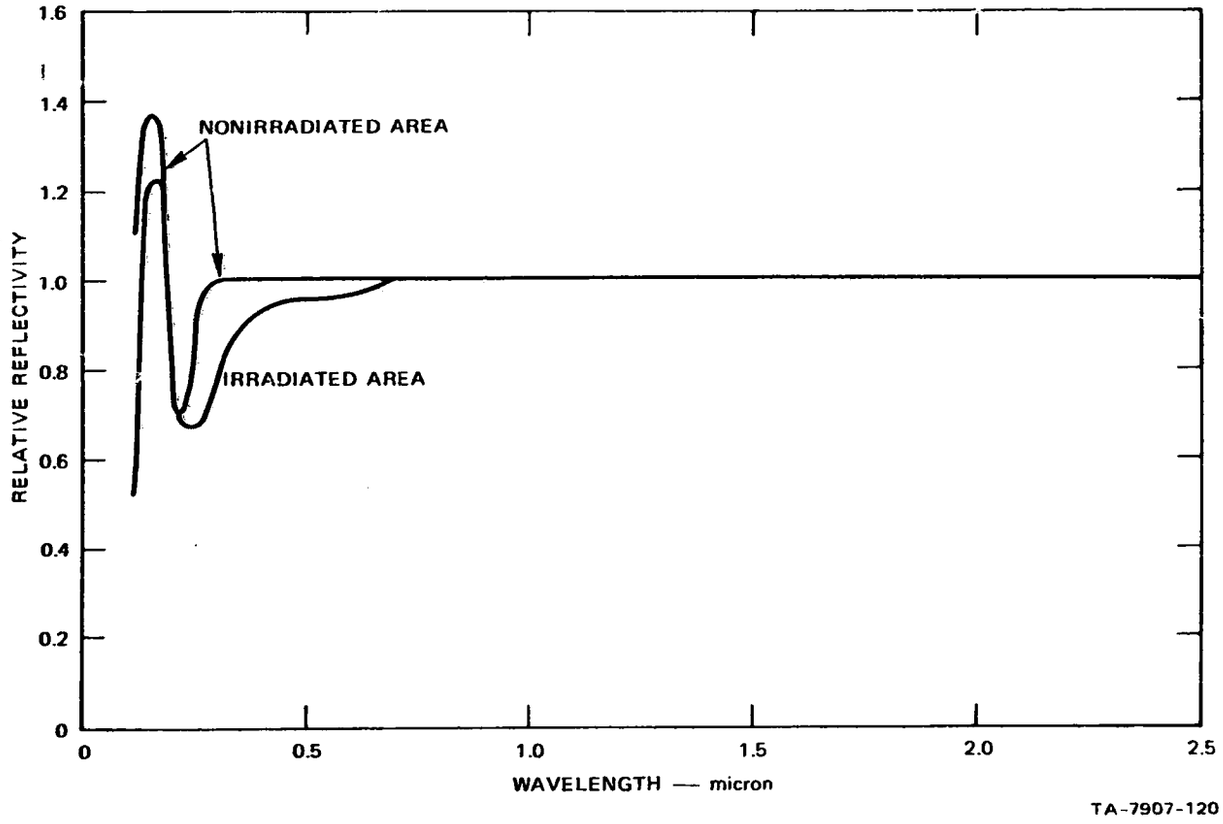

FIGURE 28 REFLECTIVITY OF A MIRROR CONTAMINATED WITH OUTGASES FROM ECCOFOAM FPH (AFTER HEATING CHILL-PLATE)

Figure 29 shows the mass spectra for the outgases of Eccofoam FPH typical of the four runs during this project. Significant peaks occur at m/e^+ of 51, 71, 91, 101, 118, 132, 145, and 174. The major peaks below m/e^+ of 51, namely, 18, 28, and 44, can be attributed to H_2O, N_2, and CO_2, respectively. This polyurethane foam has a toluene diisocyanate base. The m/e^+ peaks at 51, 132, 145, and 174 indicate its presence in the sample outgases.

RTV-41 Liquid Silicone Rubber

The material was prepared following instructions in General Electric Company's Technical Data Book S-35. A 1-g sample in pieces approximately 1 x 25 x 5 mm was exposed to a thermal-vacuum treatment of 138 hours.

Material deposited on the mirror rapidly over the first 20 hours of the run. The deposit reached a maximum weight and gradually declined over the remaining portion of the run (see Table III). The thickness of the deposit was between 0.01 and 0.03 μ, with irradiated area having a slightly heavier deposit.

The reflectivities of the mirror after 133 hours and after heating the chill-plate are presented in Figures 30 and 31, respectively. The reflectivity of the irradiated area is slightly more degraded than the nonirradiated.

Water is the only significant component seen in the mass spectrum of the sample outgases. RTV-41 is a dimethyl silicone rubber. The curing agent used was dibutyl tin dilaurate.

RTV-577 Liquid Silicone Rubber

RTV-577 was prepared following the instructions in General Electric Company's Technical Data Book S-35, using the 0.5% dibutyl tin dilaurate procedure. The material was cut into pieces approximately 3 x 2 x 1 mm. A 1-g sample was subjected to a 96-hour thermal-vacuum test.

REPRODUCIBILITY OF THE ORIGINAL PAGE

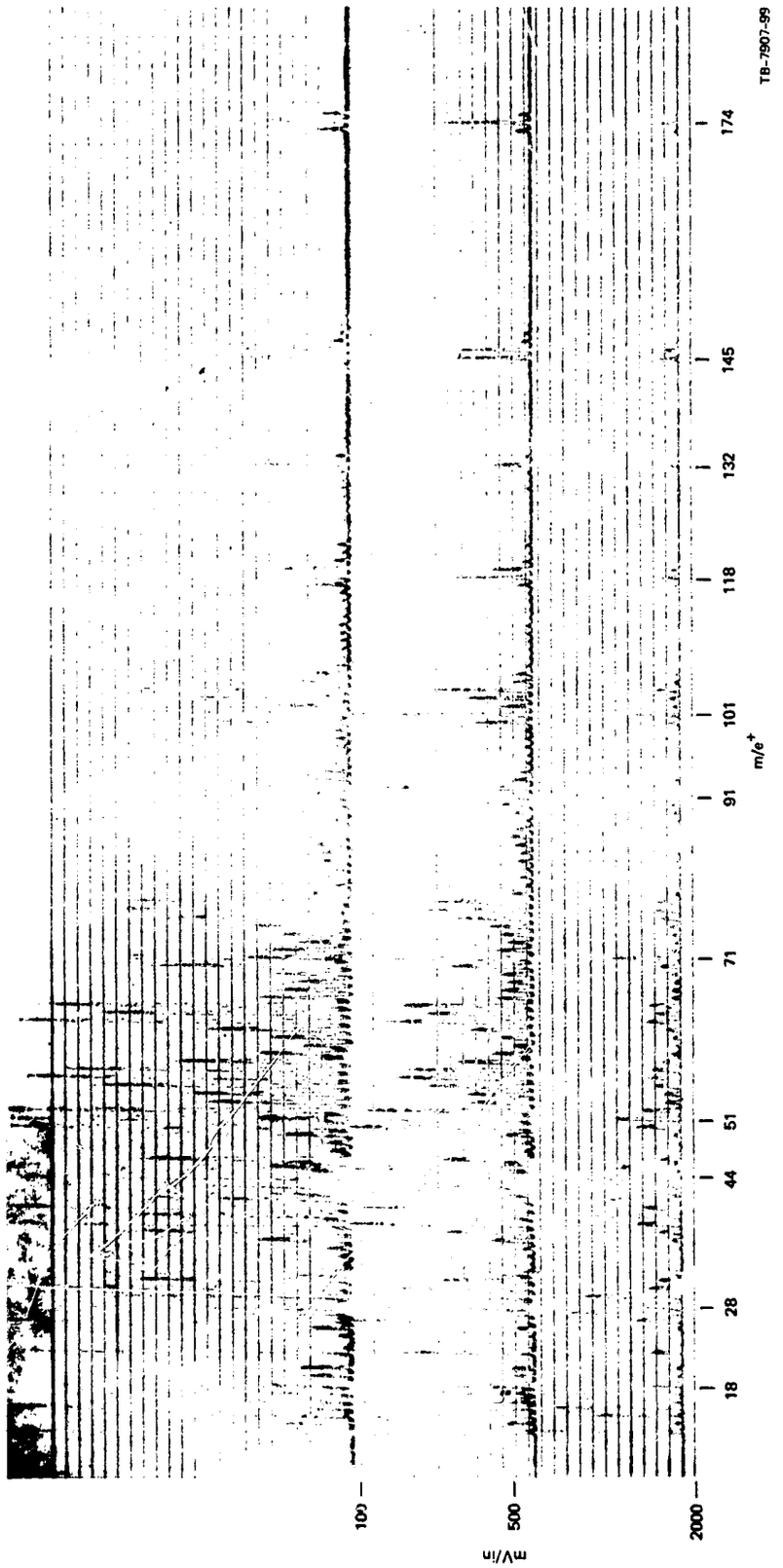

FIGURE 29 MASS SPECTRUM OF ECCOFOAM FPH (SAMPLE HEATER AT 125°C)

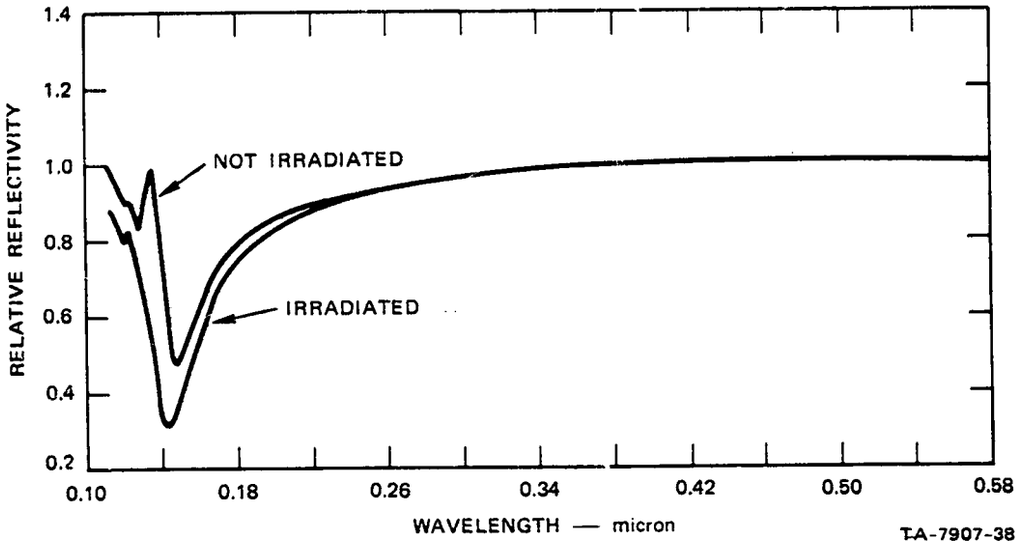

FIGURE 30 REFLECTIVITY OF A MIRROR CONTAMINATED WITH OUTGASES FROM G.E. RTV-41 (AFTER 138 HOURS)

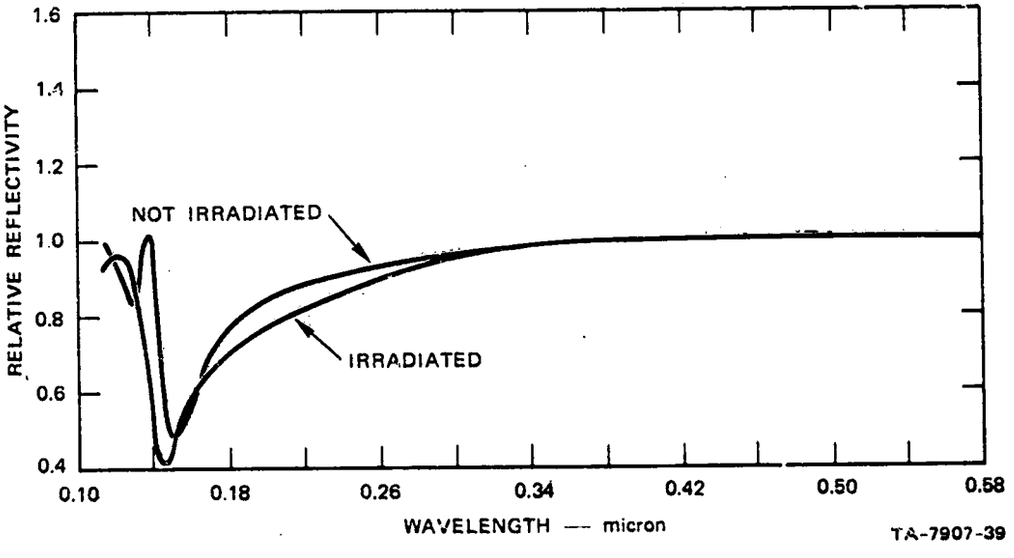

FIGURE 31 REFLECTIVITY OF A MIRROR CONTAMINATED WITH OUTGASES FROM G.E. RTV-41, AFTER CHILL-PLATE WAS HEATED AT 80°C FOR ONE-HALF HOUR

The microbalances indicate a rapid growth of the deposit during the first 10 hours of the run. The rate of deposition then slowed to only a slight increase and remained that way throughout the rest of the run (see Table III). The amount of deposit is heavy; the thickness is about 0.10 to 0.15 μ.

The reflectivity of the test mirror after heating the chill-plate is shown in Figure 32. In Figure 37 of Summary Report No. II, the reflectivity was mistakenly shown as being degraded from 0.5 to 2.5 μ. Reflectivity measurements of the wavelengths from 0.5 to 2.5 μ were made after removal of the mirror from the test chamber.

The quadrupole mass spectrum of the sample outgases indicate water as the only significant component. RTV-577 is a methyl phenyl silicone rubber.

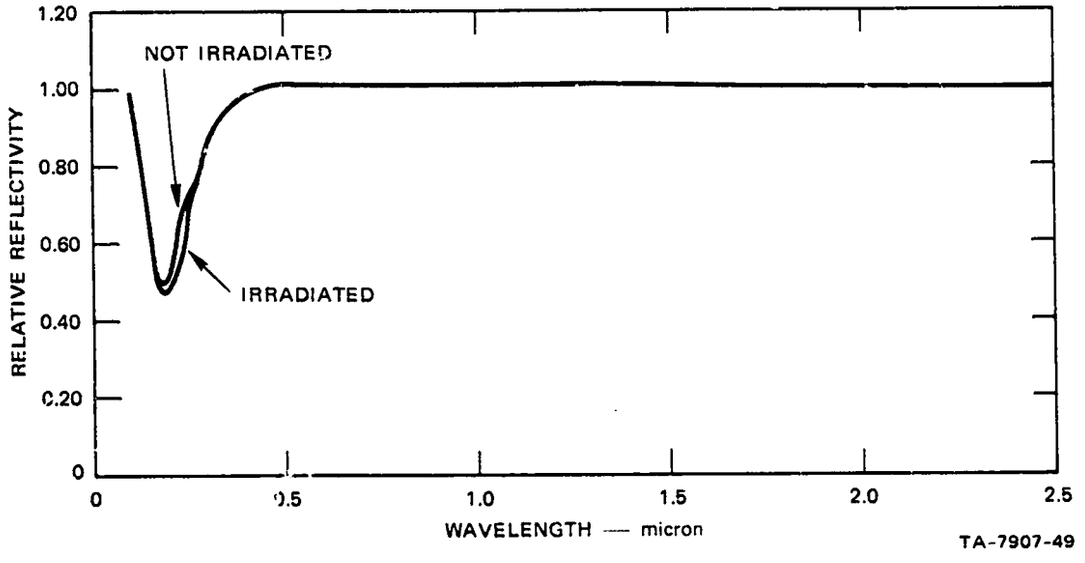

FIGURE 32 REFLECTIVITY OF A MIRROR CONTAMINATED WITH OUTGASES FROM G.E. RTV-577 (AFTER HEATING CHILL-PLATE)

RTV-602 Liquid Silicone Rubber

RTV-602 was prepared according to instructions in General Electric Technical Data Book S-35 for the 0.50% SRC-05 procedure. The material was cut into 2-mm cubes and a 1-g sample take and exposed to a 70-hour thermal-vacuum treatment.

The weight of the deposit increased rapidly for the first 10 hours of the run. The rate of deposit slowed, but continued to gain slowly for 20 more hours. The deposit then began to lose weight until the end of the run (see Table III). The thickness of the deposit after removal from the test chamber was $< 0.01\ \mu$.

Figure 33 presents the relative reflectivity of the test mirror after heating the chill-plate. The reflectivity of the nonirradiated area of the mirror is slightly more degraded than the irradiated. This is supported by a visual inspection of the mirror after its removal from the thermal-vacuum chamber.

The quadrupole mass spectrum showed that water was the only significant component. RTV-602 is a dimethyl silicone rubber. SRC-05 was used as the curing agent.

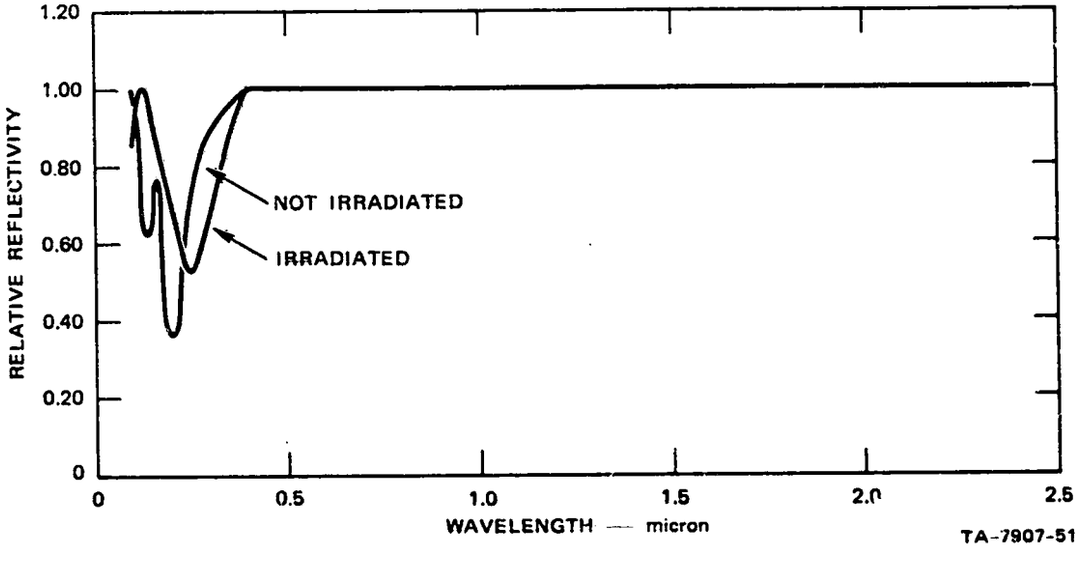

FIGURE 33 REFLECTIVITY OF A MIRROR CONTAMINATED WITH OUTGASES FROM G.E. RTV-602 (AFTER HEATING CHILL-PLATE)

Epon 934 Epoxy Adhesive

Epon 934 was prepared using the label instructions. A 1-g sample of this material, consisting of pieces 10 x 3 x 1 mm, was subjected to a 137-hour thermal-vacuum treatment.

The outgases from the sample deposited rapidly over the first 30 hours of the run. Deposit then remained constant during the rest of the run (see Table III). The deposit was light, about 0.01 to 0.03 μ thick.

Figure 34 shows the relative reflectivity of the test mirror after heating the chill-plate. The irradiated area of the mirror is less reflective than the nonirradiated. This is confirmed by visual observation of the mirror after its removal from the test chamber.

The quadrupole mass spectrum for the outgases from this material show no significant components except water. Epon 934 is an epoxy-based adhesive. Its curing agent was an organic amine.

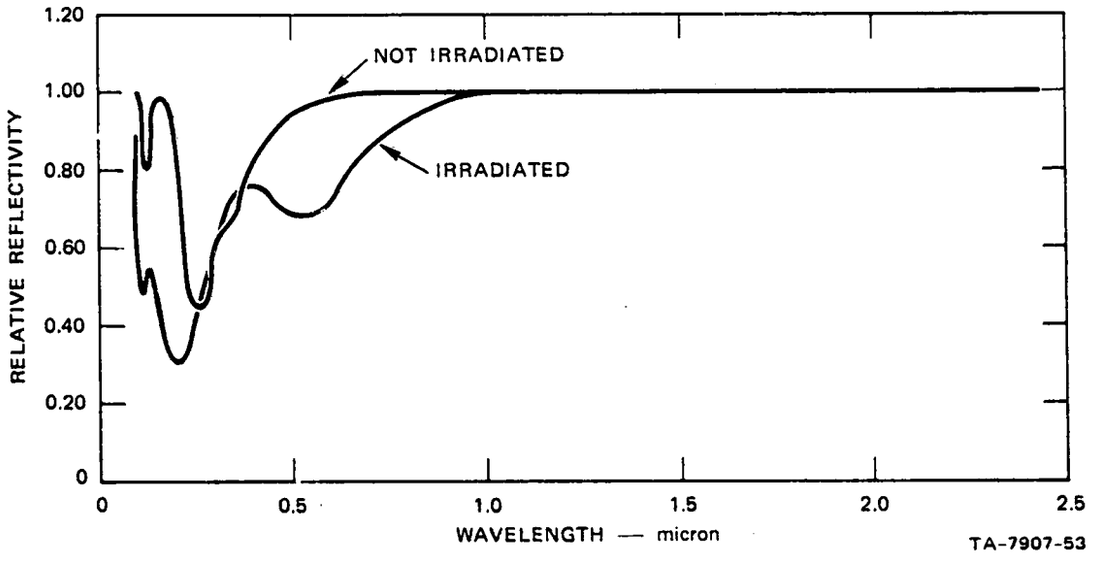

FIGURE 34 REFLECTIVITY OF A MIRROR CONTAMINATED WITH OUTGASES FROM SHELL EPON 934 (AFTER HEATING CHILL-PLATE)

Stycast 1090 Epoxy Foam

Stycast 1090 was tested several times, and this section summarizes the results of these tests. The material was prepared according to label instructions, using catalyst No. 9. The 1-g sample in pieces 2 x 1 x 0.5 mm was exposed to a 96-hour thermal-vacuum treatment.

Outgases from the sample deposited rapidly for the first few hours, then the microbalances recorded a gradual loss of deposit throughout the remainder of the run (see Table III). The thickness of the deposit is estimated to be about 0.05 to 0.08 μ after removal from the test chamber.

Relative reflectivity curves are shown in Figures 35 through 38. Both areas of the mirror are about equally degraded up to the heating of the chill-plate. After heating the chill-plate there is a marked improvement in the reflectivity of the nonirradiated area (see Figure 38). Visual inspection of the mirror after its removal from the test chamber confirmed this.

The presence of several epoxy resin pyrolysis products is indicated in the mass spectrum of the outgases in Figure 39. Significant groups of peaks occur at m/e^+ of 79, 91, 107, 119, 135, 164, and 191. Those peaks at m/e^+ of 79, 91, 107, and 135 are possibly benzene, toluene, cresols, and isopropylphenol and/or isopropenylphenol, respectively.

Epon 828 Epoxy Adhesive

Epon 828 was prepared using 50 parts Versamid 125 catalyst and 100 parts Epon 828 resin. A 1-g sample was taken from the crushed material, and exposed to a 217-hour thermal-vacuum treatment.

The deposit from the outgases of the sample accumulated rapidly during the first 20 hours of the run and then was gradually lost during the remainder of the run. The deposit was about 0.01 to 0.03 μ thick. It was the heaviest on the irradiated area of the test mirror.

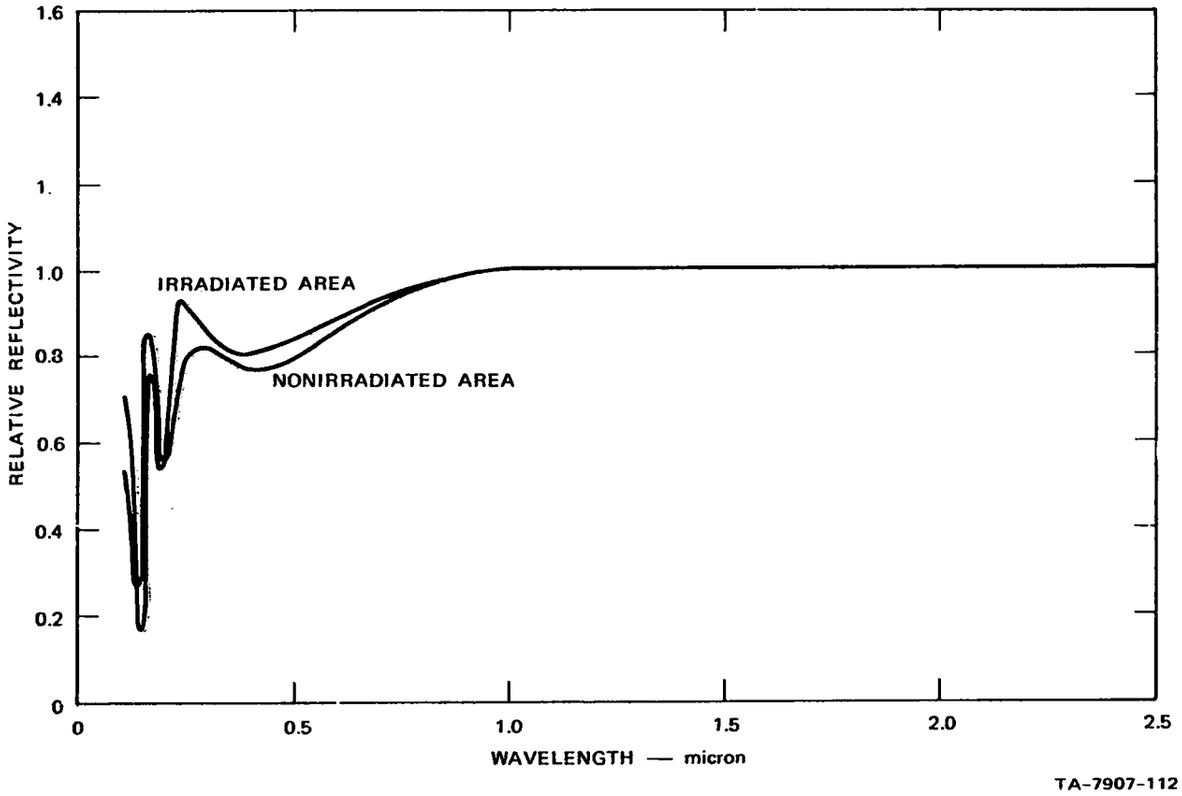

FIGURE 35 REFLECTIVITY OF A MIRROR CONTAMINATED WITH OUTGASES FROM STYCAST 1090 (AFTER 5 HOURS)

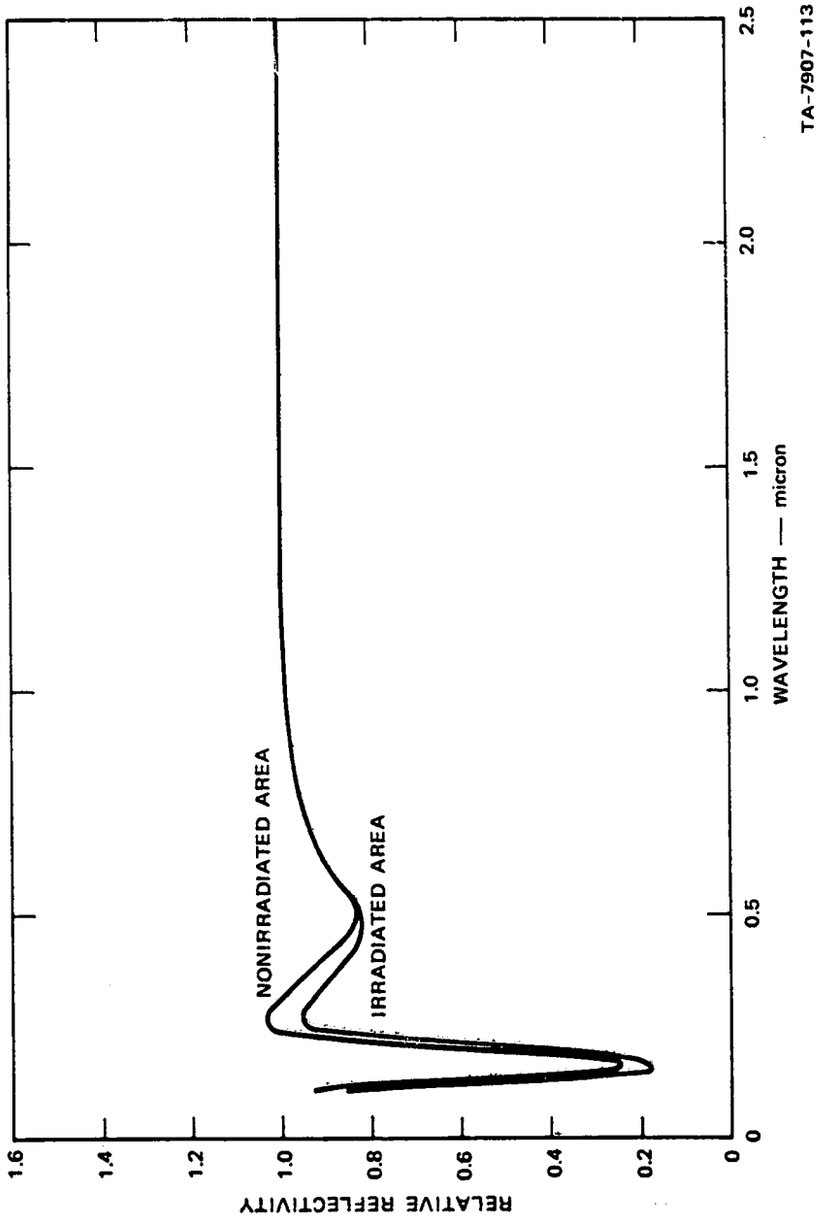

FIGURE 36 REFLECTIVITY OF A MIRROR CONTAMINATED WITH OUTGASES FROM STYCAST 1090 (AFTER 24 HOURS)

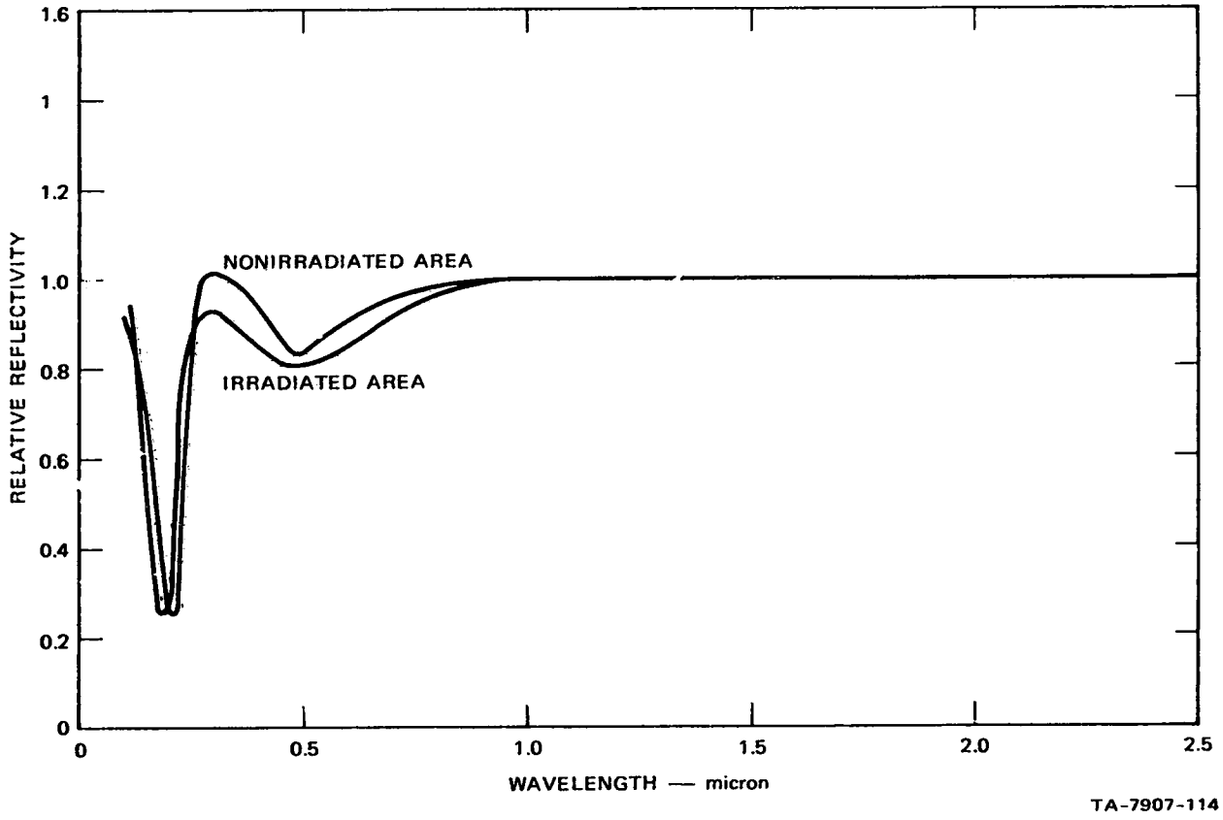

FIGURE 37 REFLECTIVITY OF A MIRROR CONTAMINATED WITH OUTGASES FROM STYCAST 1090 (AFTER 96 HOURS)

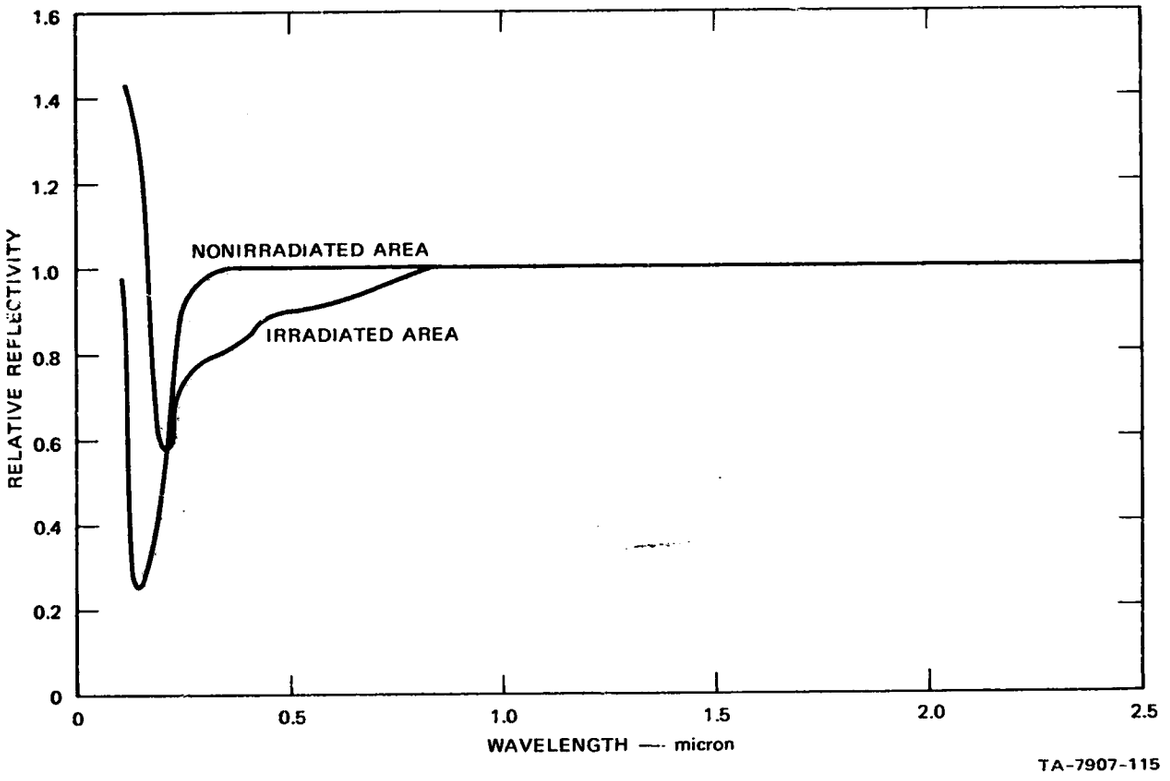

FIGURE 38 REFLECTIVITY OF A MIRROR CONTAMINATED WITH OUTGASES FROM STYCAST 1090 (AFTER HEATING CHILL-PLATE)

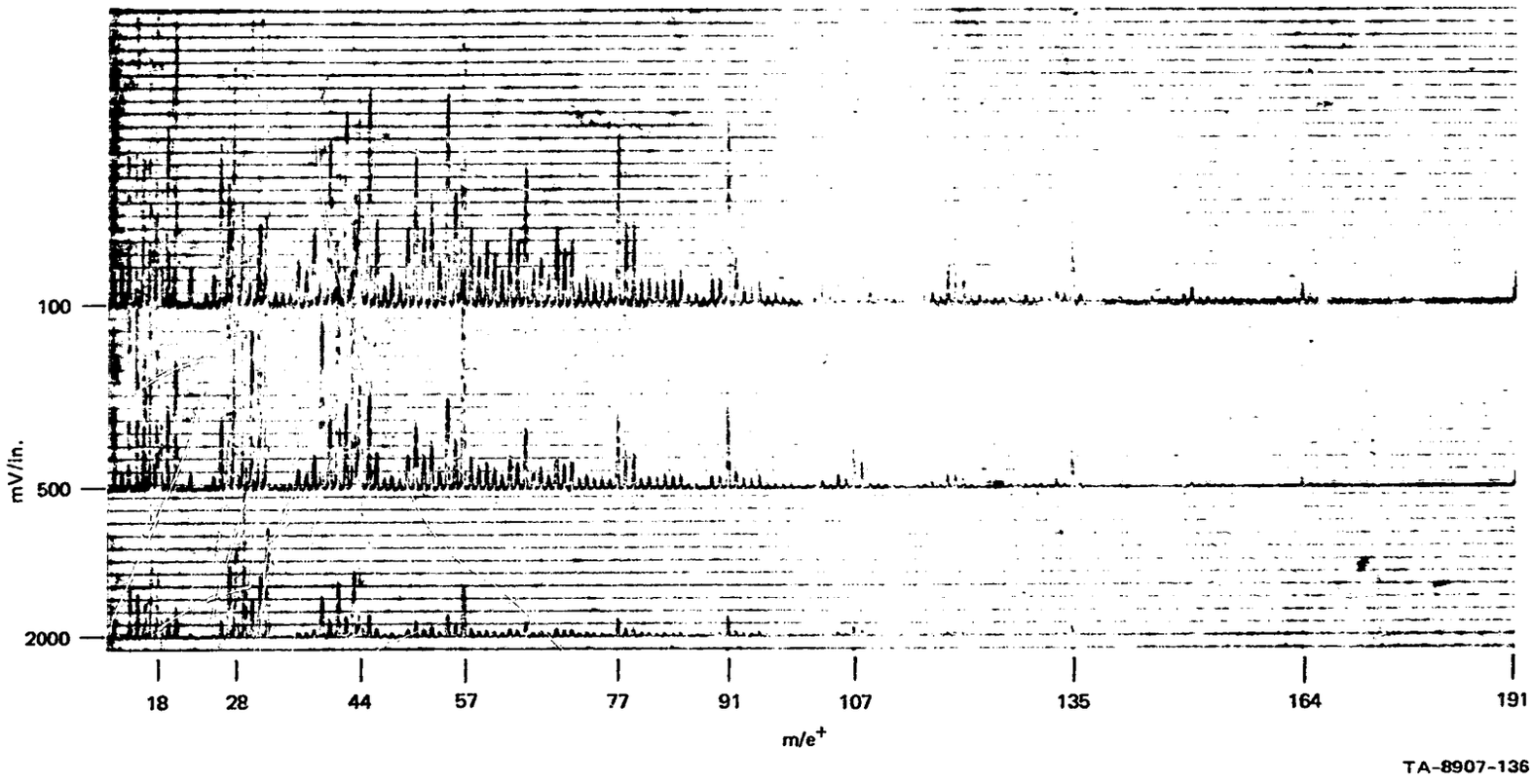

FIGURE 39 MASS SPECTRUM FOR OUTGASES FROM STYCAST 1090 (SAMPLE HEATER AT 125°C).

The relative reflectivity of the mirror after heating the chill-plate is presented in Figure 40. The irradiated area is the most degraded. The reflectivity of the mirror is impaired from 1100 to 6000 Å.

The quadrupole mass spectrum for the outgases from this sample showed that water was the only significant component present. Epon 828 is an epoxy-based adhesive. The curing agent, Versamid 125, is an organic amine.

Mystic 7100 Double-faced Tape

Mystic 7100 was the first material to be tested after the Cary spectrophotometer was optically connected to the test chamber and after sample holder No. 3 was constructed. Beginning with the test of Mystic 7100, test runs were limited to 96 hours and intermediate reflectivity measurements were made at 5, 24, and 96 hours. The reasons for these changes in apparatus and procedure are discussed in the section of Experimental Apparatus and Procedures.

Samples of this double-faced tape made by The Borden Company were prepared by cutting short strips, doubling them over, and sticking the inside sides of the strips together. The backing on one side of the tape

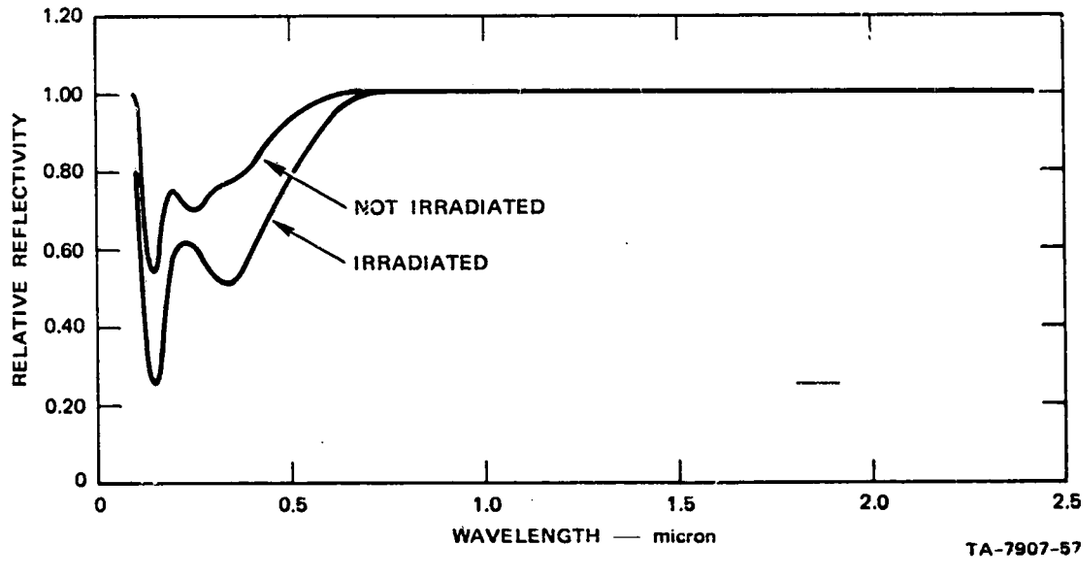

FIGURE 40 REFLECTIVITY OF A MIRROR CONTAMINATED WITH OUTGASES FROM SHELL EPON 828 (AFTER HEATING CHILL-PLATE)

was inadvertently left on the tape during the run. The test of this material should be repeated with both backings removed to get the true effects of this material under conditions in which it will be used.

The outgases deposited at a rapid rate during the first few hours of the run. The pace slowed, but material continued to deposit at the end of the run (see Table III). The thickness of the deposit is estimated to be 0.07 to 0.10 μ.

Figures 41 through 44 show the reflectivity of the mirror throughout the run. Degradation of the reflectivity of the mirror occurred at wavelengths in the region of 1100 Å to 1.0 μ.

Figure 45 presents the mass spectrum of the outgases from Mystic 7100. Molecular weights up to 223 are present in the outgases from the sample.

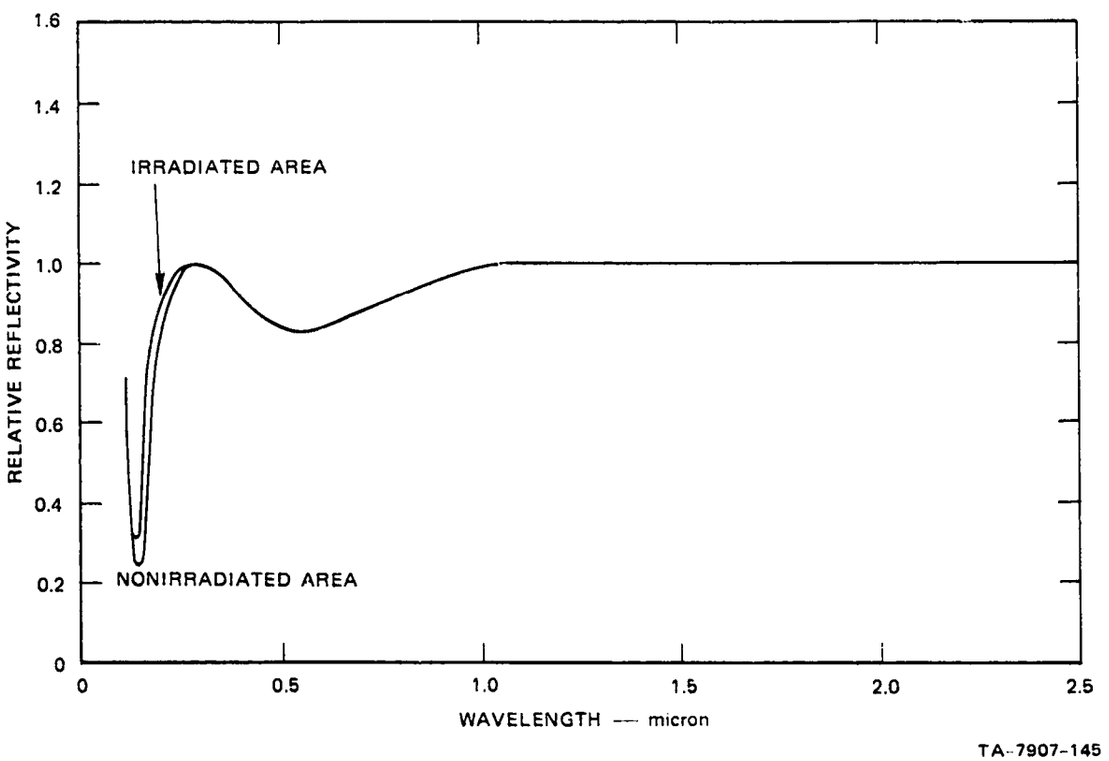

FIGURE 41 REFLECTIVITY OF A MIRROR CONTAMINATED WITH OUTGASES FROM MYSTIC TAPE NO. 7100 (AFTER 5 HOURS)

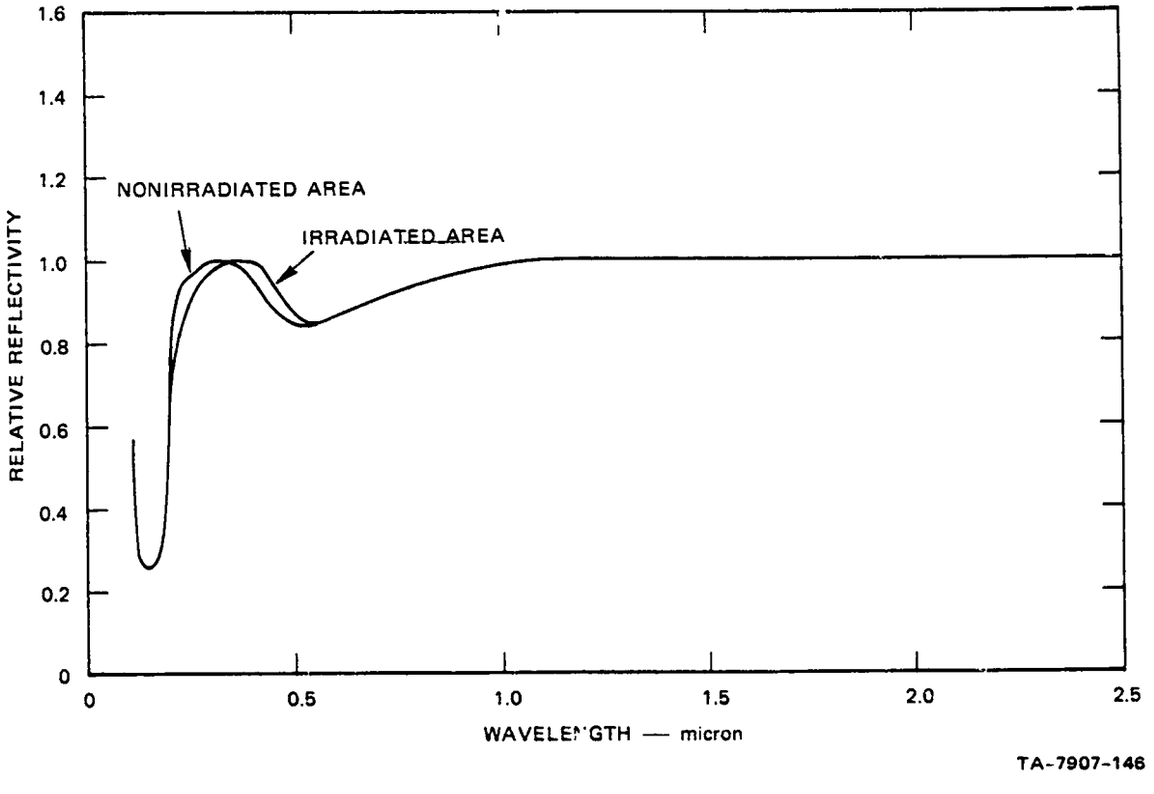

FIGURE 42 REFLECTIVITY OF A MIRROR CONTAMINATED WITH OUTGASES FROM MYSTIC TAPE NO. 7100 (AFTER 24 HOURS)

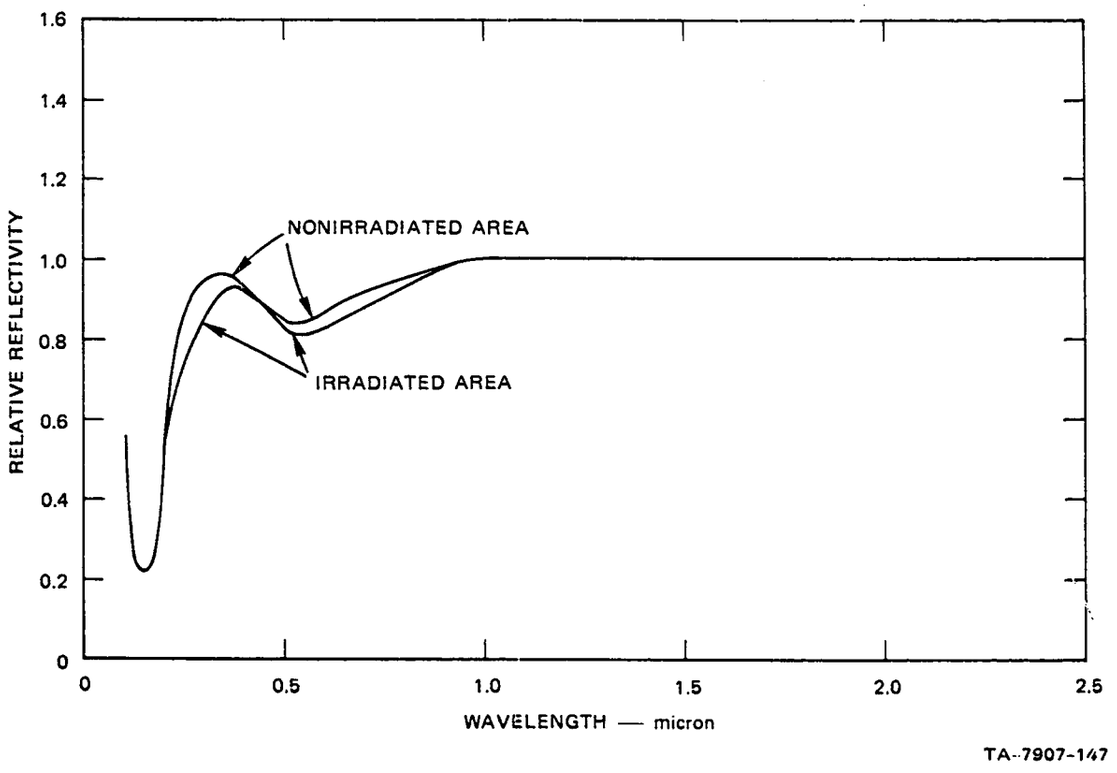

FIGURE 43 REFLECTIVITY OF A MIRROR CONTAMINATED WITH OUTGASES FROM MYSTIC TAPE NO. 7100 (AFTER 96 HOURS)

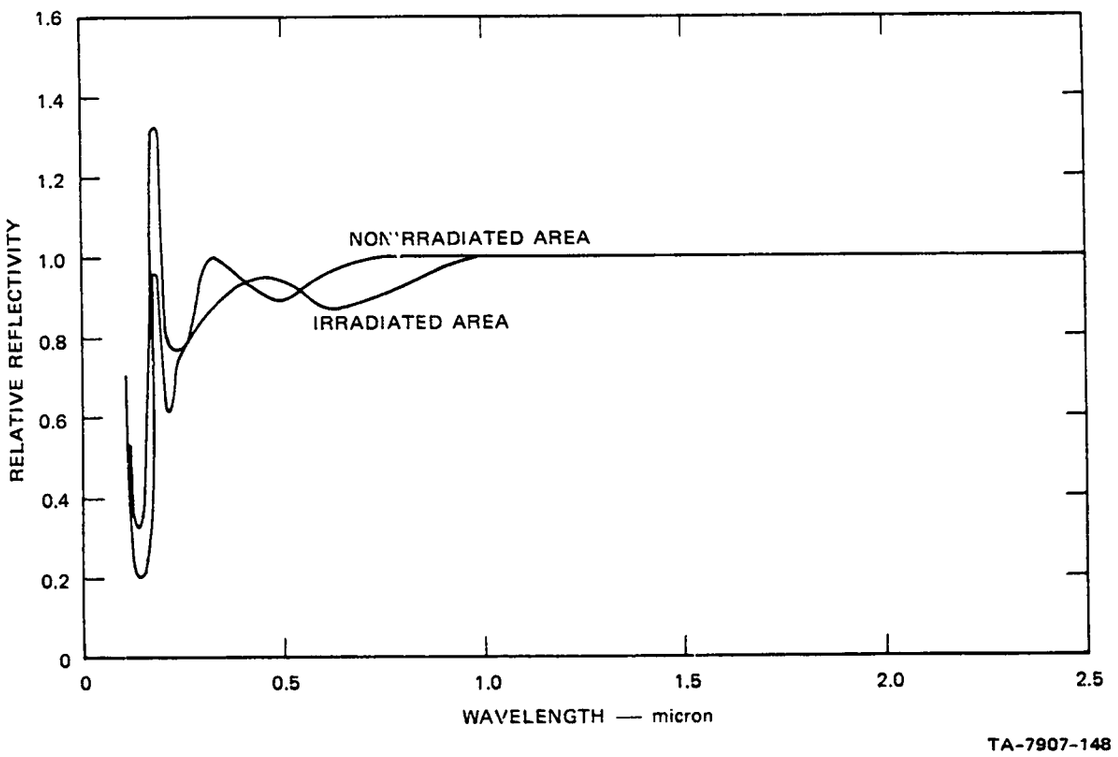

FIGURE 44 REFLECTIVITY OF A MIRROR CONTAMINATED WITH OUTGASES FROM MYSTIC TAPE NO. 7100 (AFTER HEATING CHILL-PLATE)

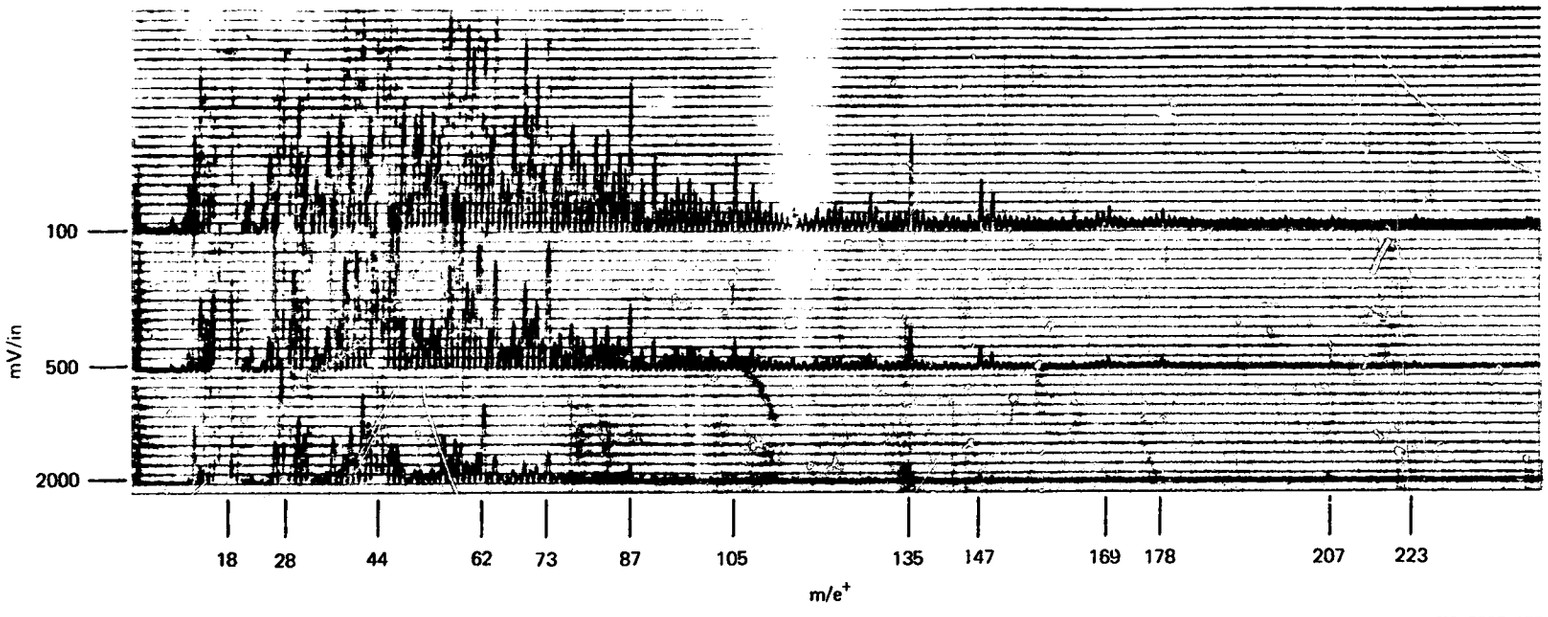

FIGURE 45 MASS SPECTRUM OF OUTGASES FROM MYSTIC TAPE NO. 7100 (SAMPLE HEATER AT 125°C)

Rexolite 2200 Copper-clad Polystyrene

A sheet of Rexolite 2200, as received, was cut into 1/4-inch cubes. A 1-g sample was placed in the sample heater and subjected to a 96-hour thermal-vacuum treatment.

No significant weight increases were recorded by the microbalances (see Table III). The mirror showed no appreciable weight gain when weighed after removal from the thermal-vacuum chamber. A very slight deposit was noticed on the mirror on visual inspection. The deposit is estimated to be $< 0.01\ \mu$ thick.

Reflectivity results are presented in Figures 46 through 49. Degradation of the reflectivity of the mirror took place in the range of 1100 Å to 0.8 μ. Relative reflectivities greater than 1 were experienced during this run as in other runs where very thin deposits were encountered.

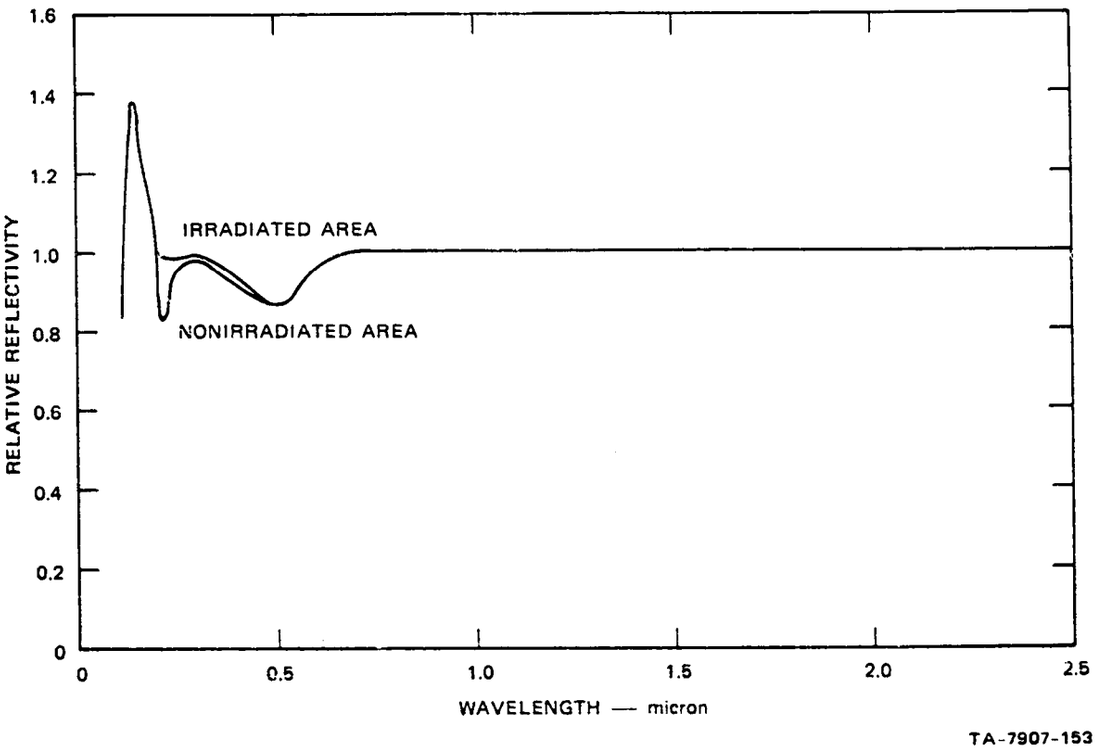

FIGURE 46 REFLECTIVITY OF A MIRROR CONTAMINATED WITH OUTGASES FROM REXOLITE 2200 (AFTER 5 HOURS)

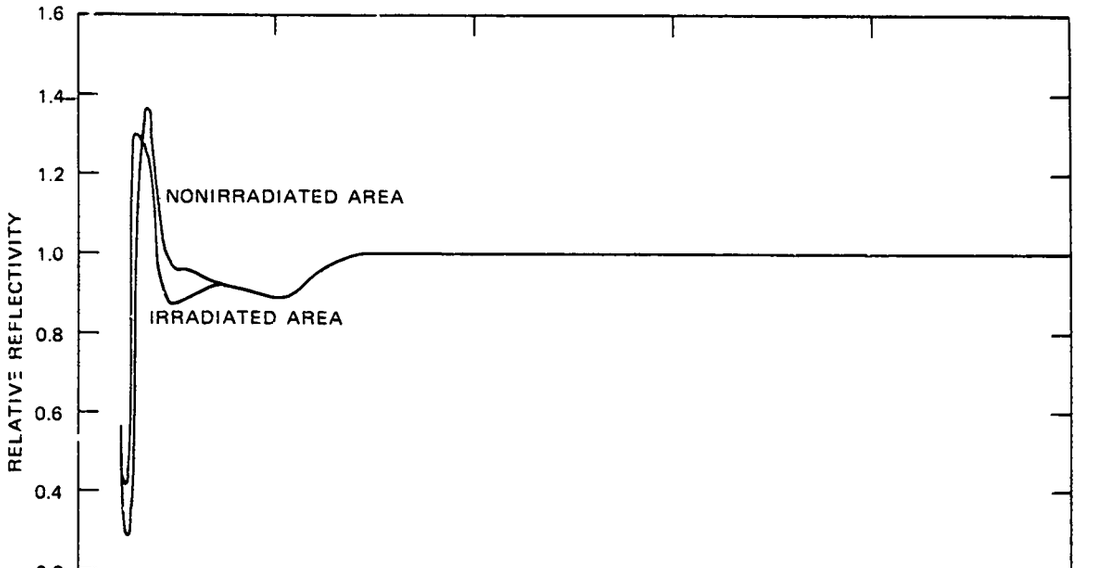

FIGURE 47 REFLECTIVITY OF A MIRROR CONTAMINATED WITH OUTGASES FROM REXOLITE 2200 (AFTER 24 HOURS)

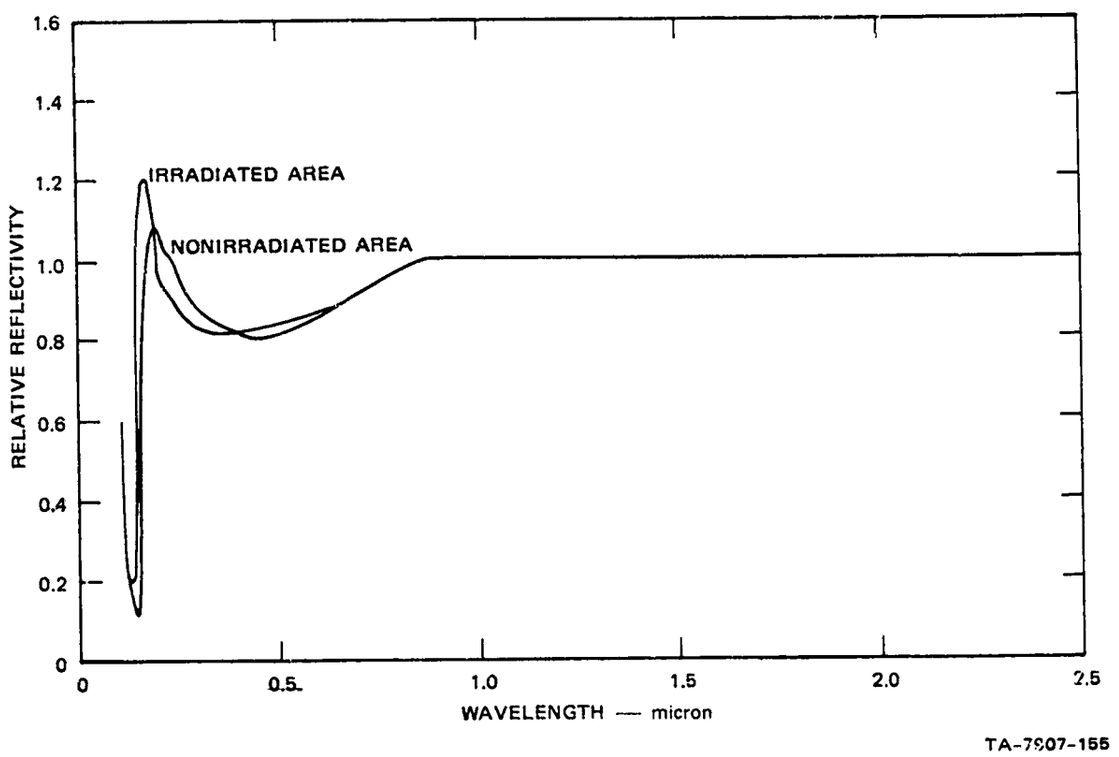

FIGURE 48 REFLECTIVITY OF A MIRROR CONTAMINATED WITH OUTGASES FROM REXOLITE 2200 (AFTER 96 HOURS)

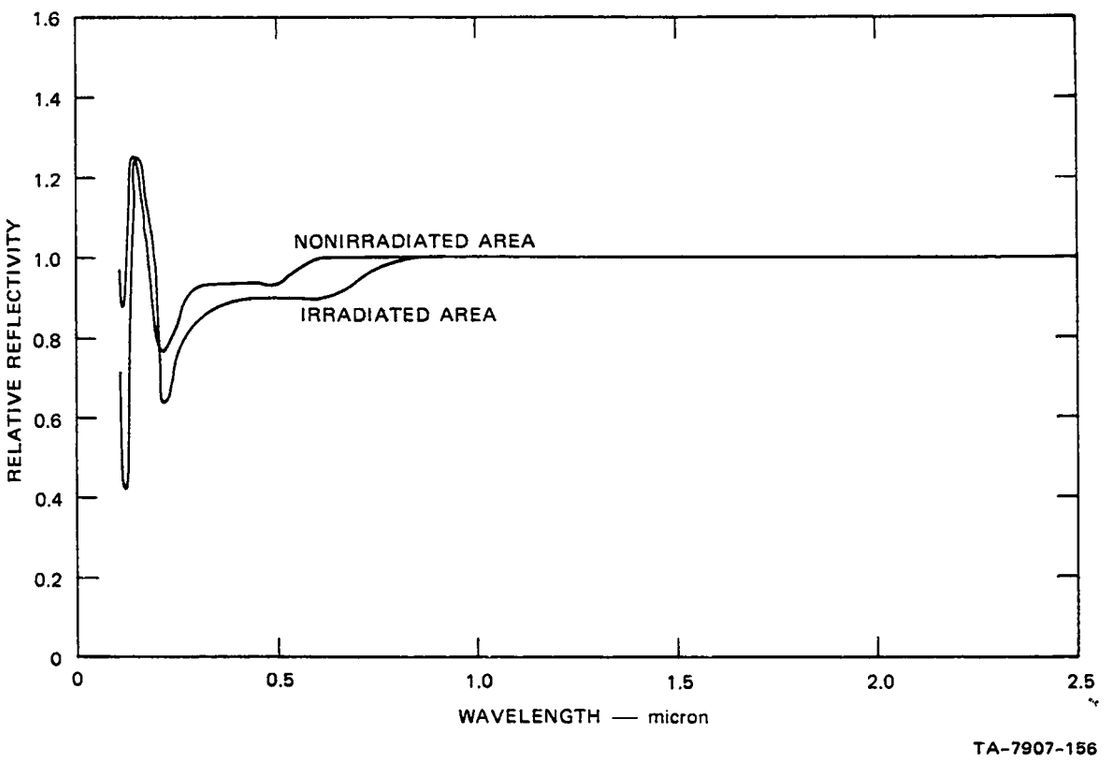

FIGURE 49 REFLECTIVITY OF A MIRROR CONTAMINATED WITH OUTGASES FROM REXOLITE 2200 (AFTER HEATING CHILL-PLATE)

The quadrupole mass spectrum of this material, shown in Figure 50, consists of several degradation products of styrene. The peaks occurring at 91, 105, 119, and 207 indicate the presence of toluene; one or a combination of xylene, styrene and ethylbenzene; methylstyrene; and the dimer of styrene, respectively.

Silastic 55U Silicone Elastomer

Silastic 55U was used as received from the manufacturer. The silicon rubber sheet was cut into 1/32-inch strips. A 1-g sample was exposed to a 96-hour thermal-vacuum treatment.

The outgases from the sample deposited rapidly on the microbalances during the first hours of the run. The rate of deposition slowed and was slowly increasing at the end of the run (see Table III). The deposit is estimated to be 0.07 to 0.10 μ thick.

The reflectivity of the test mirror shown in Figures 51 through 54, decreased during the 96-hour run. Heating the chill-plate markedly improved the reflectivity of the nonirradiated area of the mirror. The degradation of the reflectivity of the mirror occurred in the region of 1100 Å to 1.0 μ.

The quadrupole mass spectrum of the outgases from the sample is shown in Figure 55. Silastic 55U is a dimethyl silicone polymer. Catalysts used with this material include either 2,5-bis(tertbutylperoxy)-2,5-dimethylhexane and dicumyl peroxide or 2,4-dichlorobenzoyl peroxide. There was insufficient information to link these compounds or their thermal degradation products with the mass spectrum.

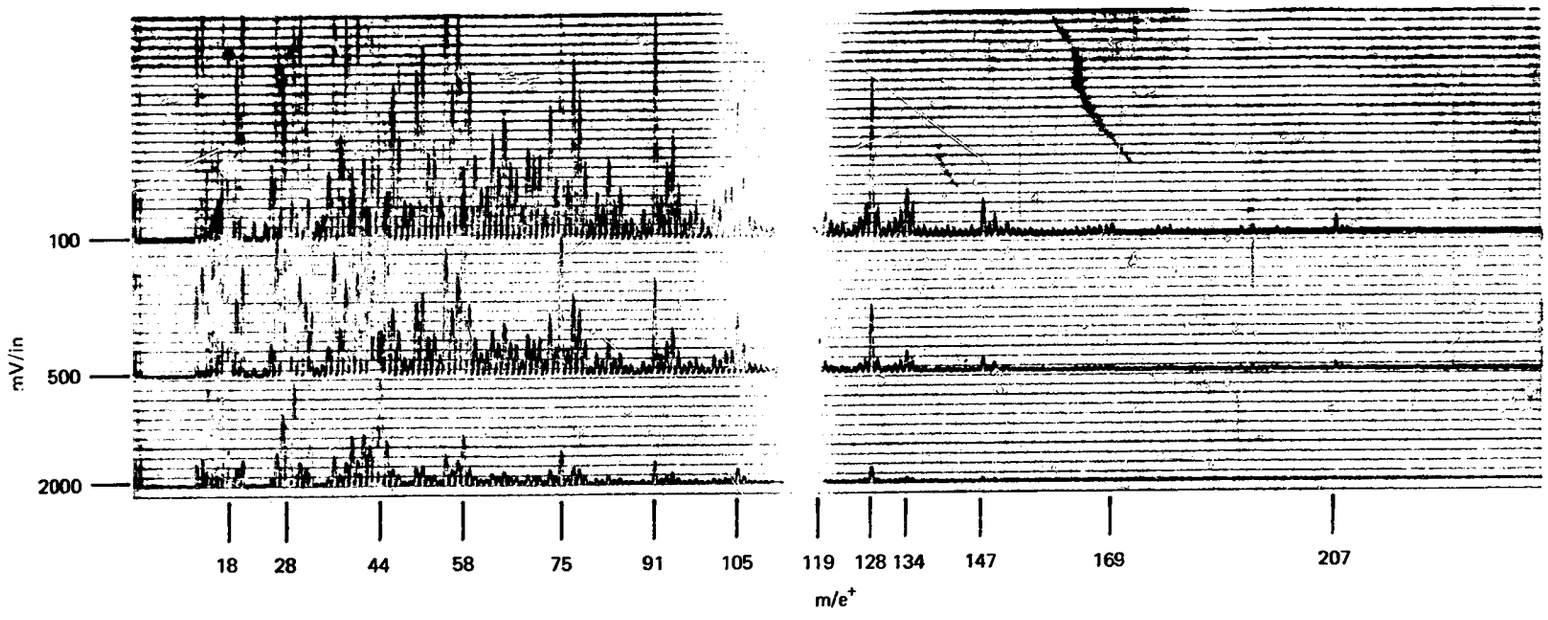

FIGURE 50 MASS SPECTRUM OF OUTGASES FROM REXOLITE 2200 (SAMPLE HEATER AT 125°C)

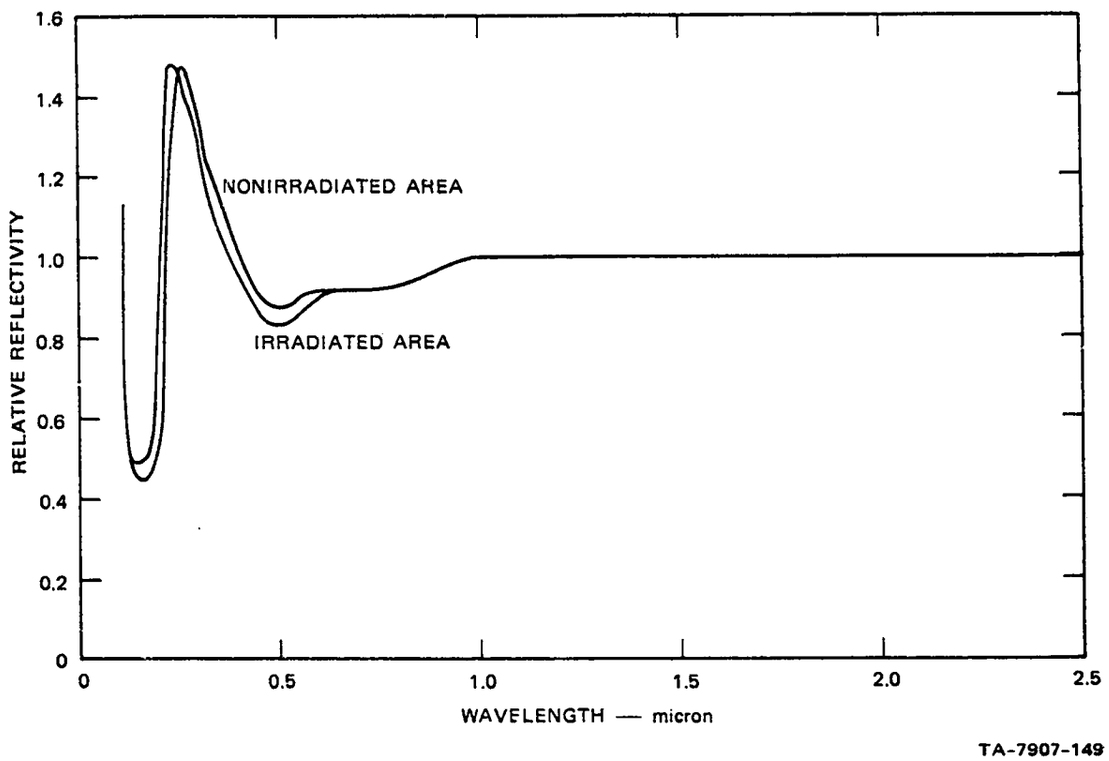

FIGURE 51 REFLECTIVITY OF A MIRROR CONTAMINATED WITH OUTGASES FROM SILASTIC 55U (AFTER 5 HOURS)

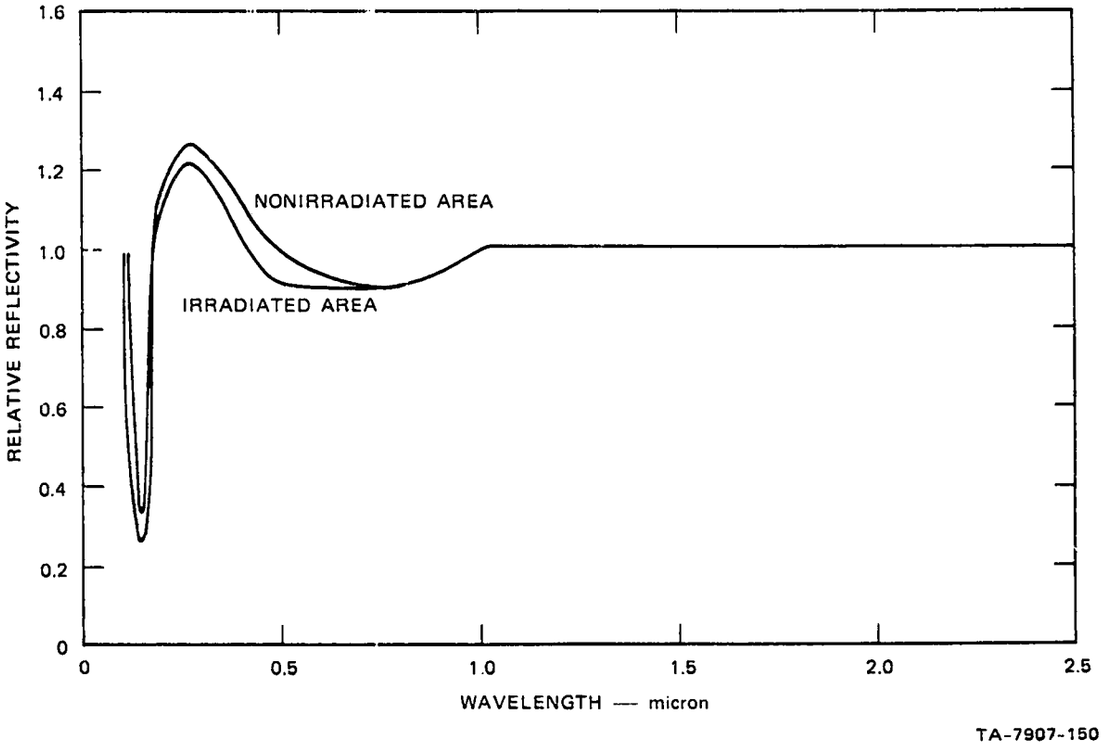

FIGURE 52 REFLECTIVITY OF A MIRROR CONTAMINATED WITH OUTGASES FROM SILASTIC 55U (AFTER 24 HOURS)

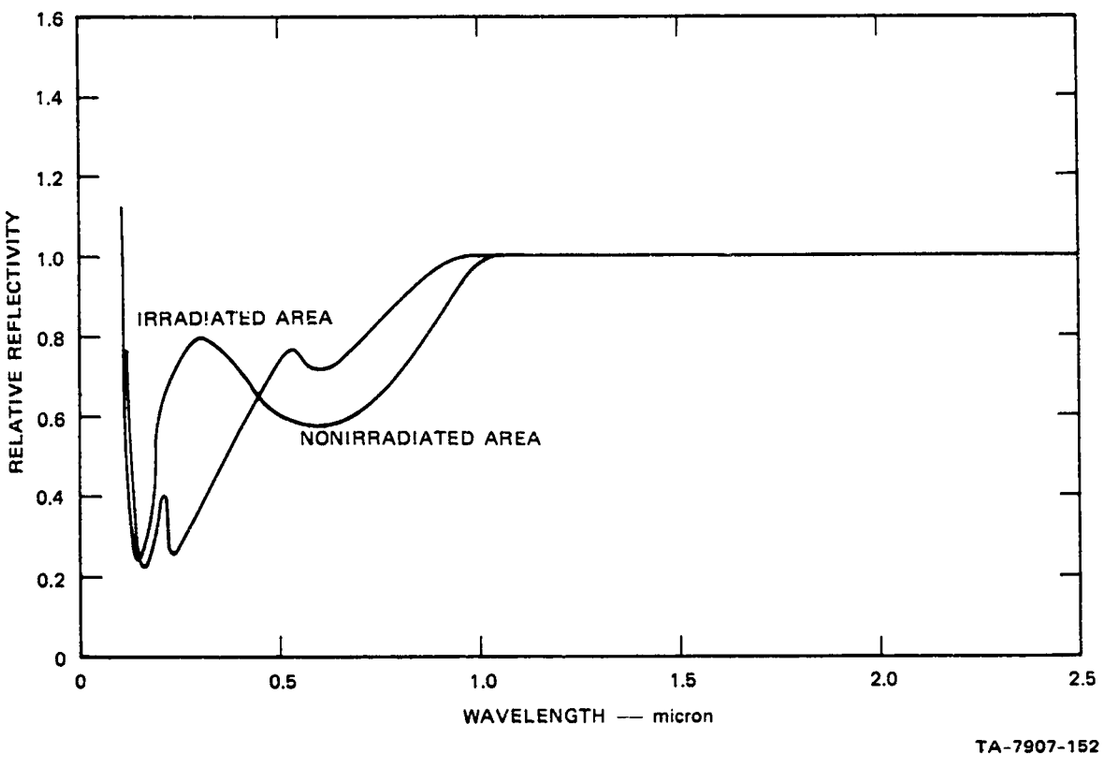

FIGURE 53 REFLECTIVITY OF A MIRROR CONTAMINATED WITH OUTGASES FROM SILASTIC 55U (AFTER 96 HOURS)

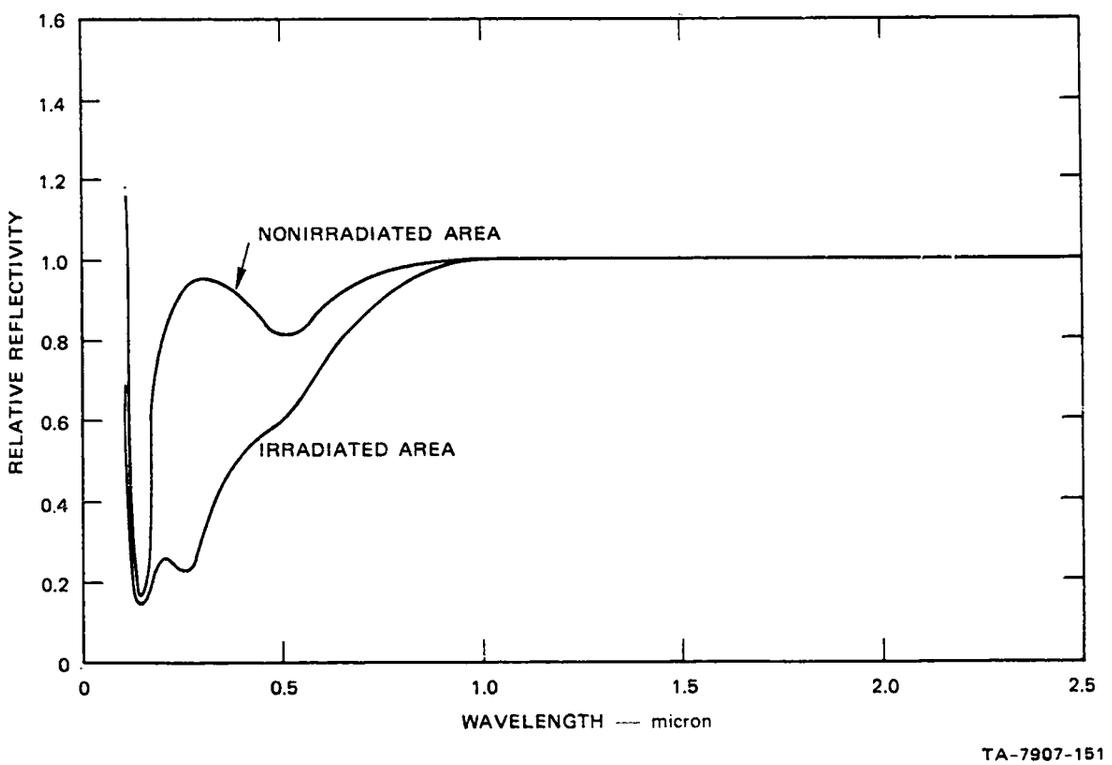

FIGURE 54 REFLECTIVITY OF A MIRROR CONTAMINATED WITH OUTGASES FROM SILASTIC 55U (AFTER HEATING CHILL-PLATE)

QUALITY OF THE ORIGINAL PAGE IS POOR.

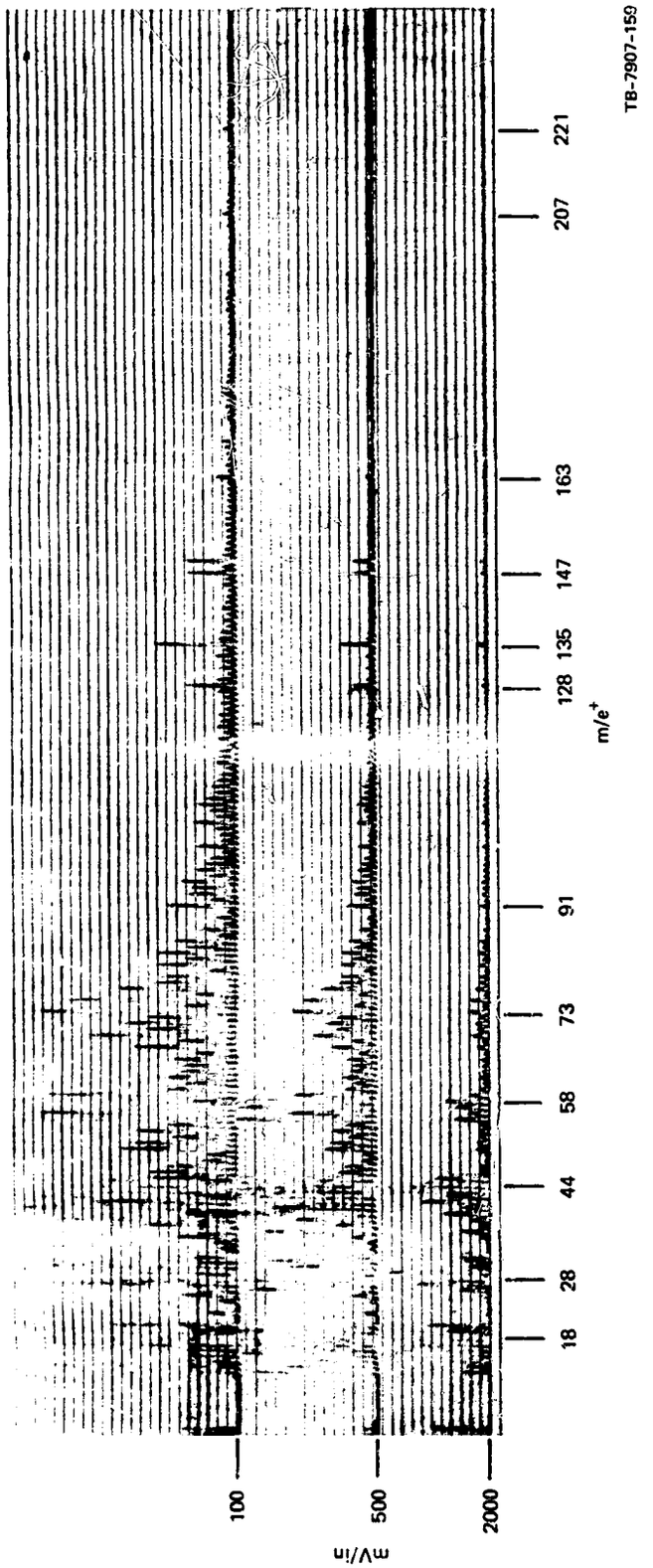

FIGURE 55 MASS SPECTRUM OF OUTGASES FROM SILASTIC 55U (SAMPLE HEATER AT 125°C)

Adiprene L-100 Polyurethane Elastomer

Adiprene L-100 was prepared using Moca curing agent according to instructions in Du Pont Adiprene Urethane Rubber Bulletin No. 7. The material was then cured for 3 hours at 100°C and 48 hours at 250°C. The product was cut into pieces 1/4 x 1/8 x 1/32 inch and subjected to a 96-hour thermal-vacuum treatment.

The outgases from the sample deposited very slowly on the microbalances throughout the run (see Table III). The total deposit after removal from the test chamber was very small and about 0.01 to 0.03 μ thick.

The reflectivity of the test mirror throughout the run is presented in Figures 56 through 59. Although the deposit is relatively light, the degradation of the mirror is marked and covers a wide wavelength range (1100 Å to 1.8 μ). Heating the chill-plate noticeably improved the reflectivity of the nonirradiated area (see Figure 59). Visual inspection of the mirror after removal from the test chamber confirmed this.

Figure 60 presents the mass spectrum of the outgases from the sample. Adiprene L-100 is a polyurethane; the catalyst used to cure it was 4,4'-methylene-bis(2-choroaniline). No information on the degradation products could be found, and no obvious degradation products could be associated with the peaks of the mass spectrum.

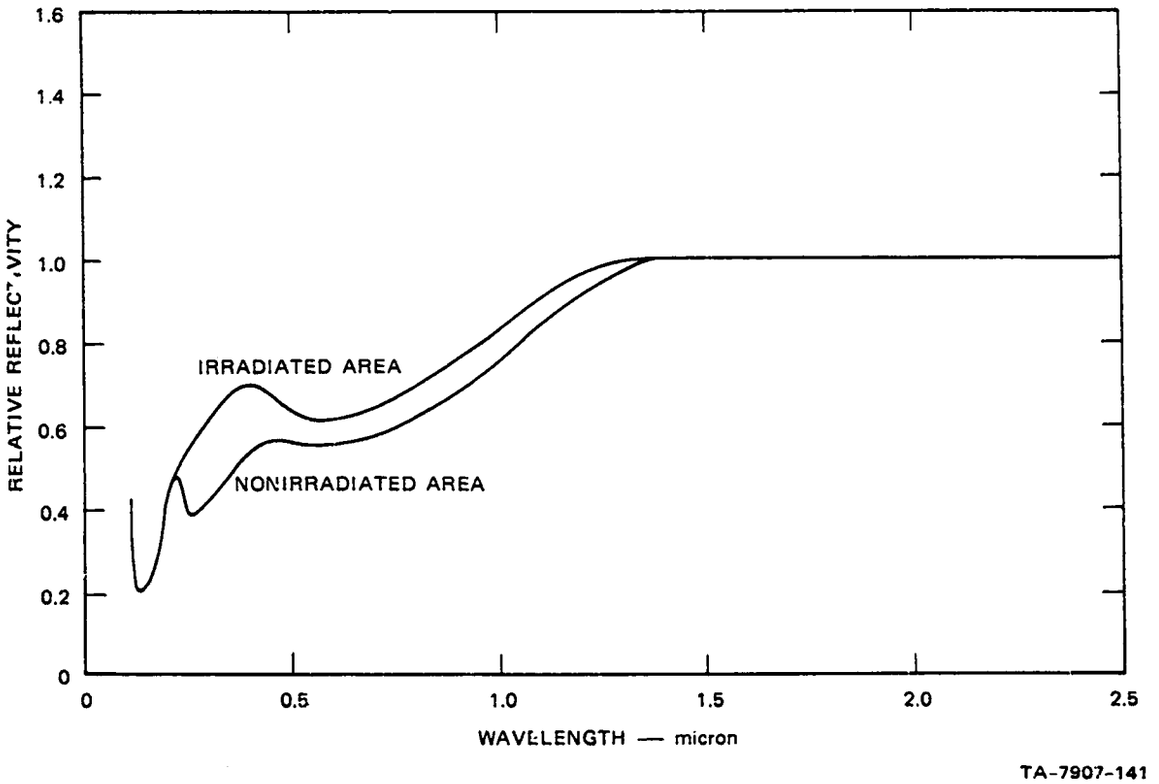

FIGURE 56 REFLECTIVITY OF A MIRROR CONTAMINATED WITH OUTGASES FROM ADIPRENE L-100 (AFTER 5 HOURS)

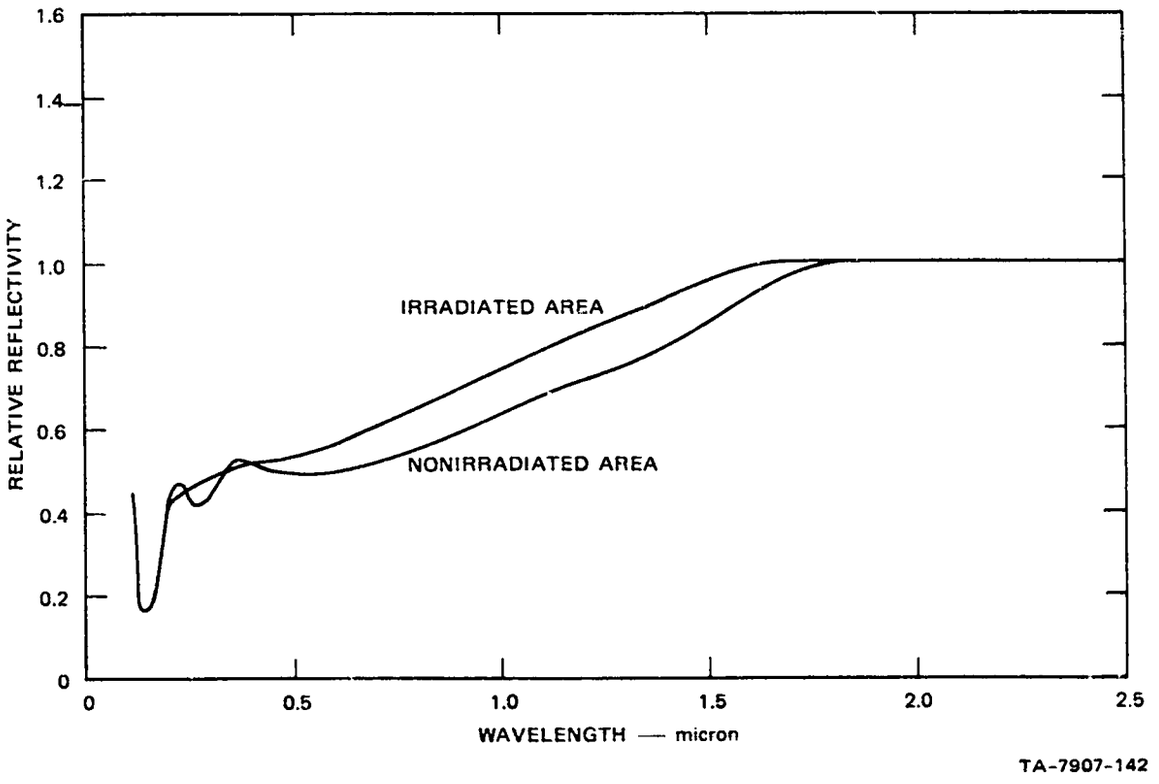

FIGURE 57 REFLECTIVITY OF A MIRROR CONTAMINATED WITH OUTGASES FROM ADIPRENE L-100 (AFTER 24 HOURS)

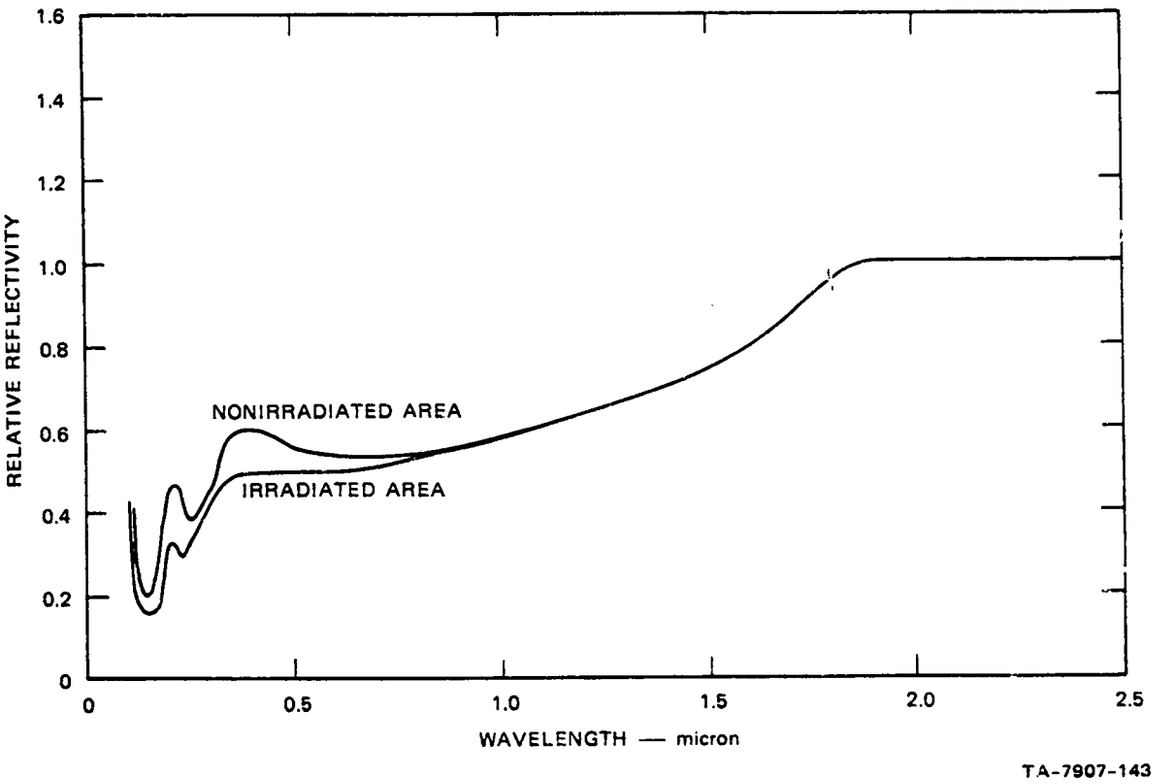

FIGURE 58 REFLECTIVITY OF A MIRROR CONTAMINATED WITH OUTGASES FROM ADIPRENE L-100 (AFTER 96 HOURS)

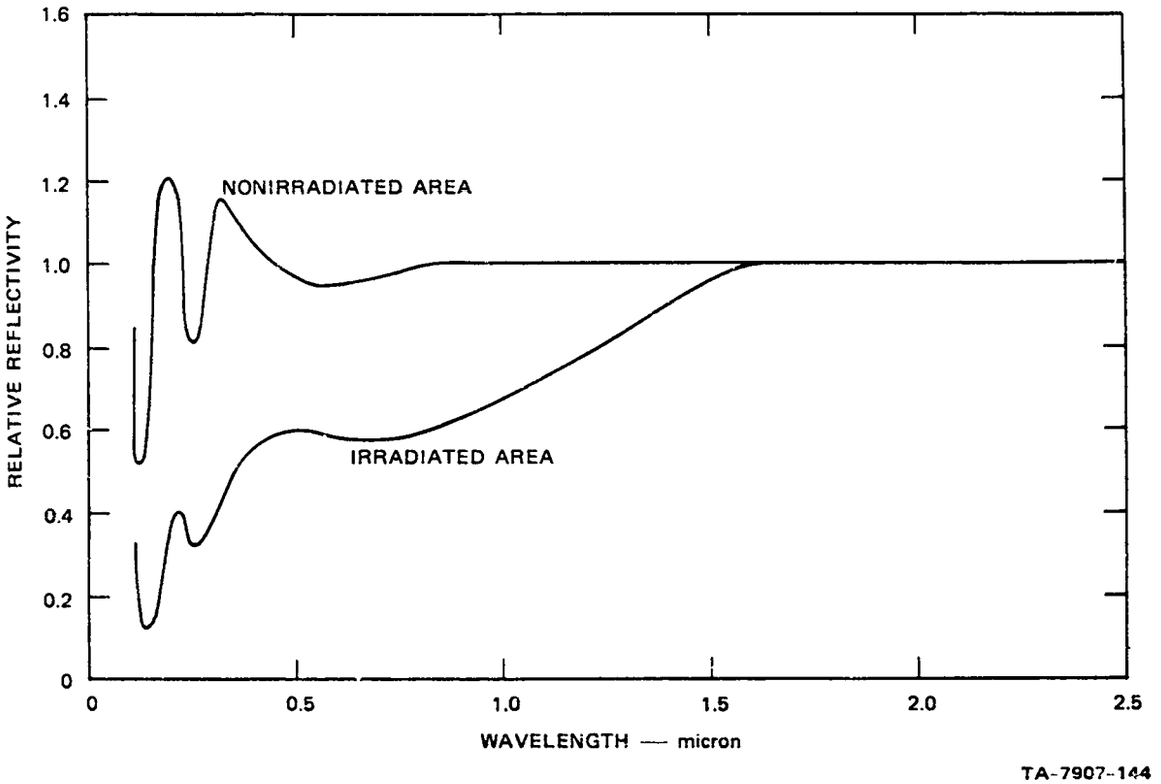

FIGURE 59 REFLECTIVITY OF A MIRROR CONTAMINATED WITH OUTGASES FROM ADIPRENE L-100 (AFTER HEATING CHILL-PLATE)

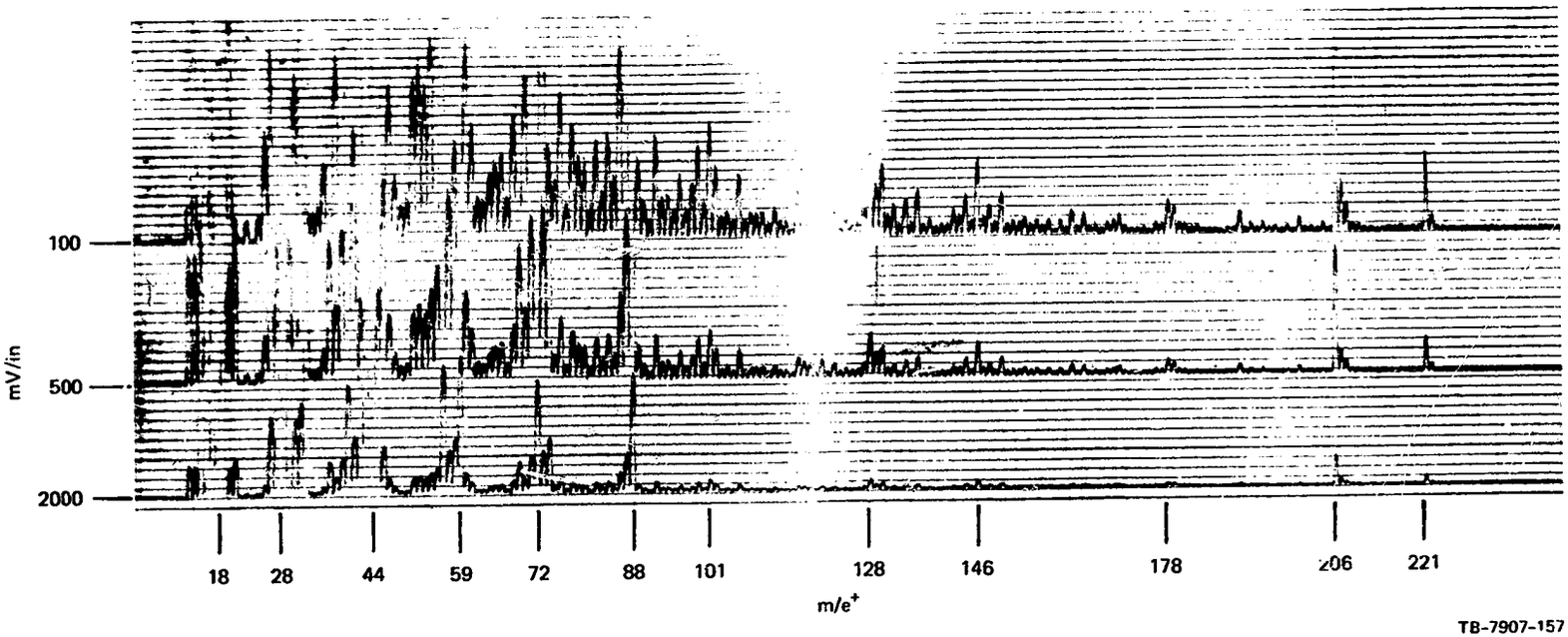

FIGURE 60 MASS SPECTRUM OF OUTGASES FROM ADIPRENE L-100 (SAMPLE HEATER AT 125°C)

CONCLUSIONS

The objective of the project was to study the contamination characteristics of selected materials used in space technology environmental testing. The effects of outgases on optical surfaces with and without the presence of ultraviolet irradiation was of particular interest. Several things were learned in this context, some expected and some not.

Some degradation of the reflectivity of the test mirror was observed with all materials tested during the course of this project. The loss of reflected light is due mainly to the light scattering caused by deposits resulting from condensation of outgases. Deposits encountered were never much greater than 1.0 μ; in most cases $< 0.1\ \mu$. This layer is generally too thin to see the effects of absorption of the light by the deposit.

A thorough theoretical evaluation of the relationship between wavelength and reflectivity of contaminated mirrors was carried out by Dr. David Falconer, Research Physicist at Stanford Research Institute. The theoretical treatment includes conductivity of aluminum, scattering, interference, and absorption. Appropriate values for these parameters were substituted into a series of equations, and a computer was used for the solutions and to present the resulting data in a useful form.

The pertinent conclusions from this evaluation are as follows:

(1) Aluminum layers thicker than 1000 Å are highly reflective throughout the wavelength range of 1000 to 10^5 Å.

(2) Aluminum mirrors with dielectric coatings thinner than 0.1 micron are highly reflective at wavelengths longer than 1.0 micron.

(3) Scattering from a rough surface is negligible if the wavelength is at least 10 times the surface roughness.

(4) Loss of light due to absorption would be negligible for dielectric films of 0.1 micron or thinner at wavelengths greater than 1.0 micron because extinction coefficients are not large enough to cause significant effects.

Details of this work are given in the Appendix.

No definite absorption bands were noted in any of the relative reflectivity curves of materials tested during this project. The scattering properties do not depend on the thickness of the deposit but on the relationship of the surface roughness to the wavelength. If the incident light remains large compared with the surface roughness, Rayleigh-type scattering is observed. If, however, the wavelength is small compared with the surface roughness, the scattering depends in a very complicated way on the complex refractive index of the dielectric deposit, and Mie-type scattering takes place. Mie mechanisms usually scatter more of the incident beam than they transmit, thus destroying the reflectivity of the mirror. In other words, the most important influence on the degradation of the reflectivity of the mirror is the surface roughness of the deposit.

Ultraviolet light has an effect on the depositing outgases. Evidence of polymerization caused by ultraviolet irradiation was found in the deposits. In some cases, such as Thermofit RNF-100, the deposit predominates on the nonirradiated area of the mirror. Other tests showed that the polymerized deposit predominates on the irradiated area, as is the case with Moxness MS60 S08 and Adiprene L-100. In still other cases, no appreciable deposit is seen on either area of the mirror, as is the case with Rexolite 2200. The condition of the deposit depends on several factors: the nature and quantity of the outgas and its susceptibility to polymerization by ultraviolet light.

In some instances, heating the chill-plate improves the reflectivity of the mirror, particularly on the nonirradiated area. This can be seen in the reflectivity curves of Adiprene L-100. Since the polymerized

deposit on the irradiated area is probably of considerably higher molecular weight, it is harder to remove by heating the chill-plate.

It was our experience that the microbalances were only a semiquantitative measure of the accumulating deposit, although they were consistent enough to determine whether the deposit was in a heavy, medium, or light deposit category. However, because the quartz crystals of the microbalances were in poor thermal contact with the chill-plate, the microbalances probably did not follow the temperature variations of the chill-plate as well as the mirror, which was in good thermal contact.

The quadrupole mass spectra of materials tested at the beginning of the project were of low intensity because of the design of the sample heater. Adding a side-arm to the sample heater to place the sample in direct line of sight of the ionizer of the quadrupole mass spectrometer greatly improved the intensity of the mass spectra. In the early work in this study, masses of only about 100 amu were distinguishable. After the introduction of sample heater No. 3, masses in the 200 to 300 amu range were easily seen.

Materials whose outgases gave deposits that degraded the reflectivity of the irradiated area more than the nonirradiated area after a thermal-vacuum treatment were Moxness MS60 S08, Scotch Tape No. Y-9050, RTV-41, Epon 934, Stycast 1090, Epon 828, Adiprene L-100, and Silastic 55U. Samples whose outgases resulted in more degradation of the reflectivity of the nonirradiated area of the mirrors were Thermofit RNF-100, TRT-24-19-V-93, and Eccofoam FS and FPH. The rest of the materials degraded the reflectivity of the mirrors only slightly after the thermal-vacuum treatment. With most of the materials, degradation of the reflectivity of the test mirror was roughly in the wavelength range of 1100 Å to 1.0 μ.

Considerable interest has been shown in this work, and several requests for information and copies of our reports have been received. Recently, Dr. Dale Coulson had the opportunity of presenting a paper on this work at the Seventh Thermophysics Conference of the American Institute of Aeronautics and Astronautics in San Antonio, Texas.

Appendix

REFLECTED AND SCATTERING FROM COATED AND UNCOATED ALUMINUM MIRRORS

Appendix

REFLECTION AND SCATTERING FROM COATED AND UNCOATED ALUMINUM MIRRORS

The material presented below discusses: the reflectivity of an aluminum layer as a function of the radiation wavelength λ and the layer thickness d; the reflectivity of a dielectric layer coated onto an aluminum surface as a function of the radiation wavelength λ, the layer thickness d, and the extinction coefficient b; and the scattering caused by a rough dielectric surface as a function of the radiation wavelength λ and surface roughness δ. It is concluded that aluminum layers thicker than 1000 Å remain highly reflective throughout the infrared, visible, and ultraviolet; that dielectric coatings with $bd < 0.1$ look highly reflective for $\lambda > 1.0$ micron; and that scattering from a rough surface remains negligible if $\lambda/\delta > 10$.

A. Reflection by Thin Layers

The reflection coefficient R associated with a smooth, metallic surface coated with a thin dielectric layer depends on the wavelength of the incident radiation, the complex refractive index of the metallic surface, and the complex refractive index and the thickness of the dielectric layer. For normally incident radiation the boundary value problem simplifies considerably and can be solved exactly with paper and pencil. The resulting formula, however, depends on the complex refractive indices in a rather complicated way, except at the longer wavelengths where some simplification results. At the shorter wavelengths one must use a digital computer to plot the reflection coefficient as a function of radiation wavelength, extinction coefficient, and layer thickness.

To solve the boundary value problem exactly, consider the geometry shown in Figure A1. The incident radiation impinges on the dielectric layer from the left and is both reflected from and transmitted by the exterior surface at z = 0. The transmitted light propagates to the interior surface at z = d, where it is reflected back toward the exterior surface and transmitted into the metal. The transmitted wave eventually suffers extinction within the metal; the reflected wave combines with the incident field at z = 0.

The three media--namely, the vacuum, dielectric, and metal--are characterized by their complex refractive indices. To solve the boundary value problem we assign instead a complex wave number to each medium:

$$k_j = d_j + i\beta_j$$

where j = 1,2,3. The complex refractive index of the j^{th} medium then takes the form:

$$ck_j/\omega$$

Here ω denotes the angular frequency of the incident illumination, and c the velocity of light in vacuo.

Without loss of generality, we can describe the incident electric and magnetic fields as

$$E_i = E_0 \exp(ik_1 z - i\omega t)$$

$$H_i = (k_1/\omega\mu_1)E_i$$

where E_0 denotes the magnitude of incident electric field and μ_1 the permeability of medium 1. The field in the dielectric layer consists of a forward traveling wave (+) and a backward traveling wave (-), that is,

$$E_\ell = E_\ell^+ + E_\ell^-$$

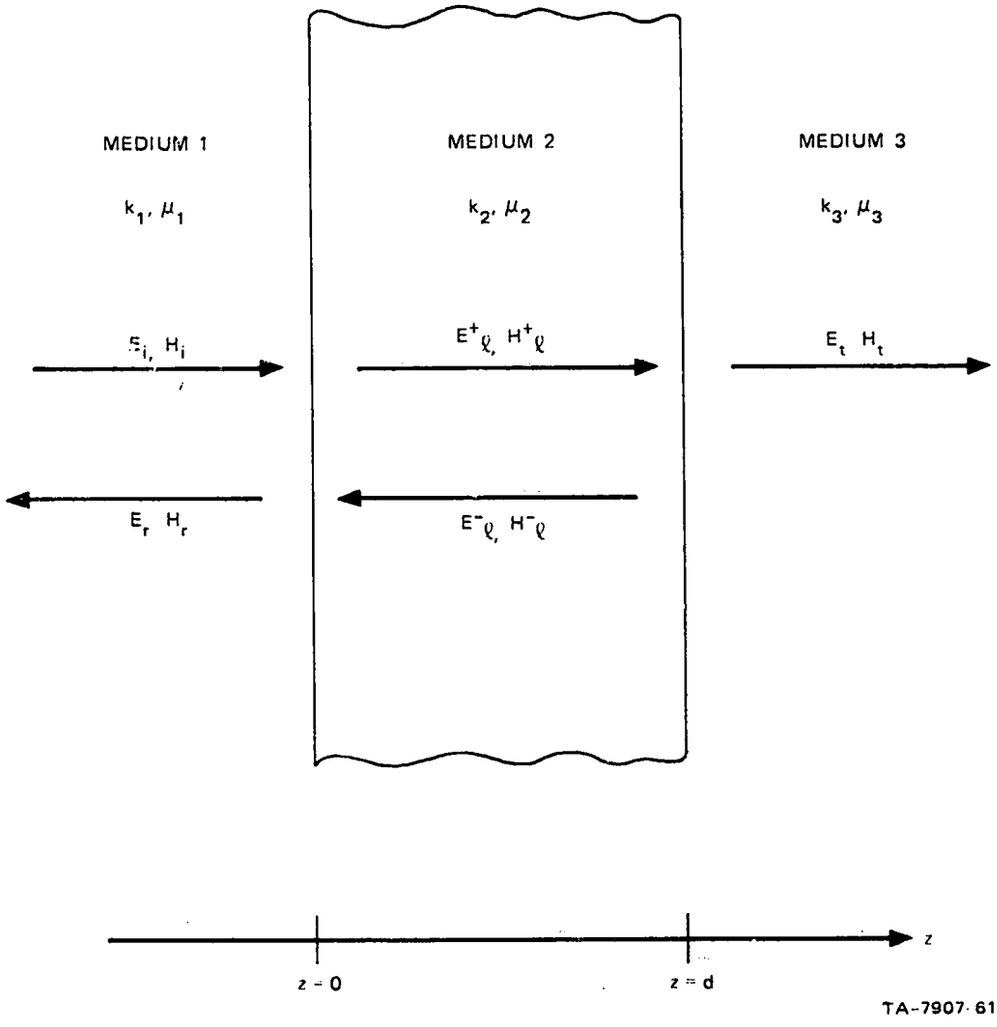

FIGURE A-1 GEOMETRY FOR BOUNDARY VALUE PROBLEM

C - 2

$$E_{\ell}^{+} = E_{2}^{+} \exp(+ik_2 z - i\omega t)$$

$$E_{i}^{-} = E_{2}^{-} \exp(-ik_2 z - i\omega t)$$

Similarly, for the magnetic field in the layer:

$$H_{\ell} = H_{\ell}^{+} + H_{\ell}^{-}$$

$$H_{\ell}^{+} = +(k_2/\omega\mu_2)\ E_{\ell}^{+}$$

$$H_{\ell}^{-} = -(k_2/\omega\mu_2)\ E_{\ell}^{-}$$

Also, the wave transmitted into the metal must have the form:

$$E_t = E_3 \exp(ik_3 z - i\omega t)$$

$$H_t = (k_3/\omega\mu_3)\ E_t$$

Finally, the wave reflected away by the dielectric layer is:

$$E_r = E_1 \exp(-ik_1 z - i\omega t)$$

Clearly, only the incident electric-field strength E_0 remains arbitrary, while E_1, E_2^{+}, E_2^{-}, E_3 all act as dependent variables.

To determine the magnitude E_r of the reflected field, we impose the electromagnetic boundary conditions. Hence, all waves propagate normally to the interior and exterior dielectric surfaces. Restrictions on the normal components of the electric and magnetic fields yield no information. On the other hand, the tangential component of the E field and the tangential component of the H field must be continuous at the dielectric surfaces. In other words,

$$E_i + E_r = E_{\ell}^{+} + E_{\ell}^{-} \qquad (z = 0)$$

$$H_i + H_r = H_{\ell}^{+} + H_{\ell}^{-} \qquad (z = 0)$$

$$E_{\ell}^{+} + E_{\ell}^{-} = E_t \qquad (z = d)$$

$$H_{\ell}^{+} + H_{\ell}^{-} = H_t \qquad (z = d)$$

Substituting for the electric fields and evaluating the results at the interior and exterior surfaces:

$$E_0 + E_1 = E_2^{+} + E_2^{-}$$

$$(k_1/\omega\mu_1)\ (E_0 - E_1) = (k_2/\omega\mu_2)\ (E_2^{+} - E_2^{-})$$

$$E_2^{+} \exp(+ikd_2) + E_2^{-} \exp(-ik_2 d) = E_3 \exp(ik_3 d)$$

$$(k_2/\omega\mu_2) E_2^{+} \exp(+ik_2 d) - (k_2/\omega\mu_2)\ E_2^{-} \exp(-ik_2 d) = (k_3/\omega\mu_2)\ E_3 \exp(ik_3 d)$$

Accordingly, we have four equations for the four unknowns E_1, E_2^{+}, E_2^{-}, E_3.

To determine the reflection coefficient R, we need the ratio of E_1 to E_0, that is,

$$R \equiv \left| E_1/E_0 \right|^2$$

Eliminating E_2^{+}, E_2^{-}, E_3 from the above equations then yields:

$$E_1/E_0 = \frac{A + B \exp(2ik_2 d)}{C + D \exp(2ik_2 d)}$$

$$A = (1 - \mu_1 k_2/\mu_2 k_1)\ (1 + \mu_2 k_3/\mu_3 k_2)$$

$$B = (1 + \mu_1 k_2/\mu_2 k_1)\ (1 + \mu_2 k_3/\mu_3 k_2)$$

$$C = (1 + \mu_1 k_2/\mu_2 k_1)\ (1 + \mu_2 k_3/\mu_3 k_2)$$

$$D = (1 - \mu_1 k_2/\mu_2 k_1)\ (1 - \mu_2 k_3/\mu_3 k_2)$$

The above equations represent the desired solution to the reflectivity problem.

The complex wave number k may be specified in terms of the medium's complex refractive index n + ik or complex conductivity σ, depending on whether one is considering a dielectric medium or a metallic one. In the case of dielectrics,

$$k = (n + ik)\ (\omega/c)$$

The imaginary part of the refractive index, k, is related to the medium's extinction coefficient, b, in the usual way:

$$b = 2k(\omega/c)$$

The extinction coefficient is in turn related to the optical density D for the medium according to

$$2.3D = b\ell$$

where ℓ denotes the thickness of the medium.

On the other hand, if one considers a metallic medium the wave number takes the alternative form:

$$k^2 = \omega^2\epsilon\mu + \omega\mu\sigma$$

For the metals considered below $\epsilon \approx \epsilon_0$ and $\mu \approx \mu_0$, so that $\epsilon\mu \approx 1/c^2$.

B. Reflection by Aluminum Films

Films of aluminum show extremely good reflectivity throughout the infrared, visible, and ultraviolet portions of the electromagnetic spectrum. In fact, experiments by R. P. Madden* indicate "that aluminum as a reflector is truly a 'wonder' material." At low temporal frequencies such reflectivities result primarily from the large number of free electrons in the metal; at high frequencies the reflectivity remains good owing to the apparent lack of drag forces on the electrons at optical frequencies.

As suggested above, aluminum's high reflectivity derives from its high conductivity at infrared, visible, and ultraviolet frequencies.

---

* R. P. Madden, "Preparation and Measurement of Reflecting Coatings for the Vacuum Ultraviolet," in Physics of Thin Films, Vol. I, ed. G. Hass (Academic Press, New York, 1963), p. 155.

The simplest model for conduction--oringinally due to Drude (1908)--pictures the metal as containing N free electrons per unit volume. Under the action of an applied electric field the electrons oscillate back and forth and dissipate the driving energy by mechanisms such as collisions with other electrons, lattice vibrations, lattice imperfections, and chemical impurities. To first order, the equation of motion for such an electron takes the basic form:

$$mx'' + mgx' = eE_0 \exp(-i\omega t)$$

Here m represents the mass of an electron, e its charge, and g an empirical damping constant. (The form of the applied electric field presumes the electron's motion is small compared with the radiation wave length.)

The conductivity σ of a metallic substance is defined as the ratio of the current density in the substance to the applied electric field:

$$\sigma = eNx'/E_0 \exp(-i\omega t)$$

where, of course, x' denotes the instantaneous velocity of the electron. The steady-state solution to the above differential equation, however, has the form:

$$x' = \frac{eE_0 \exp(-i\omega t)}{mg\ (1 - i\omega/g)}$$

Accordingly, the conductivity σ becomes

$$\sigma = \frac{Ne^2}{mg(1 - i\omega/g)} \equiv \frac{\sigma_0}{1 - i\omega/g}$$

Here σ_0 represents the metal's conductivity with a DC ($\omega = 0$) electric field.

Experience with aluminum indicates that the damping constant g becomes active at optical frequencies, that is, $g \approx 10^{14}$ radians/second. At temporal frequencies ω less than g, little damping is observed, and

the conductivity remains real and large. At frequencies above g, the electron fails to follow the changes in the applied electric field, and the conductivity becomes small and imaginary. The real part of the conductivity and the skin depth, $1/\beta$, are plotted as a function of wave length in Figures A2 and A3, respectively.

The reflectivity of an aluminum layer coated onto a glass substrate follows from the formula for R quoted above. To determine the reflectivity as a function of the layer thickness, we take the following values.

Medium One (Vacuum):

$n = 1.0$

$k = 0.0$

Medium Two (Aluminum):

$\sigma_0 = 3.54 \times 10^7$ mhos/meter

$\epsilon_0 = 8.85 \times 10^{-12}$ farads/meter

$g = 10^{14}$ radians/second

$d = 1.0, 0.1, 0.01$ microns

Medium Three (Glass):

$n = 1.5$

$k = 0.0$

The curves shown in Figures A4, A5, and A6 give the reflectivity of the aluminum layer as a function of wave length for layer thickness d of 1.0, 0.1, 0.01 microns, respectively. From these curves one concludes that aluminum layers 1000 Å thick reflect better than 95% of the incident radiation.

C. Reflection by Dielectric Films

The reflectivity of a dielectric layer coated onto an aluminum substrate depends, among other things, on the thickness d of the layer and on the dielectric's extinction coefficient b. The formula for R given in

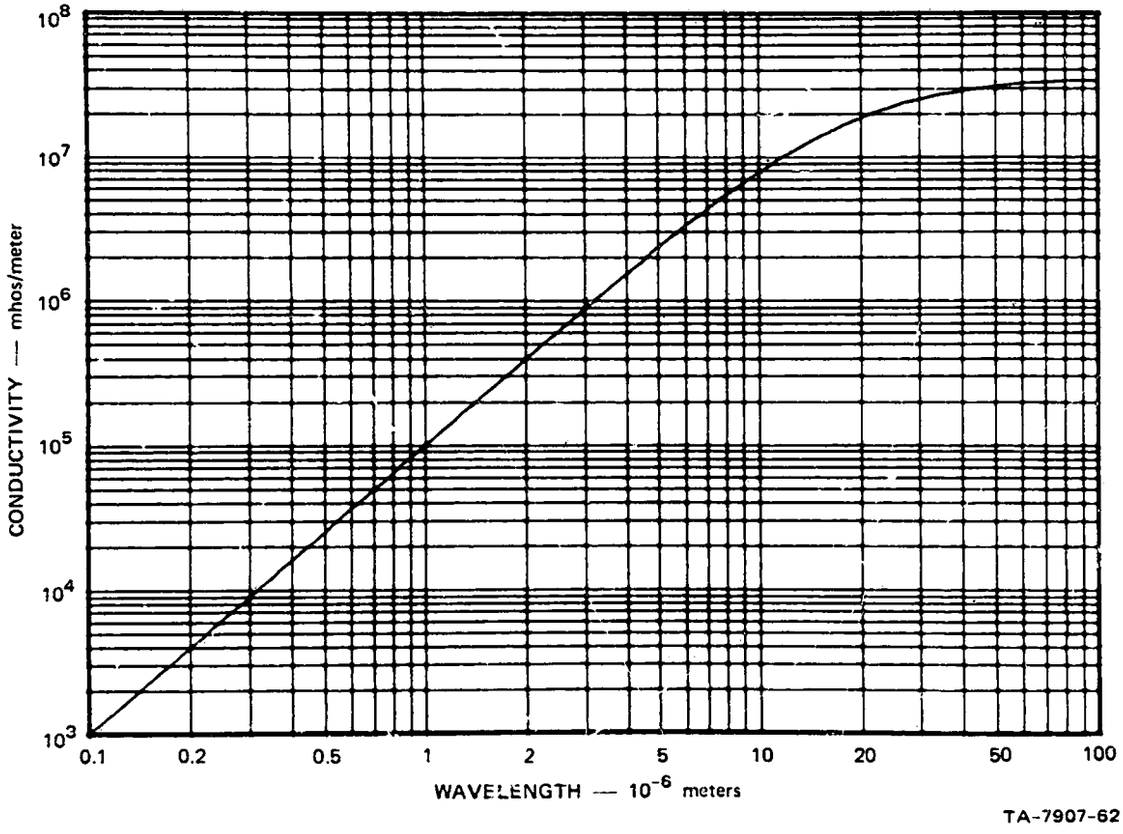

FIGURE A-2 ALUMINUM CONDUCTIVITY VERSUS WAVELENGTH
$\sigma_o = 3.54 \times 10^7$ mhos/meter, $g = 10^{14}$ radians/second

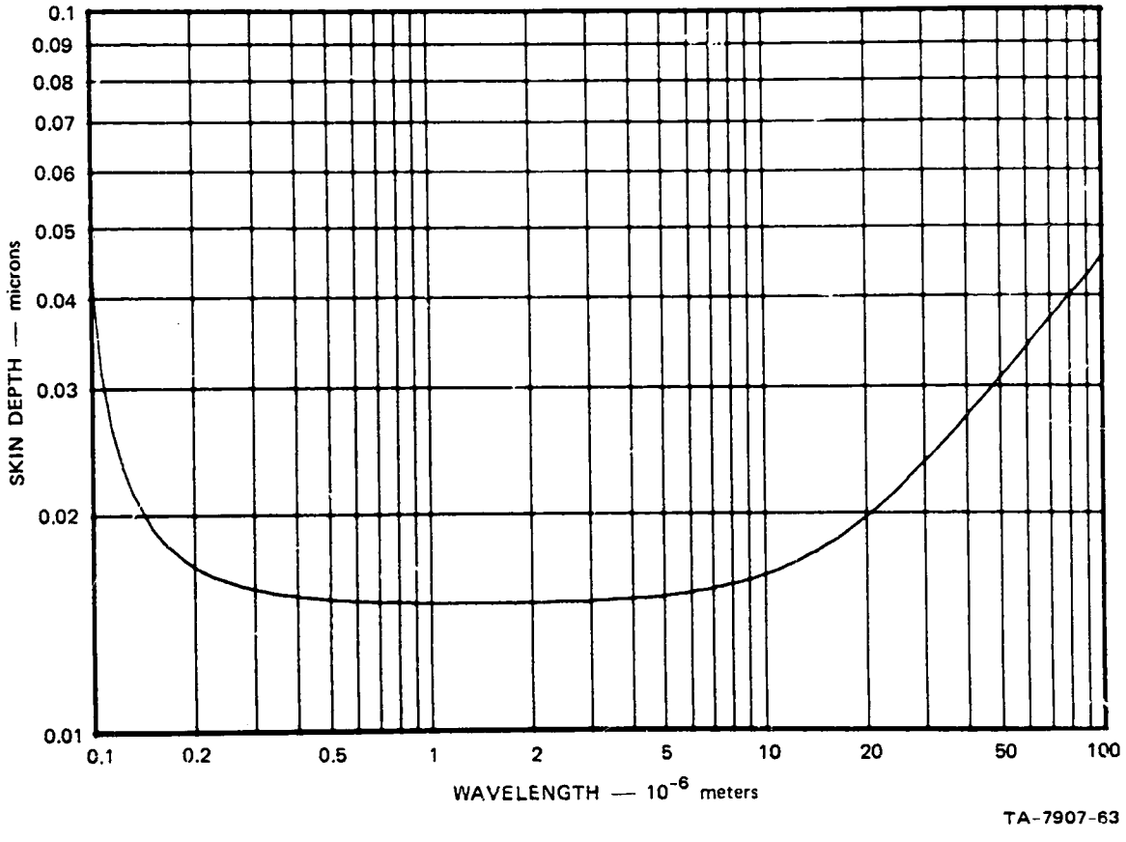

FIGURE A-3 ALUMINUM SKIN DEPTH VERSUS WAVELENGTH
$\sigma_o = 3.54 \times 10^7$ mhos/meter, $g = 10^{14}$ radians/second, $\mu = \mu_o$

REPRODUCIBILITY OF THE ORIGINAL PAGE IS POOR

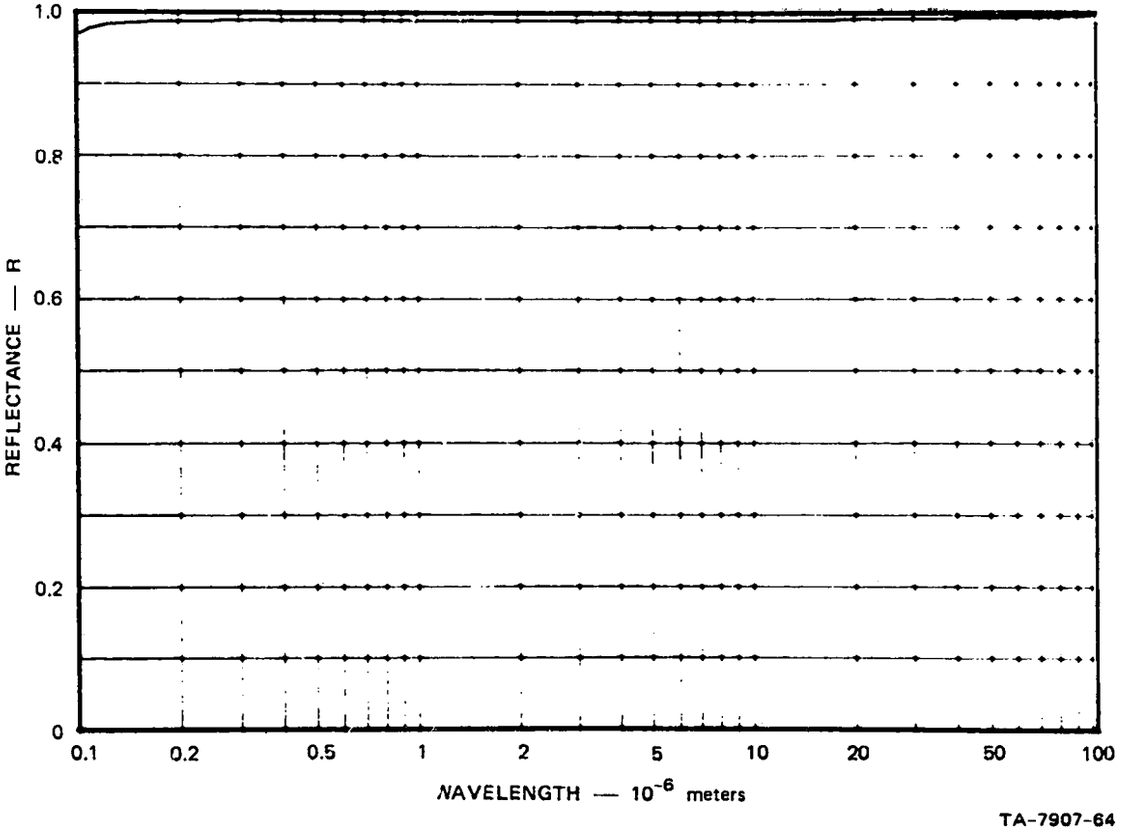

FIGURE A-4 ALUMINUM REFLECTANCE VERSUS WAVELENGTH
$d = 10^{-6}$ meters. (See text for parameter assignments.)

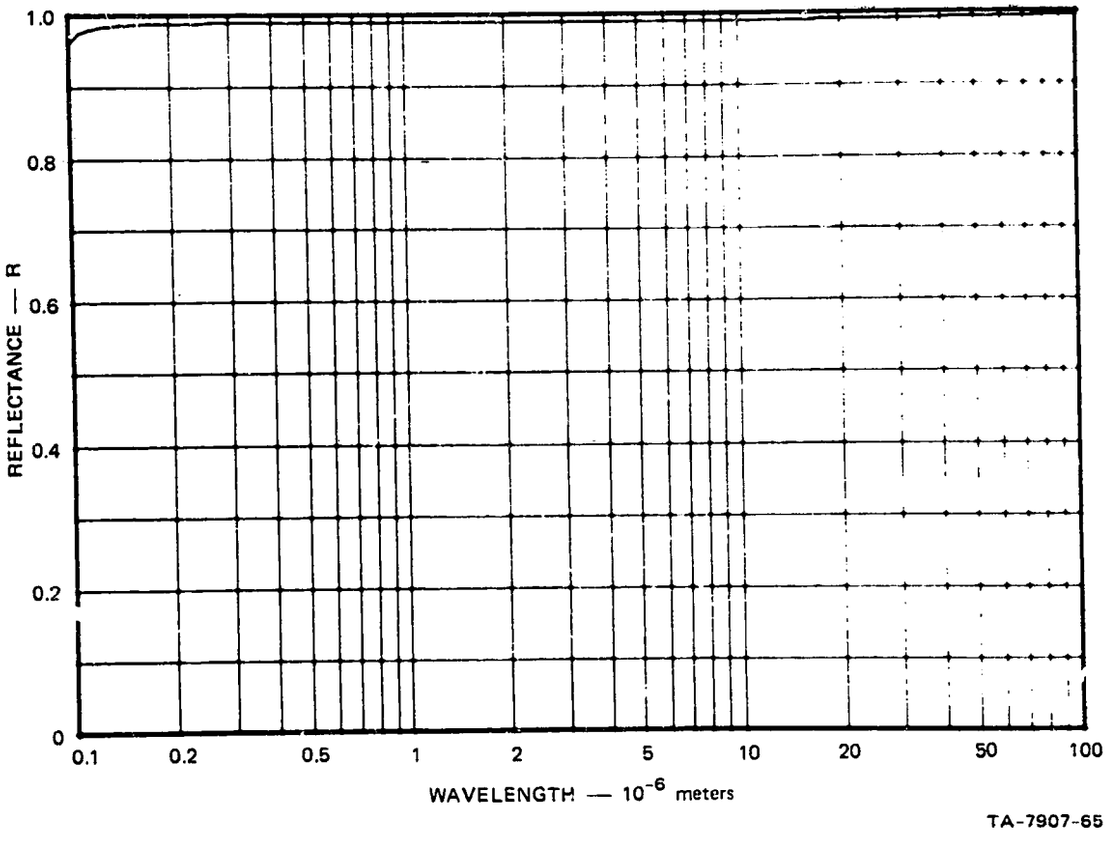

FIGURE A-5 ALUMINUM REFLECTANCE VERSUS WAVELENGTH
$d = 10^{-7}$ meters. (See text for parameter assignments.)

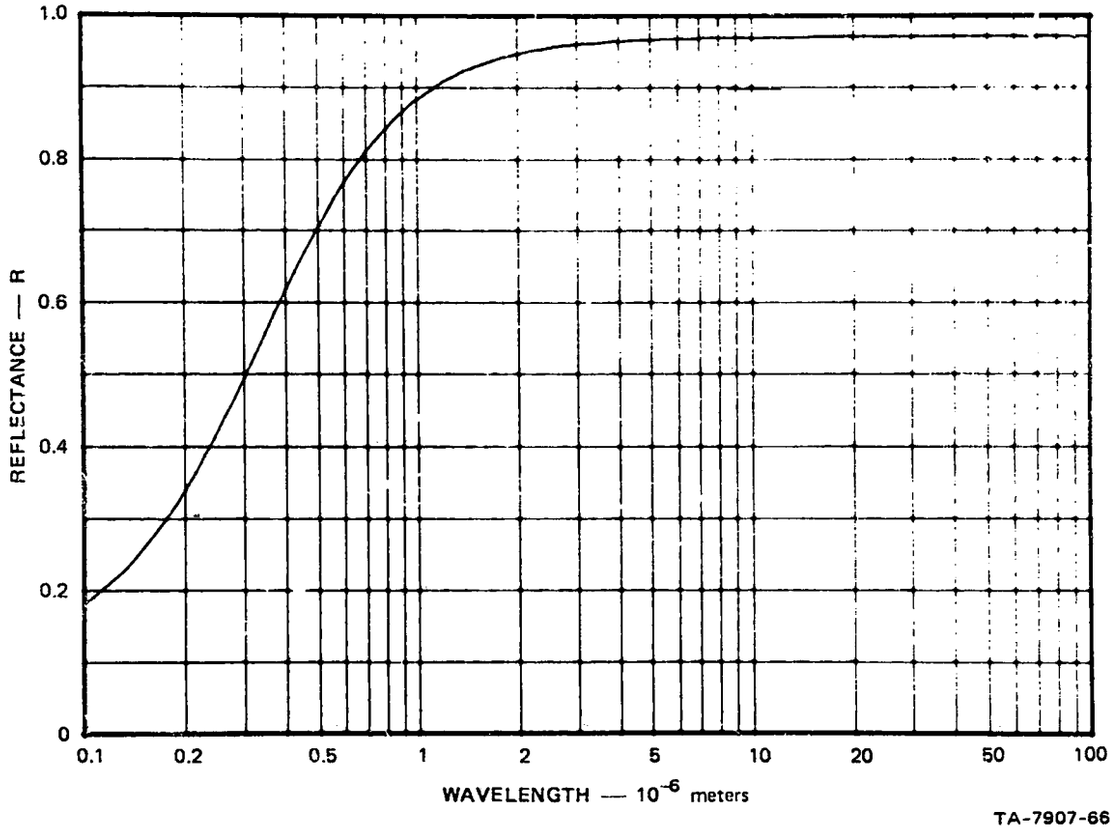

FIGURE A-6 ALUMINUM REFLECTANCE VERSUS WAVELENGTH
$d = 10^{-8}$ meters. (See text for parameter assignments.)

Section A above allows one to study the reflectivity as a function of wavelength λ, given typical values for d and b. Toward this end we make the following parameter selection:

Medium One (Vacuum):

$n = 1.0$

$k = 0.0$

Medium Two (Dielectric):

$n = 1.5$

$b = 1.0, 10, 100, 1000$ microns^{-1}

$d = 1.0, 0.1, 0.01$ microns

Medium Three (Aluminum):

$\sigma_0 = 3.54 \times 10^7$ mhos/meter

$\epsilon_0 = 8.85 \times 10^{-12}$ farads/meter

$g = 10^{14}$ radians/second

The curves shown in Figures A7 through A18 give the reflectivity R as a function of λ for the values of b and d quoted above. These figures indicate that the reflection coefficient R remains near unity if the product $bd < 0.1$ and the wavelength $\lambda > 1.0$ micron. The oscillating structure observed in Figures A10, A13, and A14 arises because the dielectric layer acts as an interference filter at certain frequencies. For $b = 10^8$ meters^{-1} the extinction is so great that little light reaches the aluminum substrate. In this case the dielectric surface looks black at the shorter wave lengths, as suggested by Figures A16 and A17.

D. Scattering by Thin Films

As suggested by Figure A17, a rough dielectric surface will scatter some of the radiation incident upon it. If the wavelength λ of the incident light remains large compared with the rms surface roughness δ,

REPRODUCIBILITY OF THE ORIGINAL PAGE IS POOR.

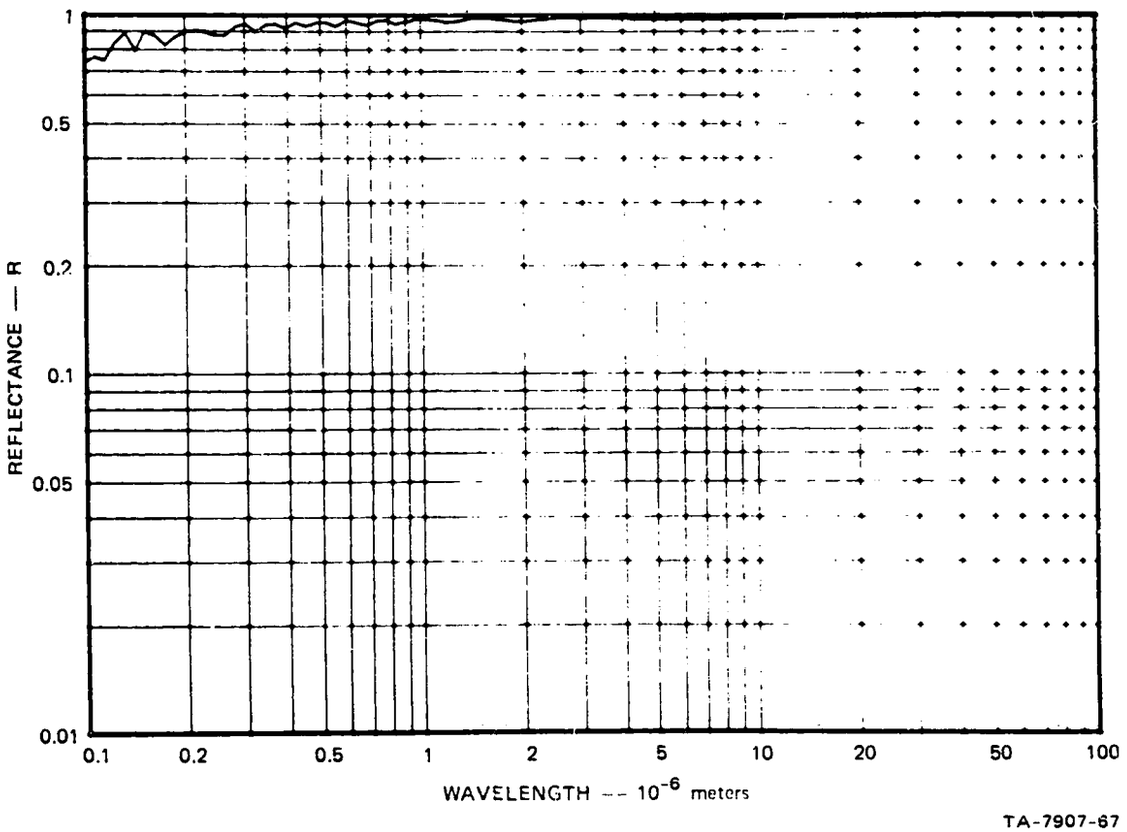

FIGURE A-7 REFLECTANCE VERSUS WAVELENGTH
$d = 10^{-6}$ meters, $1/b = 10^{-5}$ meters

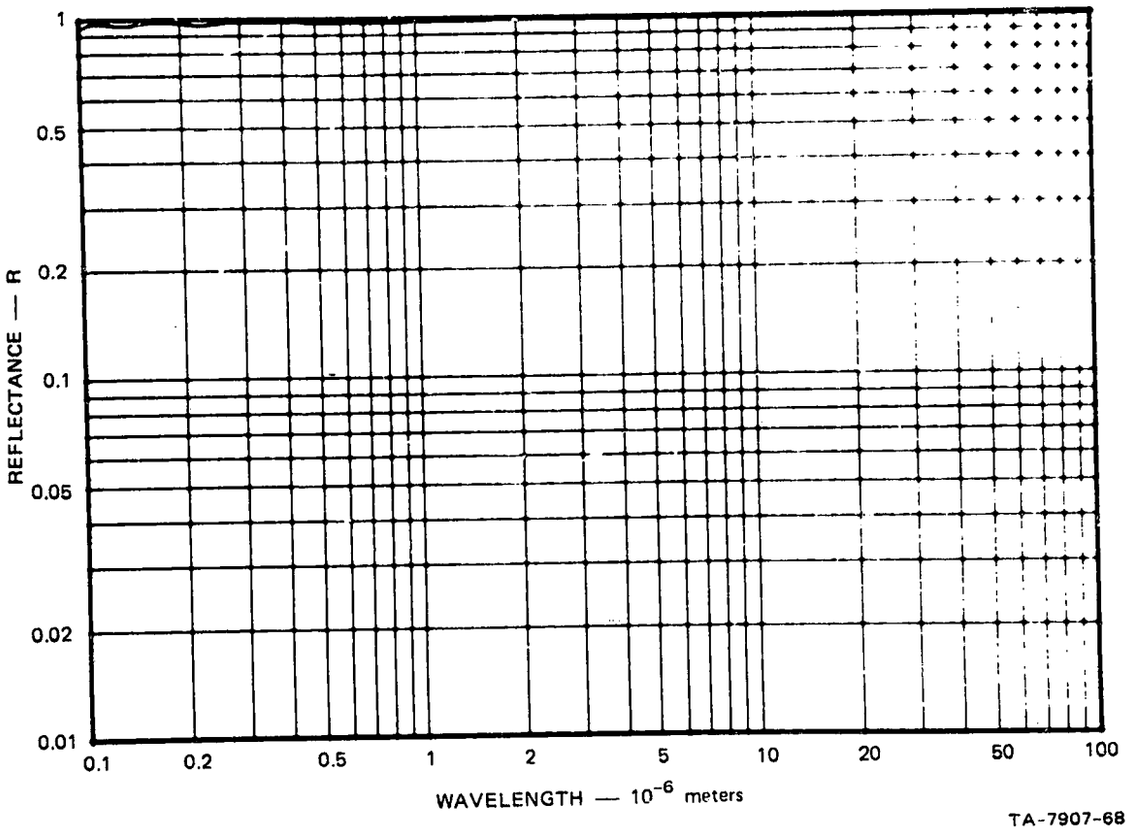

FIGURE A-8 REFLECTANCE VERSUS WAVELENGTH
$d = 10^{-7}$ meters, $1/b = 10^{-5}$ meters

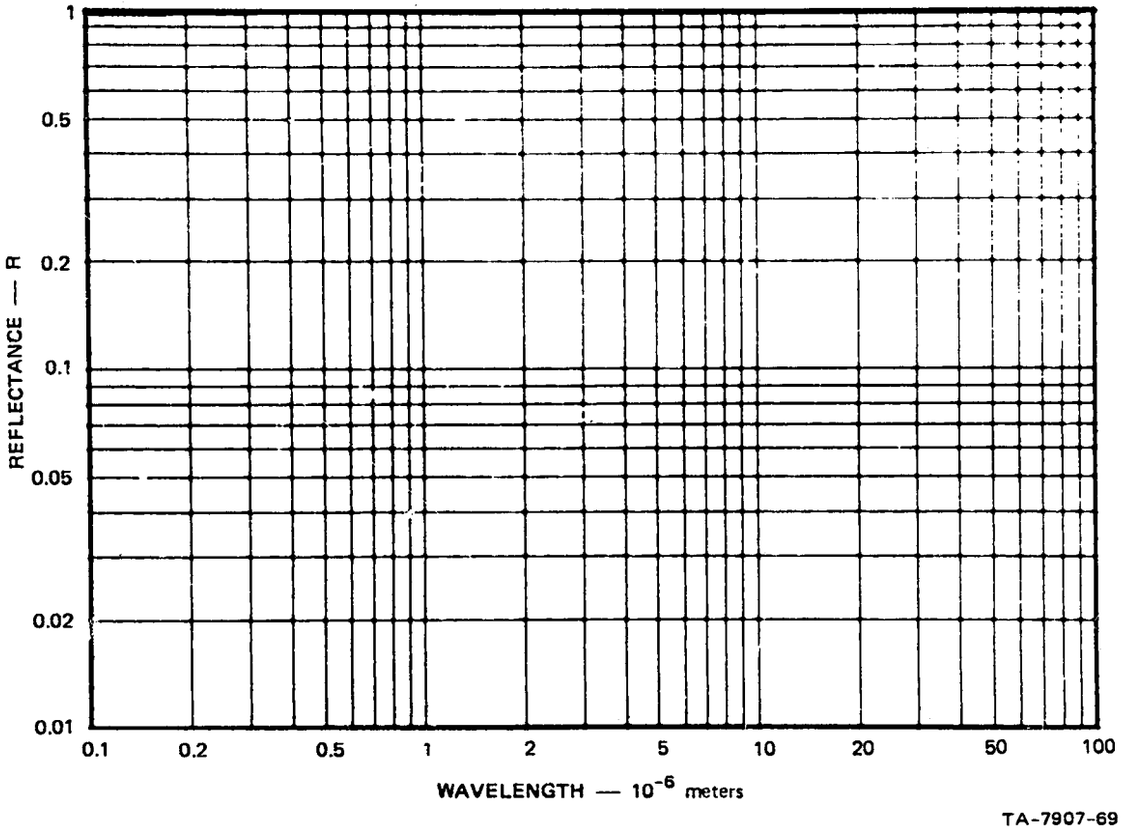

FIGURE A-9 REFLECTANCE VERSUS WAVELENGTH
$d = 10^{-8}$ meters, $1/b = 10^{-5}$ meters

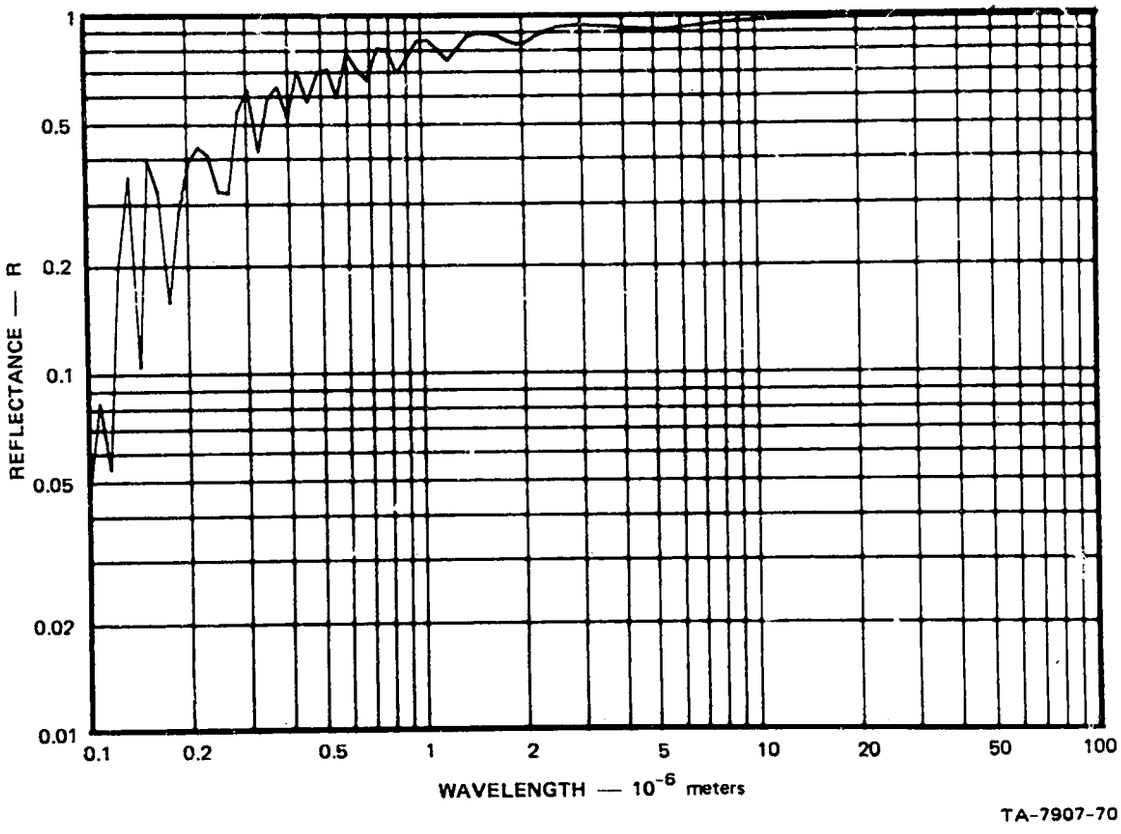

FIGURE A-10 REFLECTANCE VERSUS WAVELENGTH
$d = 10^{-6}$ meters, $1/b = 10^{-6}$ meters

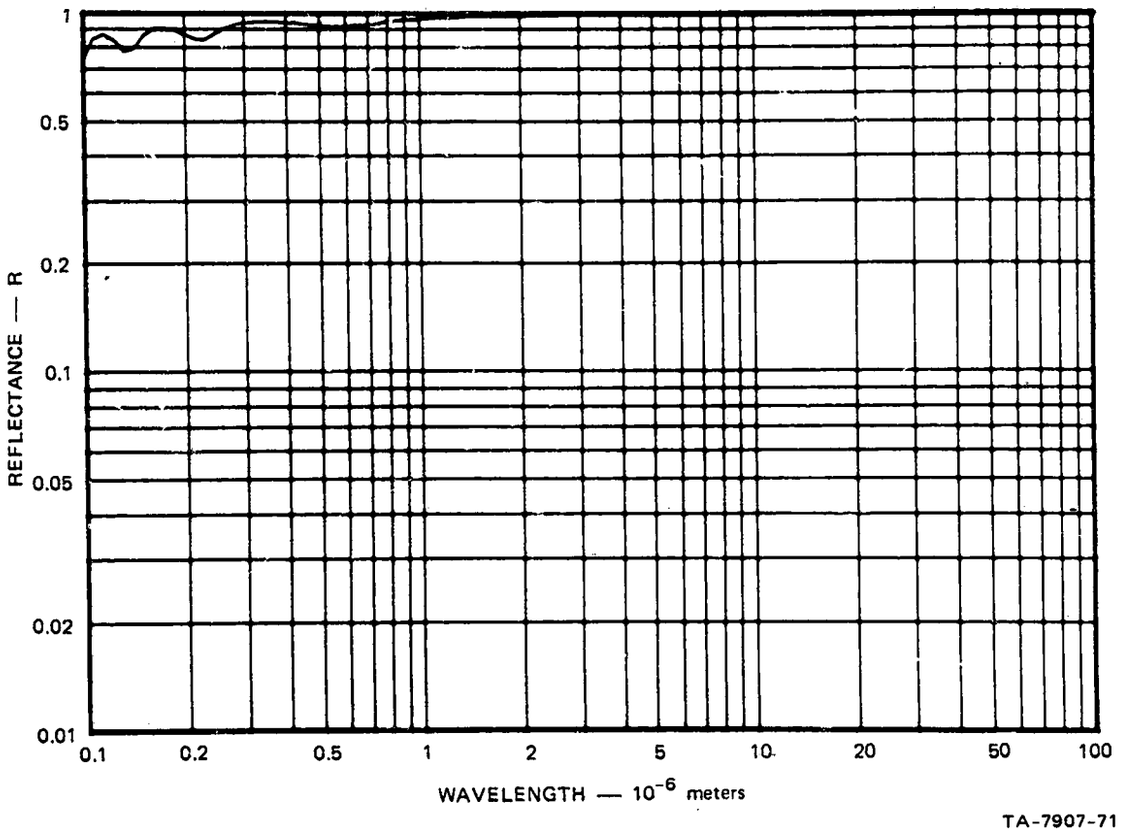

FIGURE A-11 REFLECTANCE VERSUS WAVELENGTH
$d = 10^{-7}$ meters, $1/b = 10^{-6}$ meters

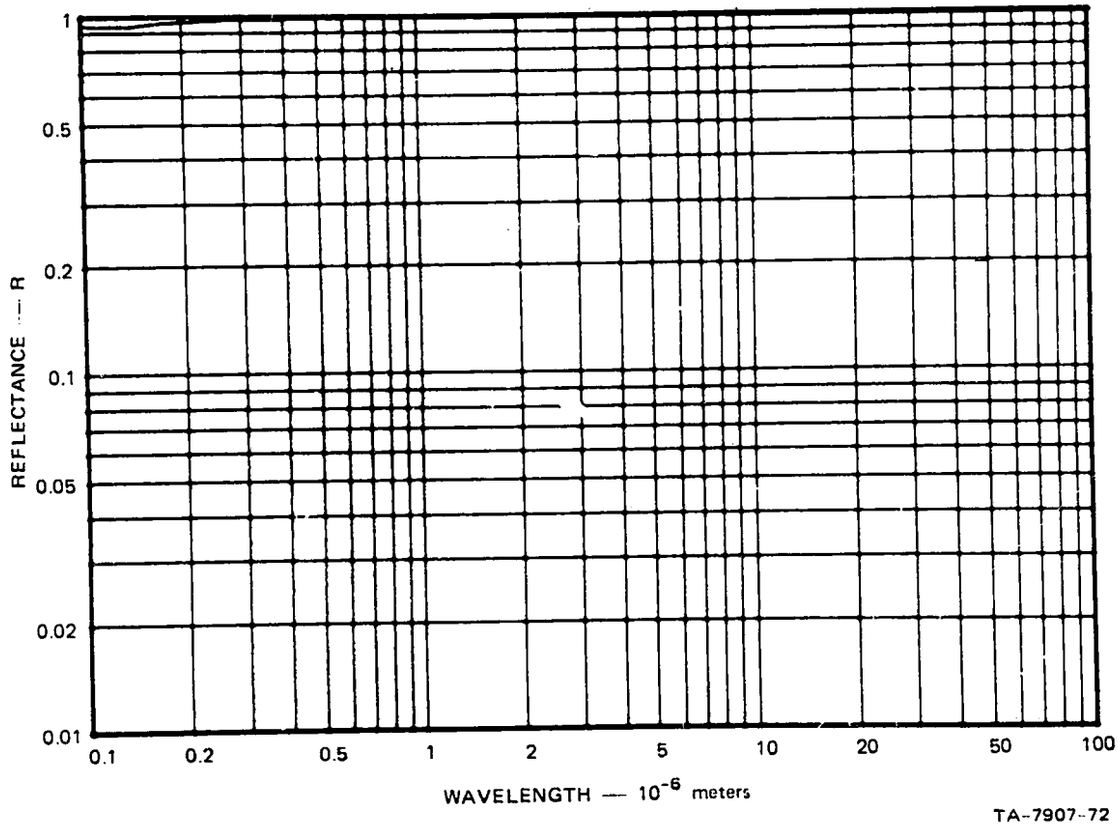

FIGURE A-12 REFLECTANCE VERSUS WAVELENGTH
$d = 10^{-8}$ meters, $1/b = 10^{-6}$ meters

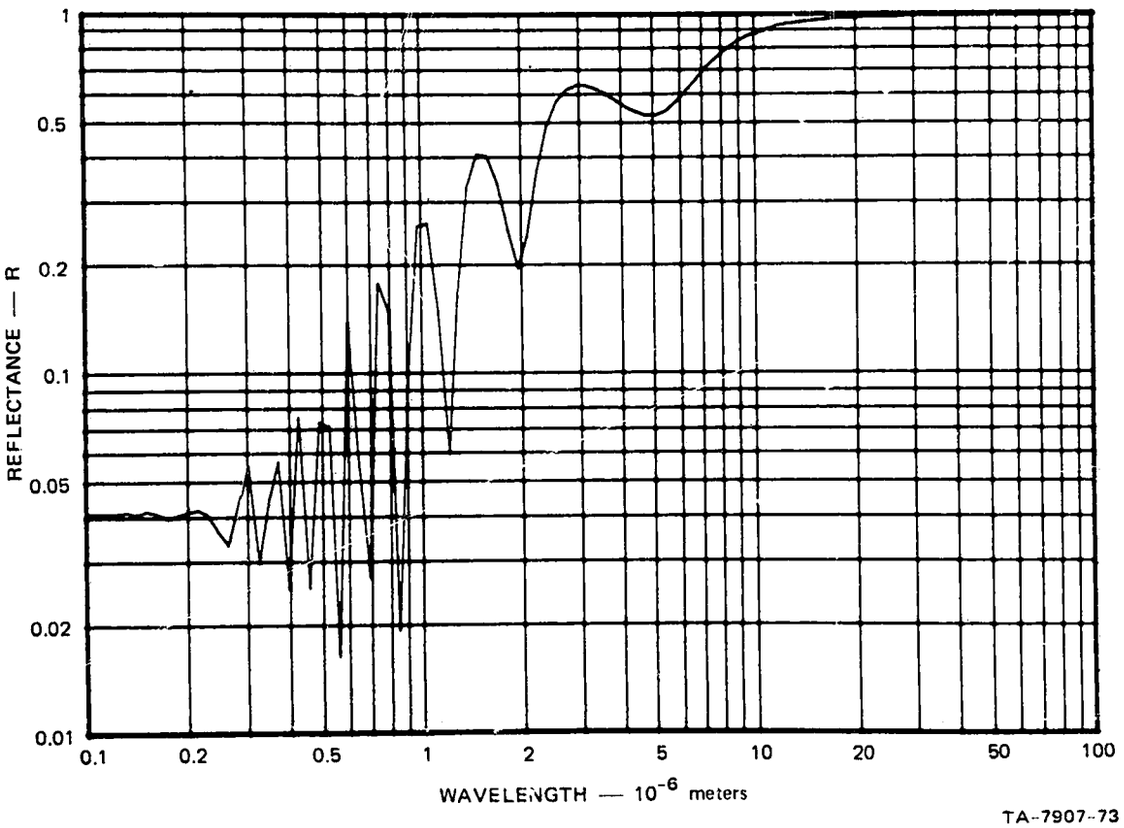

FIGURE A-13 REFLECTANCE VERSUS WAVELENGTH
$d = 10^{-6}$ meters, $1/b = 10^{-7}$ meters

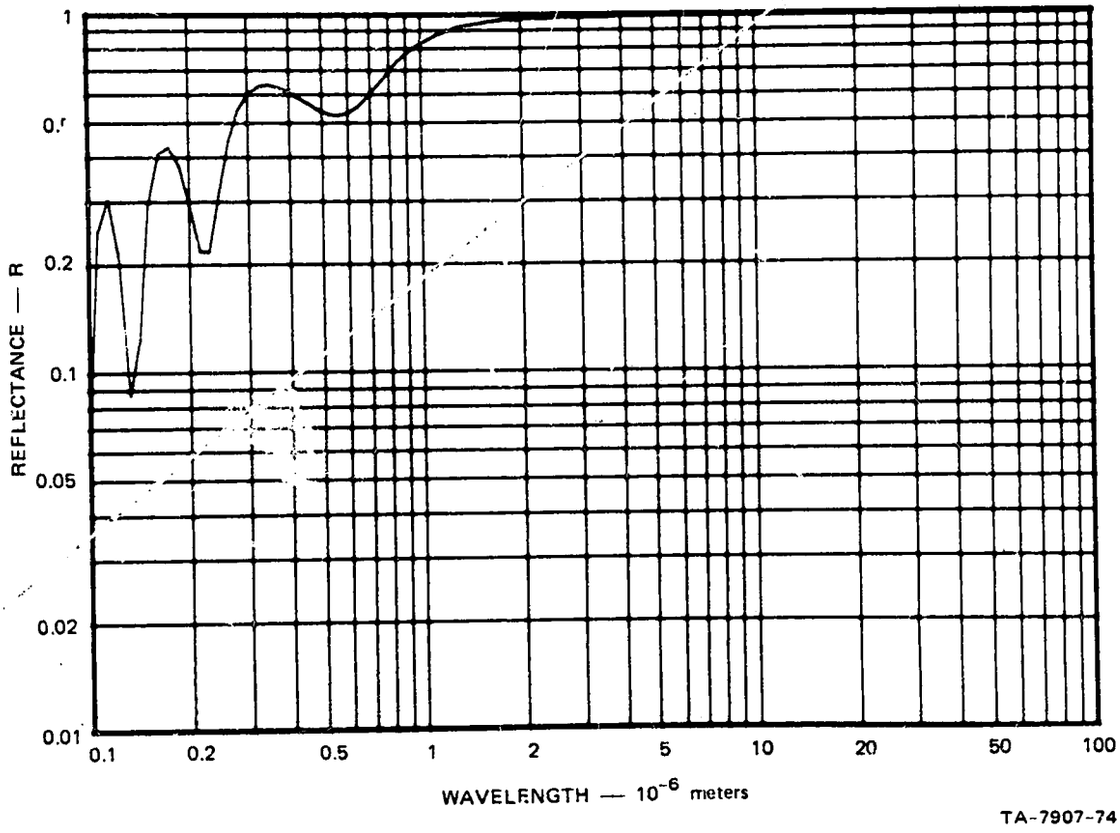

FIGURE A-14 REFLECTANCE VERSUS WAVELENGTH
$d = 10^{-7}$ meters, $1/b = 10^{-7}$ meters

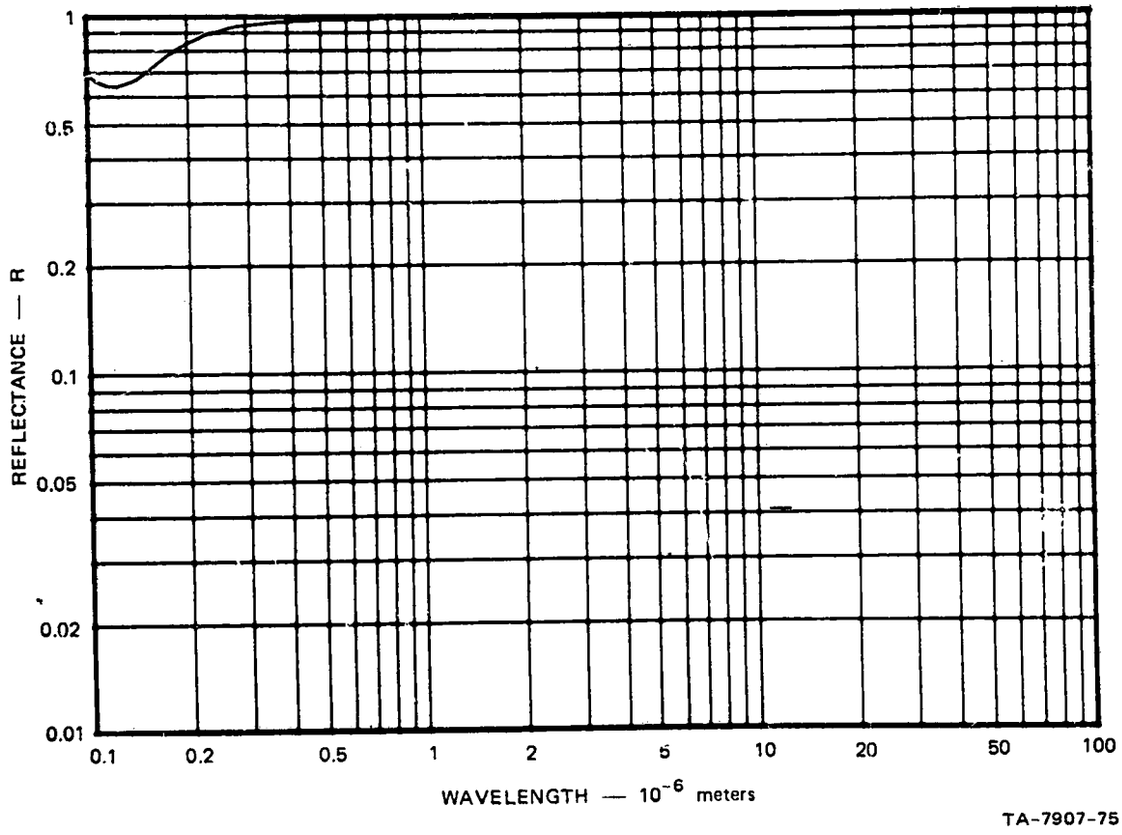

FIGURE A-15 REFLECTANCE VERSUS WAVELENGTH
$d = 10^{-8}$ meters, $1/b = 10^{-7}$ meters

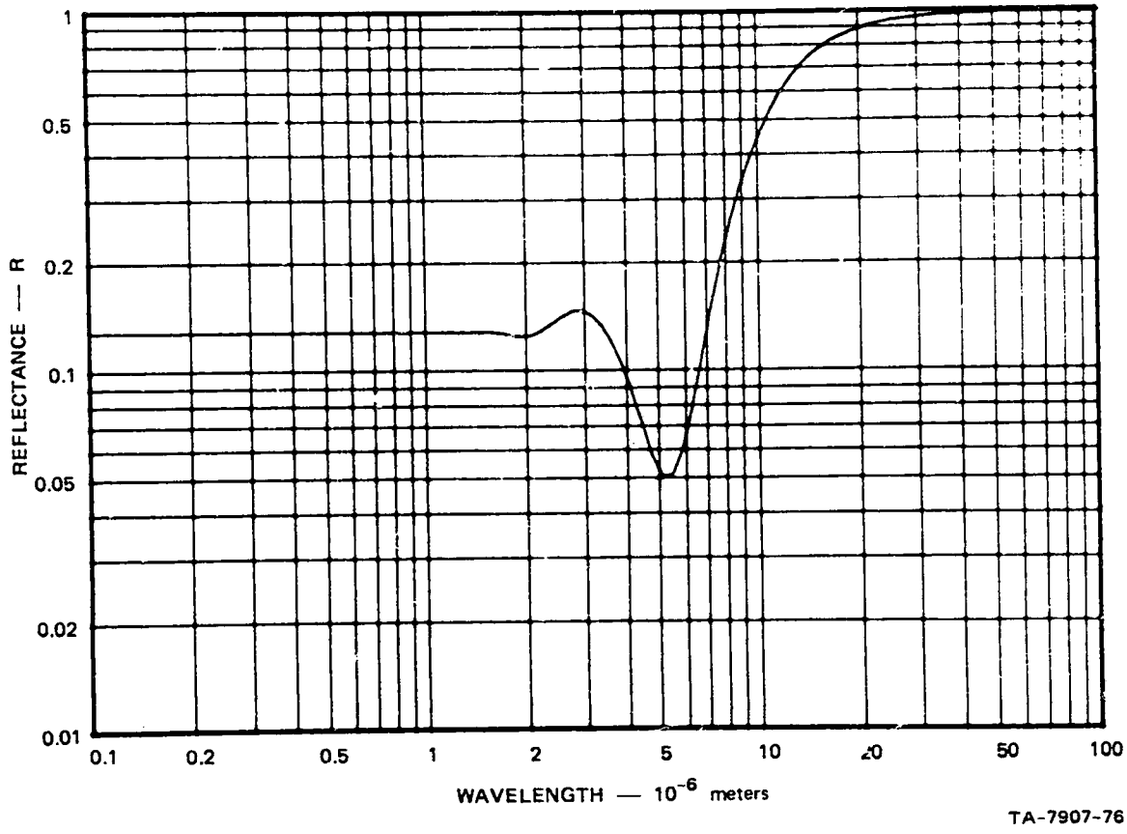

FIGURE A-16 REFLECTANCE VERSUS WAVELENGTH
$d = 10^{-6}$ meters, $1/b = 10^{-8}$ meters

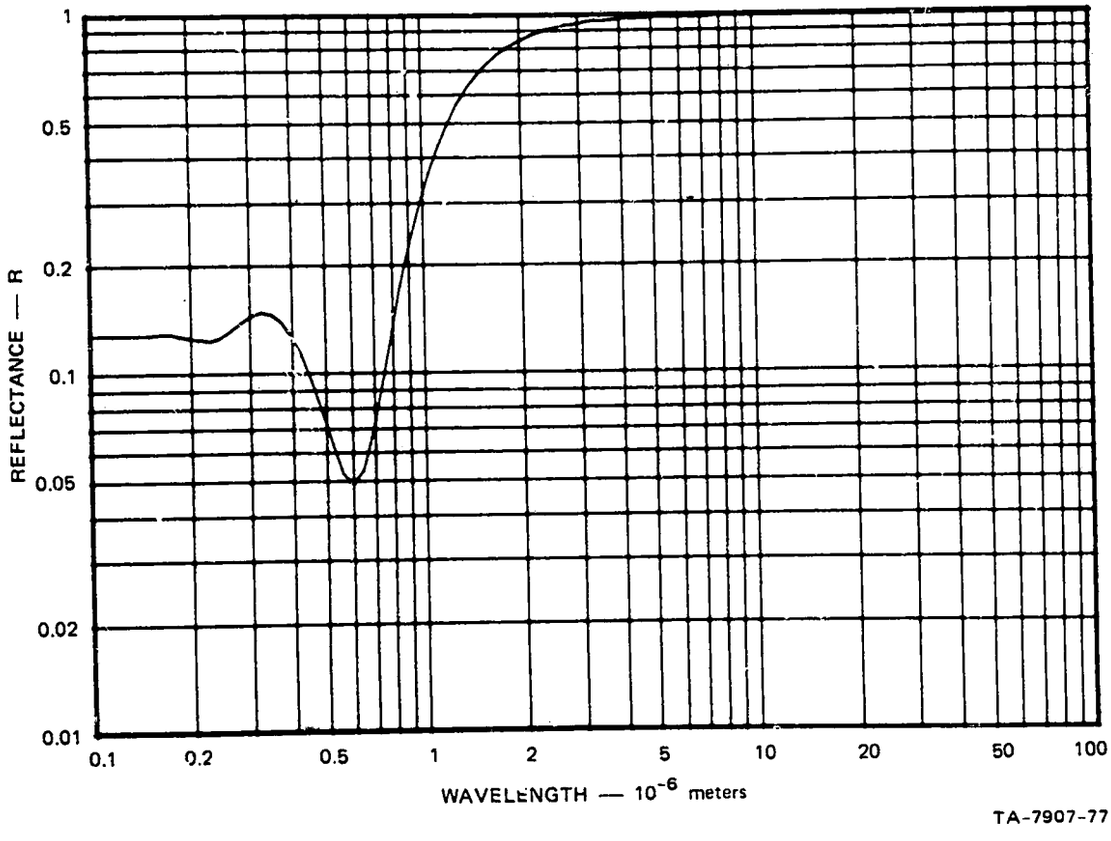

FIGURE A-17 REFLECTANCE VERSUS WAVELENGTH
$d = 10^{-7}$ meters, $1/b = 10^{-8}$ meters

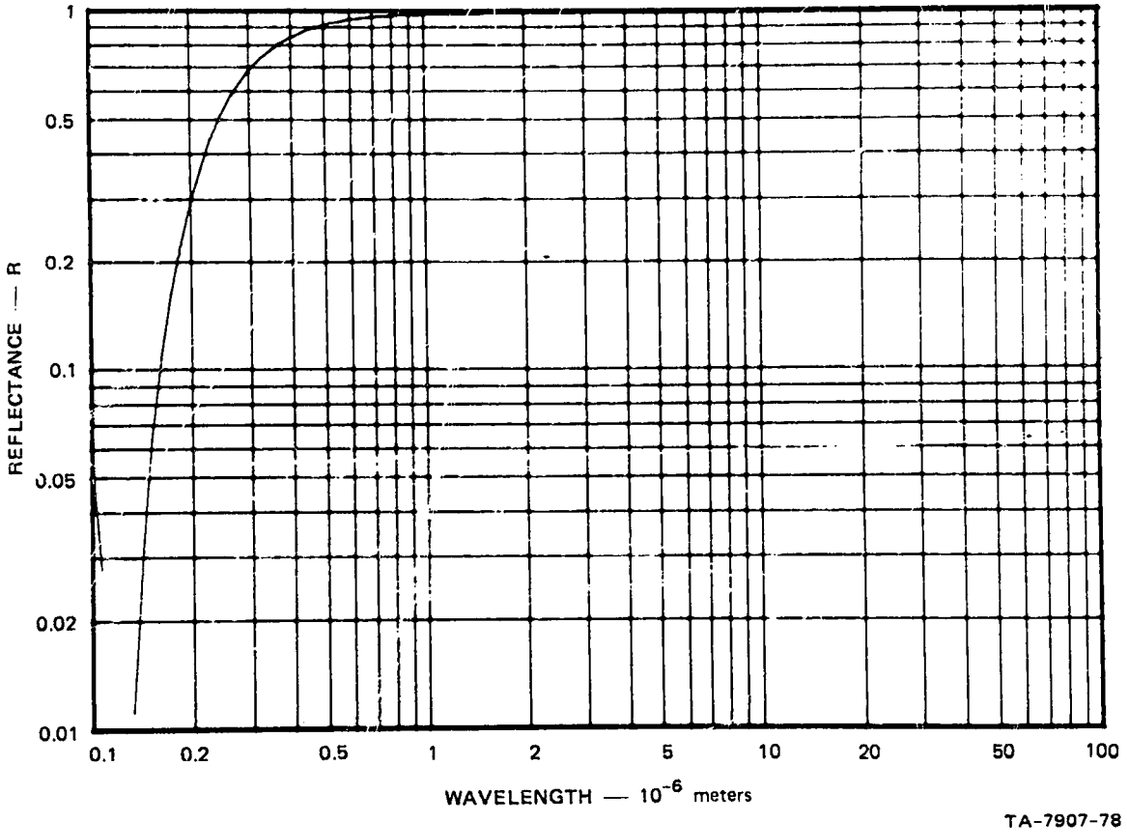

FIGURE A-18 REFLECTANCE VERSUS WAVELENGTH
$d = 10^{-8}$ meters, $1/b = 10^{-8}$ meters

one observes Rayleigh-type, rather than Mie-type scattering at the dielectric surface. If, on the other hand, the wavelength λ looks small compared with δ, the scattering depends in a very complicated way on the surface geometry and complex refractive index of the dielectric medium. Moreover, in contrast to Rayleigh scattering, the Mie mechanisms usually scatter more of the incident beam than they transmit, thus destroying the mirror-like qualities of the aluminum surface shown in Figure A19.

According to the Rayleigh theory, the amount of light scattered by a body with dimensions much smaller than the wavelength λ depends only on the volume V of that body. In particular, the scattering cross section σ_s is directly proportional to the volume squared and inversely proportional to the fourth power of the wavelength λ

$$\sigma_s \propto V^2/\lambda^4$$

In addition, if the body has a complex refractive index n + ik, then the cross section increases as the modulus squared of this index:

$$\sigma_s \propto \left| n + ik \right|^2 V^2/\lambda^4$$

To determine the constant of proportionality, however, one must solve the associated scattering problem for the for-field radiation pattern.

The electric field $E_s(\vec{x})$ scattered by a body centered on the origin and illuminated with the plane wave exp(ikz) takes the usual form:

$$E_s(\vec{x}) = (-1/4\pi) \int_{\infty} \exp(ikz')\ U(\vec{x}').\exp(ikR)/R\ \ d\vec{x}'$$

As shown in Figure A20, R denotes the distance between the observation point $\vec{x}'$:

$$R = \left| \vec{x} - \vec{x}' \right|$$

The optical scattering potential $U(\vec{x}')$ may be real or complex and is related to the medium's complex refractive index n + 1k in the following

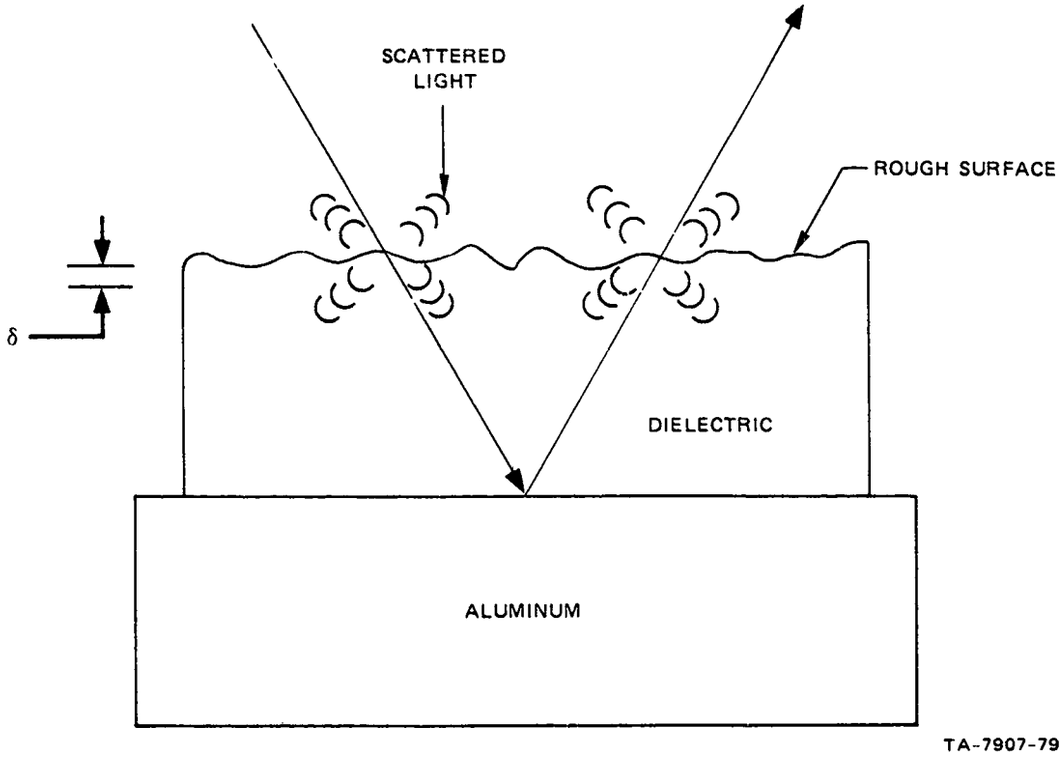

FIGURE A-19 LIGHT SCATTERING BY ROUGH DIELECTRIC SURFACE.
δ is the rms surface roughness.

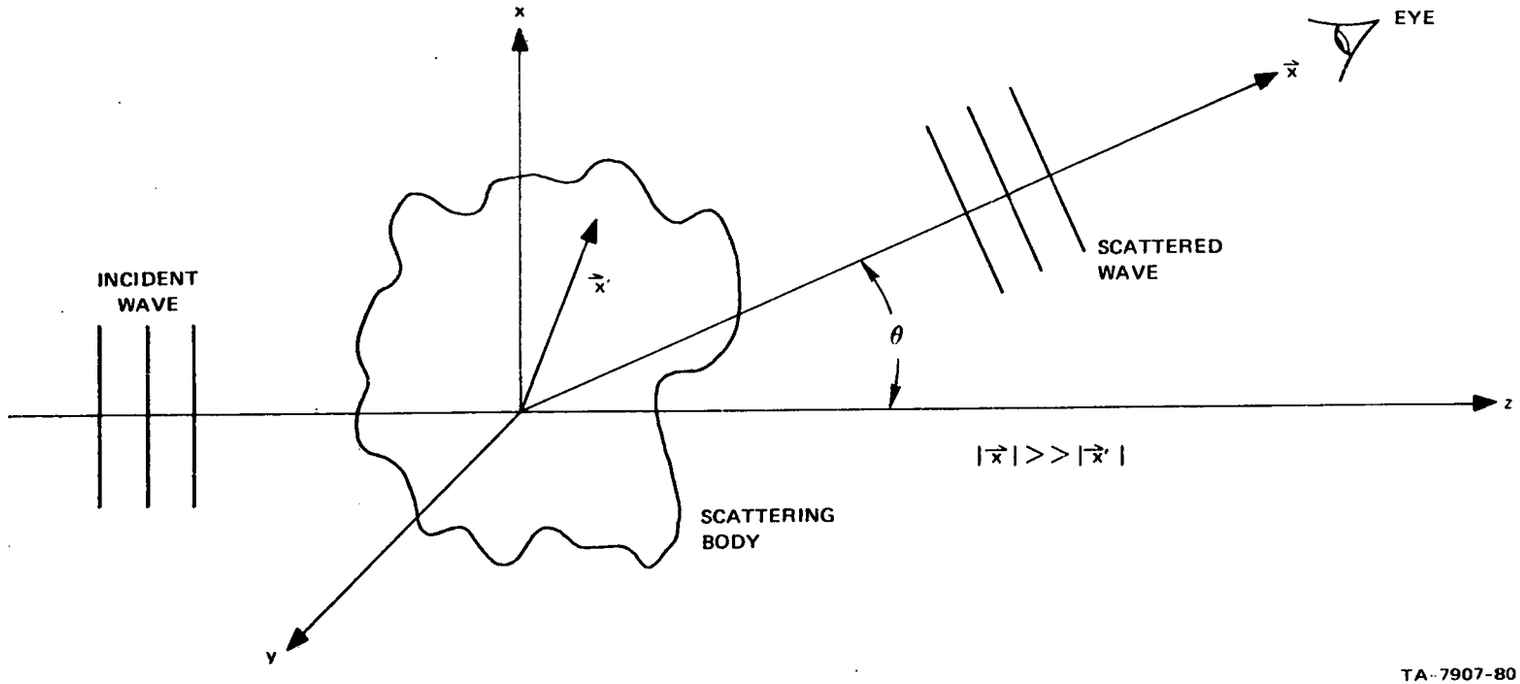

FIGURE A-20 SCATTERING PROBLEM GEOMETRY

way:

$$U(\vec{x}') \approx 2k^2 [n(\vec{x}') + ik(\vec{x}') - 1]$$

Here and in what follows, k is real and equal to its free-space value ω/c.

At large distances from the scattering body, R may be replaced by r in the denominator of the intergrand and by

$$kR \approx kr - k\vec{x} \cdot \vec{x}'/r = kr - k_f \cdot \vec{x}'$$

in its exponent. Here, of course, $r = |\vec{x}|$ and

$$\vec{k}_f \equiv k\vec{x}/r$$

denotes the final wave vector for the scattered photons. Using the same notation, the initial wave vector for the photons takes the form:

$$\vec{k}_i = k\vec{e}_z$$

Accordingly, we may write

$$\vec{\Delta} = \vec{k}_i - \vec{k}_f$$

and call $\vec{\Delta}$ the three-momentum transfer to the body by the incident photons.

Substituting into the formula for the scattered electric field then yields:

$$E_s(\vec{x}) = (-k^2/2\pi) \exp(ikr)/r \cdot \int_{\infty} [n(\vec{x}') + k(\vec{x}') - 1] \exp(i\vec{\Delta} \cdot \vec{x}') \, d\vec{x}'$$

For scattering bodies small compared with the radiation wavelength λ, the dot product $\vec{\Delta} \cdot \vec{x}'$ remains small for all points on the body. In addition, if the complex refractive index remains uniform within the body, the above formula simplified to

$$E_s(\vec{x}) = (-k^2/2\pi) \exp(ikr)/r \cdot (n + ik - 1) \int d\vec{x}'$$

The indicated integral goes over the volume V of the body.

The scattering amplitude $f(k, \vec{\Delta})$ follows by deleting the factor $\exp(ikr)/r$ from the above expression:

$$f(k, \vec{\Delta}) = (-k^2/2\pi)\ (n + ik - 1)V,$$

where V denotes the volume of the scattering body. The differential scattering cross section follows immediately from the above formula:

$$d\sigma_s/d\Omega = \left| f(k, \vec{\Delta}) \right|^2 = (k^4/4\pi^2) \left| n + ik - 1 \right| V^2$$

The total scattering cross section obtains by integrating the above expression over all solid angles:

$$\sigma_s = 16\pi^3 \left| n + ik - 1 \right|^2 V^2/\lambda^4$$

Accordingly, the sought after constant of proportionality is just $16\pi^3$.

The surface of the dielectric film consists of many randomly located imperfections--all presumed small compared with the wavelength λ. If δ^3 represents the average volume of such imperfections, then the scattering cross section takes the form:

$$\sigma_s = 16\pi^3 \left| n + ik - 1 \right|^2 \delta^6/\lambda^4$$

If N such imperfections occur per unit area, then the fraction of the incident light scattered by the imperfections is just

$$I_s/I_o = N\sigma_s$$

The maximum number of imperfections one can expect per unit area is clearly

$$N = 1/\delta^2$$

Thus, an upper limit on the amount of Rayleigh scattered light is given by the expression:

$$I_s/I_0 = 32\pi^3 \left| n + ik - 1 \right|^2 \delta^4/\lambda^4$$

The extra factor of two has been inserted because scattering occurs when the light enters the dielectric and again when it leaves it.

To estimate amount of Rayleigh scattering as a function of wavelength λ and surface roughness d, we rather arbitrarily take

$$\left| n + ik - 1 \right|^2 = 1/2$$

In this case the fraction of light scattered by surface roughness becomes

$$I_s/I_0 = 16\pi^3 \delta^4/\lambda^4$$

The above equation is plotted in Figures A21, A22, and A23 for $\delta = 10^{-6}$, 10^{-7}, and 10^{-8} meters, respectively. (All curves have been truncated when I_s/I_0 exceeds 1.0 because the integral formula used for $E_s(\vec{x})$ becomes inaccurate when the amount of scattered light becomes comparable to the amount of incident light.)

REPRODUCIBILITY OF THE ORIGINAL PAGE IS POOR.

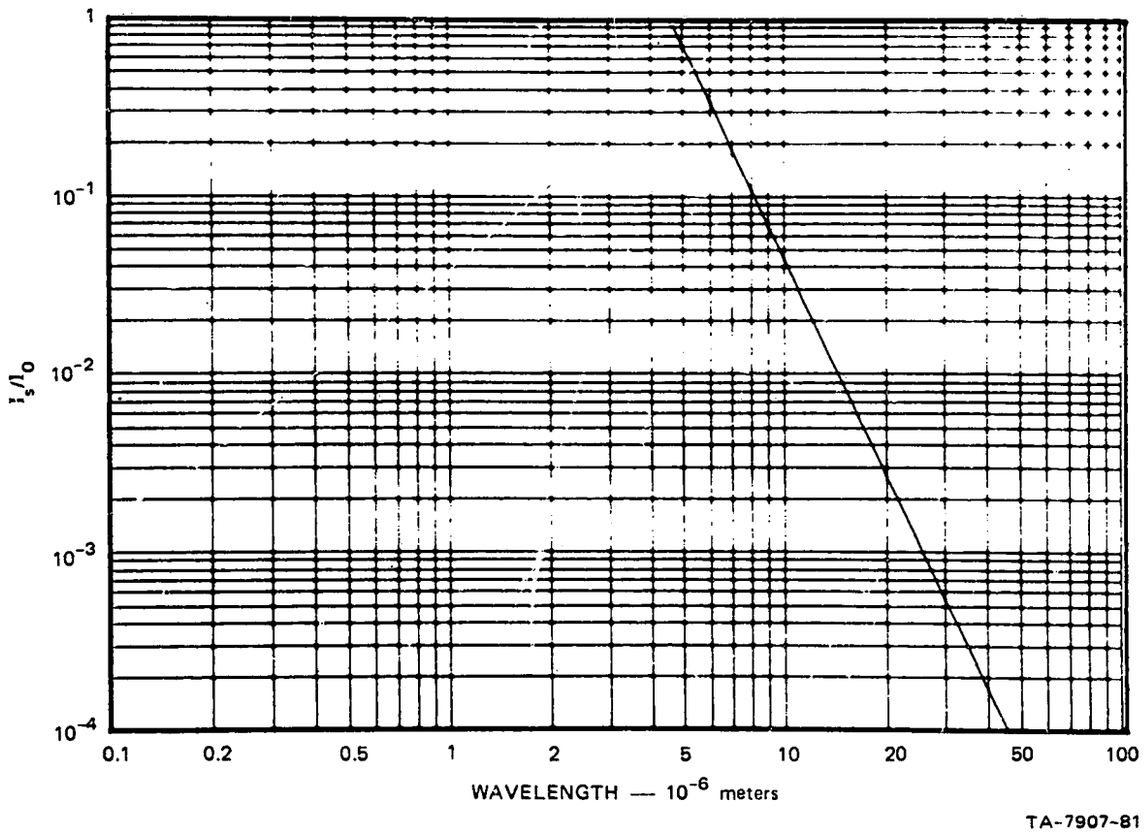

FIGURE A-21 SCATTERING VERSUS WAVELENGTH
$\delta = 10^{-6}$ meters

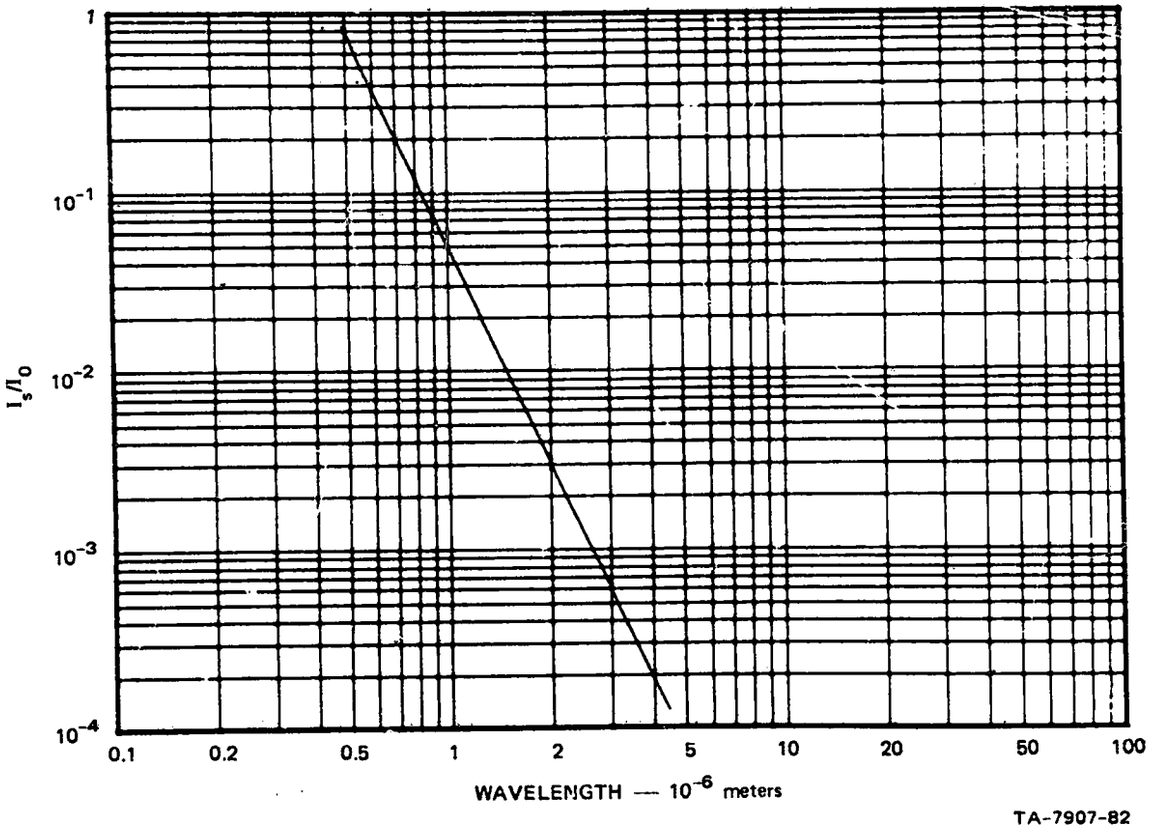

FIGURE A-22 SCATTERING VERSUS WAVELENGTH
$\delta = 10^{-7}$ meters

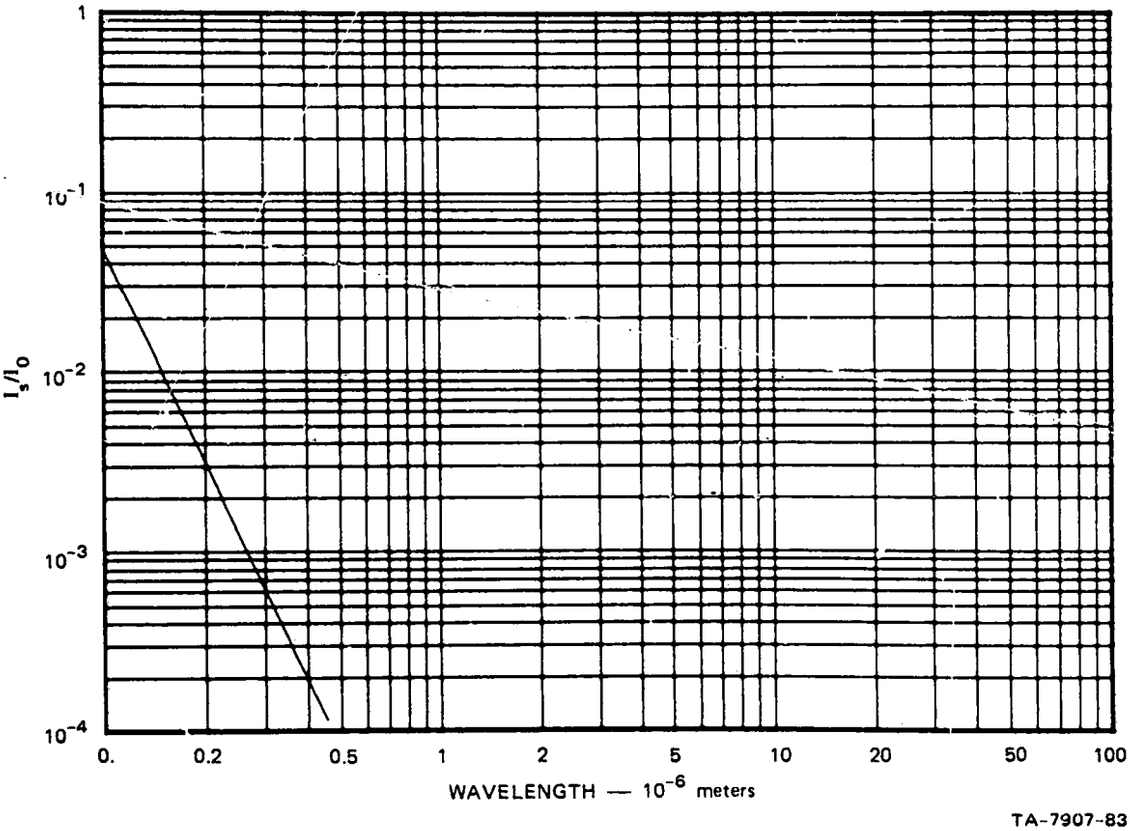

FIGURE A-23 SCATTERING VERSUS WAVELENGTH
$\delta = 10^{-8}$ meters